



**ADEKUNLE AJASIN UNIVERSITY**

P.M.B. 001 AKUNGBA AKOKO,  
ONDO STATE, NIGERIA

**ANTI-DIABETIC STUDIES OF *Chromolaena odorata* FLAVONOID FRACTION IN  
STREPTOZOTOCIN - TREATED RATS: INVOLVEMENT OF TGR5/INSULIN/PDX-1 PATHWAY**

**BY**

**Ojochenemi Aladi ENEJOH**

**MATRIC NO. 169418002**

**NOVEMBER 2021**

ANTI-DIABETIC STUDIES OF *Chromolaena odorata* FLAVONOID FRACTION IN  
STREPTOZOTOCIN-TREATED RATS: INVOLVEMENT OF TGR5/INSULIN/PDX-  
1 PATHWAY

BY

Ojochenemi Aladi ENEJOH

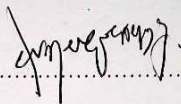
MATRIC. NUMBER: 169418002

BEING A Ph.D THESIS IN THE DEPARTMENT OF BIOCHEMISTRY, FACULTY  
OF SCIENCE, AND SUBMITTED TO THE POST GRADUATE SCHOOL,  
ADEKUNLE AJASIN UNIVERSITY, AKUNGBA AKOKO, ONDO STATE, NIGERIA  
IN PARTIAL FULFILMENT OF THE REQUIREMENTS FOR THE AWARD OF  
DEGREE OF DOCTOR OF PHILOSOPHY (Ph.D) IN BIOCHEMISTRY

NOVEMBER, 2021

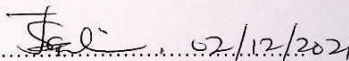
## CERTIFICATION

This is to certify that this thesis was carried out and reported by **Ojochenemi Aladi ENEJOH** with Matriculation Number **169418002** in the Department of Biochemistry, Faculty of Science, Adekunle Ajasin University, Akungba-Akoko, Ondo State, Nigeria.



OMOTUYI, Idowu O. Ph.D

Supervisor



SALIU, Jamiyu A. Ph.D

Head of Department

## DEDICATION

This thesis is dedicated to my loving grandfather, Mr Samuel J. Akpotabore.

## ACKNOWLEDGEMENTS

My acknowledgement goes to my maker, the Lord Almighty, for the gift of life, and the grace to start and finish this Ph.D programme successfully. Father, I thank you for your unspeakable gift. To you alone be all the glory.

My deep and profound gratitude goes to my indefatigable supervisor, Dr Olaposi I. Omotuyi, for his relentless efforts to see to the completion of my Ph.D. You are a mentor whose excellence I reflect and upon whose shoulders I have risen to this level today.

My gratitude goes to other lecturers of the Department of Biochemistry: Dr J. A. Saliu, Dr O. Y. Adeniran, Dr A. O. Olusola, Dr D. S. Metibemu, Dr (Mrs) S. A. Shodehinde, Dr (Mrs) V. O. Odubanjo, Dr A. Fakoya, Mr G. J. Oluwadahunsi, Dr O. S. Bakare, Dr O. E. Ekun, Dr S. A. Emaleku, and other non-academic staff, I appreciate all their assistance in my academic pursuit.

To my Centre for Bio-computing and Drug Development family, Eunice Oribamise, Ayo, Wale, Inyang, Niyi, Bamidele thank you for being there.

My bagging another degree would not have been possible, if I was not granted study leave from my place of work. To this effect, I wish to say a big thank you to the Director General, National Biotechnology Development Agency (NABDA) Abuja, for releasing me to study for a Ph.D programme. To my boss, Dr. Oyekanmi Nash, thank you Sir, for the encouragement, support and push to bring out excellence in me. I also thank all staff of Genomics and Bioinformatics Department, NABDA.

I especially appreciate my parents, Mr Adams U. Enejoh, Mrs Eunice O. Enejoh and only brother, Mr Omakoji D. Enejoh for their tremendous support throughout the period of this programme. My handsome, master Ajirioghene Faith Otovoh, thank you for your patience and understanding, mummy loves you very much. From the depth of my heart, I sincerely

appreciate the prayers, support and encouragement I received from my Aunties, Uncles, Cousin and well-wishers. If I were to mention everyone by name, I would run out of space.

To my darling husband, Mr Afolabi Owoloye, thank you for being a pillar of support and encouragement all through my study time. You are the best! Last, but not least, to my baby Jordan; thank you for your smile that always melts my heart.

## TABLE OF CONTENTS

	Page
Title Page	i
Certification	ii
Dedication	iii
Acknowledgements	iv
Table of Contents	vi
List of Figures	xi
List of Table	xvi
Abstract	xvii
<b>CHAPTER ONE</b>	
1.0 Introduction	1
<b>CHAPTER TWO</b>	
2.0 Literature Review	6
2.1 Insulin Signaling Pathway	6
2.1.1 Insulin Secretion	6
2.2 Diabetes Mellitus	9
2.3 Types of Diabetes Mellitus	10
2.3.1 Type 1 Diabetes	10
2.3.2 Type 2 Diabetes	11
2.4 Diabetes Oxidative Stress and Inflammation	15
2.5 Management of Diabetes Mellitus	18

2.6 Pharmacological Interventions	18
2.6.1 Insulin Therapies	19
2.6.2 Sulfonylureas	19
2.6.3 Incretins	20
2.6.3.1GLP-1 mediated insulin production	21
2.6.4 Biguanides	22
2.6.5 Thiazolidinediones	23
2.6.6 Alpha-Glucosidase Inhibitors	23
2.7 Medicinal Plants	23
2.8 Antidiabetic Potential of Medicinal Plants	24
2.9 <i>Chromolaena odorata</i> (L.)	25
2.9.1 Phytochemical Constituents of <i>Chromolaena odorata</i> (L.) Leaves	28
2.9.2 Biological Activities of <i>Chromolaena odorata</i> (L.)	29
2.10 Flavonoids	30
2.10.1Structure and Classes of Flavonoids	31
2.10.2Biosynthesis of Flavonoids	33
2.11 Roles of Flavonoids in Diseases	33
2.11.1Anti-oxidant Properties	33
2.11.2Antimicrobial Properties	34
2.11.3 Role in Cardiovascular Diseases	34
2.11.4 Anti-inflammatory Properties	35
2.11.5 Anti-diabetic Properties	35
2.12 Flavonoids and Diabetes	35
2.12.1 Role of Flavonoids in Streptozotocin-Induced Diabetes	37
2.13 Takeda G-protein receptor 5/ glucagon- like peptide-1 (TGR5/GLP-1) signaling	38

### **CHAPTER THREE**

3.0	Materials and methods	41
3.1	Plant material	41
3.1.1.	Preparation of Plant Extract and Flavonoid Isolation	41
3.2	Experimental Animals	41
3.2.1	Induction and Confirmation of Diabetes in Experimental Animals	41
3.3	Experimental Design	42
3.4	Gene Expression Studies	42
3.4.1	PCR Conditions	43
3.5	Blood Urea Nitrogen and Serum Creatine Estimation	44
3.6	NOAEL Experiments	44
3.6.1	Experimental Design	44
3.6.2	Liver Function Test	44
3.6.3	Kidney Function Test	44
3.7	Histological Examination	44
3.8	Statistical Analysis	45
3.9	Starting TGR5 Model for Molecular Docking Studies	45
3.10	2D Coordinates of Ligands and Docking Protocols	46
3.11	Biosystems Setup and Molecular Dynamics (MD) Simulation	46
3.12	Post-Simulation Trajectory Quality Assessment	47
3.13	Data Analysis	48

### **CHAPTER FOUR**

4.0	Results	49
4.1	CoF Reverses STZ-Induced Hyperglycemia	49
4.2	CoF Reverses Pancreatic Beta Cell Damage in STZ-Induced Hyperglycemia	49

4.3	STZ Treatment is Associated with Organ Histo-Structural Damages in the Pancreas; Reversible with CoF Treatment	49
4.4	CoF Restores STZ-Induced Loss of Kidney Function in Experimental Nephropathy	57
4.5	STZ Treatment is Associated with Up-Regulation of Antioxidant and Pro-Inflammatory Genes in the Kidney; Reversal by CoF	57
4.6	STZ Treatment is Associated with Organ Histo-Structural Damages in the Kidney; Reversible with CoF Treatment	58
4.7	CoF Restores Protein Glycosylation Enzymes in the Aorta to Normal Levels in STZ-Induced Rats	69
4.8	STZ Treatment is Associated with Up-Regulation of Antioxidant and Pro-Inflammatory Genes in the Aorta; Reversal by CoF	69
4.9	STZ Treatment is Associated with Organ Histo-Structural Damages in the Aorta; Reversible with CoF Treatment	69
4.10	No observed adverse effect level (NOAEL)	80
4.11	CoF Elicits Similar TGR5 Interaction as Known Agonist in Molecular Docking Studies	88
4.12	TGR5 in CoF Bound State Elicits Continuous Internal Water Pathway That Sinks in the (E)-Dry Motif	90
4.13	Ligand-Sensitive Toggle Switches in TGR5	92
4.14	Pancreatic Response to CoF and Metformin	95
4.15	CoF, but not Metformin, Modulates Circulating GLP-1 and GLP-2 in Intestinal Crypt	98
4.16	Action of CoF And Metformin on the Aorta of Experimental Animals	101
4.17	Action of CoF And Metformin on the Kidney of Experimental Animals	110

## **CHAPTER FIVE**

<b>5.0</b>	Discussion	117
------------	------------	-----

## **CHAPTER SIX**

<b>6.0</b>	Conclusion, Recommendation and Contributions to Knowledge	128
------------	---	-----

<b>6.1</b>	Conclusion	128
------------	------------	-----

<b>6.2</b>	Recommendation	128
------------	----------------	-----

<b>6.3</b>	Contributions to Knowledge	129
------------	----------------------------	-----

<b>REFERENCES</b>		130
-------------------	--	-----

## LIST OF FIGURES

Figure 2.1	Insulin signal transduction pathway	8
Figure 2.2.	Molecular mechanisms of the link between obesity and diabetes	14
Figure 2.3	<i>Chromolaena odorata</i> (L.) leaves collected from Akungba-Akoko	27
Figure 2.4	Structures of various flavonoid classes and subclasses	32
Figure 2.5:	TGR-5-stimulated GLP-1 production in improved glycemic control	40
Figure 4.1	Fasting blood glucose levels of treatment and control groups	51
Figure 4.2	Expression pattern of insulin gene in the pancreas of treatment and control groups	52
Figure 4.3	Expression pattern of pancreatic duodenal box - 1 (PDX-1) gene in the pancreas of treatment and control groups	53
Figure 4.4	Islet cell density of pancreas	54
Plate 4.5	Representative Hematoxylin and Eosin stained photomicrograph (x400 objective) sections of pancreas	55
Figure 4.6	Expression pattern of glucagon-like peptide - 1 (GLP-1) gene in the intestinal crypt of treatment and control groups	56
Figure 4.7	Kidney function tests: Bar graph representing mean and SEM values of Blood Urea Nitrogen and Serum Creatinine in control, STZ and STZ+CoF treatment groups	59
Plate 4.8	Haematoxylin and Eosin stained photomicrographs of kidney histomorphological presentations (x400) in Adult male Wistar rats across the various groups	60
Figure 4.9	Expression pattern of inflammatory gene, Tumor necrosis Factor-alpha (TNF- $\alpha$ ), in kidney of treatment and control groups	61
Figure 4.10	Expression pattern of inflammatory gene, Tumor Necrosis Factor Receptor (TNF-R), in kidney of treatment and control groups	62

Figure 4.11 Expression pattern of inflammatory gene, Interleukin -10 (IL-10), in kidney of treatment and control groups	63
Figure 4.12 Expression pattern of inflammatory gene, Monocyte Chemoattractant Protein -1 (MCP-1), in kidney of treatment and control groups	64
Figure 4.13 Expression pattern of antioxidant gene, Glutathione Peroxidase - 1 (GPx-1), in kidney of treatment and control groups	65
Figure 4.14 Expression pattern of antioxidant gene, Catalase (CAT), in kidney of treatment and control groups	66
Figure 4.15 Expression pattern of Occludin (OCC) in kidney of treatment and control groups	67
Figure 4.16 Expression pattern of Kidney Injury Molecule - 1 (KIM-1) in kidney of treatment and control groups	68
Figure 4.17 Mean Aorta Diameter (mm) in treatment and control groups	70
Figure 4.18 Expression pattern of protein glycosylation enzyme, O-GlcNAc transferase (OGT) gene in the aorta of treatment and control groups	71
Figure 4.19 Expression pattern of protein glycosylation enzyme, $\beta$ -N-Acetylglucosaminidase (OGA) gene in the aorta of treatment and control groups	72
Figure 4.20 Expression pattern of inflammatory gene, Interleukin 6 (IL-6), in the aorta of treatment and control groups	73
Figure 4.21 Expression pattern of inflammatory gene, Interleukin -1 beta (IL-1 $\beta$ ), in the aorta of treatment and control groups	74
Figure 4.22 Expression pattern of inflammatory gene, Tumor necrosis Factor-alpha (TNF- $\alpha$ ), in the aorta of treatment and control groups	75
Figure 4.23 Expression pattern of inflammatory gene, Monocyte Chemoattractant Protein -1 (MCP-1), in the aorta of treatment and control groups	76

Figure 4.24	Expression pattern of antioxidant gene, Catalase (CAT), in the aorta of treatment and control groups	77
Figure 4.25	Expression pattern of antioxidant gene, Glutathione Peroxidase - 1 (GPx-1), in the aorta of treatment and control groups	78
Plate 4.26	Photomicrographs showing panoramic views of aorta general histomorphological presentations (x100) in Adult male Wistar rats across the various groups	79
Figure 4.27	Graph of Mean Body Weight of control and treated groups for NOAEL Experiment	81
Figure 4.28	Graph of Urea Concentration in blood plasma of control and treated groups for NOAEL Experiment	82
Figure 4.29	Graph of alanine aminotransferase (ALT) levels in blood plasma of control and treated groups for NOAEL Experiment	83
Figure 4.30:	Graph of aspartate aminotransferase (AST) levels in blood plasma of control and treated groups for NOAEL Experiment	84
Plate 4.31:	Photomicrographs showing panoramic views of pancreas for NOAEL experiment (x400)	85
Plate 4.32:	Photomicrographs showing kidney sections for NOAEL experiment (x400)	86
Plate 4.33:	Photomicrographs showing liver sections for NOAEL experiment (x400)	87
Figure 4.34:	Binding Pose of ligand within TGR5 orthosteric site	89
Figure 4.35:	TGR5 evolves continuous internal water pathway in CoF and INT-777 bound states	91
Figure 4.36:	Dynamic network and free-energy surface plots	93
Figure 4.37:	Rotameric Switch candidates in the orthosteric site of TGR5	94
Figure 4.38:	Expression pattern of insulin gene in the pancreas of treatment and control groups	96

Figure 4.39: Expression pattern of pancreatic duodenal box-1 gene in the pancreas of treatment and control groups	97
Figure 4.40: Expression pattern of glucagon-like peptide-1 gene in the intestinal crypt of treatment and control groups	99
Figure 4.41: Expression pattern of glucagon-like peptide-2 gene in the intestinal crypt of treatment and control groups	100
Figure 4.42: Expression pattern of O-GlcNAc transferase gene in the aorta of treatment and control groups	102
Figure 4.43: Expression pattern of $\beta$ -N-Acetylglucosaminidase gene in the aorta of treatment and control groups	103
Figure 4.44: Expression pattern of glutathione peroxidase-1 in the aorta of treatment and control groups	104
Figure 4.45: Expression pattern of catalase gene in the aorta of treatment and control groups	105
Figure 4.46: Expression pattern of tumor necrosis factor-alpha gene in the aorta of treatment and control groups	106
Figure 4.47: Expression pattern of monocyte chemoattractant protein-1 gene in the aorta of treatment and control groups	107
Figure 4.48: Expression pattern of Interleukin-1 beta gene in the aorta of treatment and control groups	108
Figure 4.49: Expression pattern of Interleukin-6 gene in the aorta of treatment and control groups	109
Figure 4.50: Expression pattern of kidney injury molecule-1 gene in kidney of treatment and control groups	111
Figure 4.51: Expression pattern of glutathione peroxidase-1 gene in kidney of treatment and control groups	112

Figure 4.52: Expression pattern of tumor necrosis factor-alpha gene in kidney of treatment and control groups	113
Figure 4.53: Expression pattern of tumor necrosis factor receptor gene in kidney of treatment and control groups	114
Figure 4.54: Expression pattern of monocyte chemoattractant protein-1 gene in kidney of treatment and control groups	115
Figure 4.55: Expression pattern of Interleukin-10 gene in kidney of treatment and control groups.	116

**LIST OF TABLE**

Table 3.1 Primer sequences of genes studies

43

## ABSTRACT

Diabetes is a metabolic disorder, which when aggravated by associated complications can lead to premature death. Medicinal plants have played a key role in the management and treatment of diabetes. Here, plants previously reported to have anti-diabetic properties were screened using gene expression profiling technique. *Chromolaena odorata* displayed characteristics of a good glucagon-like peptide 1 (GLP-1) agonist. Molecular docking studies traced the insulin enhancing mechanism of *C. odorata* to its flavonoid-enriched fraction, acting via Takeda G-protein receptor 5 (TGR5) activation and GLP-1 release. Streptozotocin (STZ)-induced diabetes and its associated complications, were challenged by *Chromolaena odorata* flavonoids (CoF) to validate molecular docking studies.

Twenty-one Wistar rats were divided into control (n=7), STZ (n=7) (40 mg/kg body weight (b.w.)) and STZ+CoF (n=7) (CoF=30 mg/kg b.w.) groups. Blood glucose levels of the animals were monitored once weekly for forty-two days. At the end of the experiment, blood urea nitrogen (BUN) and serum creatinine (SC) levels were quantified using standard methods. Kidney and liver functions were assayed using standard kits. Gene expression levels were also evaluated using reverse-transcription and polymerase chain reaction protocols. Histological assessment was performed using haematoxylin and eosin staining protocols. No observed adverse effect level (NOAEL) experiments were also carried out.

The results showed that CoF up-regulated the expression of insulin and pancreatic duodenal homeobox-1 genes in the pancreas, and GLP-1 in the intestine. In the kidney, BUN/SC levels were restored to pre-STZ treatment states following CoF treatment. Inflammatory and kidney injury molecule -1 genes were equally significantly down-regulated ( $p < 0.05$ ) in STZ-CoF treated group in comparison with STZ-only group. In the aorta, the significant increase of inflammatory genes as a result of STZ treatment, were down-regulated by CoF intervention. CoF also significantly increased antioxidant genes that were down-regulated in the STZ-only group. Histo-structural alterations associated with STZ treatment were completely reversed in STZ-CoF group in the pancreas, kidney and aorta. NOAEL experiments revealed that CoF is relatively safe up to doses of 100 mg/kg b.w. Molecular dynamics simulation confirmed TGR5 as the putative target, where it evolved active state conformation from a starting intermediate state conformation when bound to CoF. Further studies revealed that the performance of CoF was highly comparable with metformin (an anti-diabetic drug).

The outcome of this study showed that CoF reversed hyperglycemia and its associated comorbidities, as well as modulated the expression of GLP-1 and its release via TGR5. This finding may underscore its anti-diabetic potency.

**Keywords:** *Chromolaena odorata*, flavonoid, TGR5, GLP-1, molecular docking, gene expression

## CHAPTER ONE

### 1.0 INTRODUCTION

Diabetes is a metabolic disorder characterized by hyperglycaemia. Persistently high amounts of glucose in the blood stream leads to life-threatening micro- and macrovascular complications, responsible for high risk of morbidity and mortality of affected persons (Baena-Diez *et al.*, 2016).

Type 1 diabetes (T1D) and Type-2 diabetes (T2D) are the most common forms of diabetes. Pathophysiologically, lack of insulin secretion due to autoimmune-mediated dysfunctional pancreatic  $\beta$ -cell loss (Atkinson, 2012) and dysfunctional metabolism-induced insulin resistance (Scheen, 2003) explain T1D and T2D, respectively. T1D is managed with insulinotropic drugs (Atkinson, 2012) while T2D relies chiefly on the improved metabolic status of the patient (Scheen, 2003, Scheen and Paquot, 2015). Nephropathy, retinopathy, cardiomyopathy and peripheral neuropathy are all recognized as major complications associated with 50% of diabetic patients, mostly due to poor glycemic control or to improper management of the pathology (Ghaed *et al.*, 2012; Baharvand-Ahmadi *et al.*, 2016).

The prevalence of diabetes in adults, according to International Diabetes Federation, was estimated to be 8.4% in 2017 with a projected rise to 9.9% in 2045 (Cho *et al.*, 2018); this means that one in every ten (10) adults will be diagnosed with diabetes by 2030 (Whiting *et al.*, 2011). These predictions, indicate a growing burden of diabetes, particularly in developing countries.

Africa and Asia are said to experience diabetes at an estimated two- to three-times more than in other regions (Eidi *et al.*, 2007). The global prevalence of diabetes and diabetes-related deaths occurs in low- and medium-income countries (Mendenhall *et al.*, 2014), where access to quality health care is rare and the cost of drugs are high. It is in light of this

that cheaper alternative medicines are sought to reduce the mortality rate, cut down current epidemiology as well as combat future projections.

The use of plants and plant products for medicinal purposes has been an age-long practice in traditional communities which is regaining global relevance. The presence of secondary metabolites found in medicinal plants are said to be the key drivers of their pharmacological actions (Hussein and El-Anssary, 2019). It has been estimated that 80% of the African population use herbal regimen for treatment and control of diseases (Mahomoodally, 2013); this is due to the belief that these products are of natural origin, and so may be quite safe and potent. Most plants and plant products are probably safe when normal doses are taken/administered; however, some of them are known to be toxic at high doses, while many others can cause undesirable adverse side effects (Frantisek, 1991). Plant-derived compounds, mainly their secondary metabolites, have been used for the treatment of diabetes, as they have a wide range of anti-diabetic effects (Oh, 2015, Ebrahimi *et al.*, 2017).

Indigenous solutions to diabetes may depend on tapping the vast heterogeneous phytochemical deposit in plants, microbes and natural bio-resources. An increasing number of reports now establish that some secondary metabolites of plant origin possess insulintropic activities and may represent a new therapeutic strategy for managing diabetes (Lokman *et al.*, 2013, Shen *et al.*, 2012, Oh, 2015, Ebrahimi *et al.*, 2017). Recently, the World Health Organization recommended the use of medicinal plants for the management of diabetes and further encouraged the expansion of the frontiers of scientific evaluation of the hypoglycaemic properties of diverse plant species. Consequently, current estimates show that over 70% of the global population applies resources derived from traditional medicine for the management and alleviation of diabetes and its complications (Haq, 2004; Remuzzi *et al.*, 2007; Abdel-Azim *et al.*, 2011). Studies have shown that bioactive-constituents of natural resources, such as medicinal plants, have anti-diabetic effects

(Bhattacharya and Chirangeebee, 2006), which have also been confirmed in animal and *in vitro* studies. The most biologically active secondary metabolites with anti-diabetic activity include alkaloids, flavonoids, terpenes and phenolics (Bahmani *et al.*, 2014).

Flavonoids, a phenomenal group of plant secondary metabolites have been credited with diverse key functions in plant growth and development, many of which are critical for survival. At the molecular level, they interact with multiple biological targets involved in different physiological activities (Andersen and Markham, 2005). They possess anticancer, anti-diabetic, antioxidant properties. More than 5000 naturally occurring flavonoids have been reported in various plants; these flavonoids show many beneficial effects with advantages over some conventional drugs (Hossain *et al.*, 2016). Several studies have shown the potential health benefits of natural flavonoids against obesity and diabetes (Zeka *et al.*, 2017, Hossain *et al.*, 2016). They may also influence the synthesis and release of insulin from  $\beta$ -cells (EILatif *et al.*, 2014).

*Chromoleana odorata* is one plant that recently gained research attention as a result of its ability to reverse hyperglycemia (Onkaramurthy *et al.*, 2013; Adedapo *et al.*, 2016a). It is said to have a wide spectrum of activities (Vijayaraghavan *et al.*, 2017). Reports of the use of *C. odorata* as an effective therapy against diarrhea, malarial, toothache, diabetes, skin diseases, dysentery, and colitis are also available (Odugbemi, and Akinsulire, 2006; Akinmoladun *et al.*, 2007).

Takeda-G-protein-receptor-5 (TGR5), a member of G protein coupled receptor (GPCR) family plays an important role in energy metabolism. It responds to bile acids (Maruyama *et al.*, 2002) stimulating glucagon-like peptide-1 (GLP-1) release *via* cAMP production at the proximal ligated ileum or its cell lines (Brighton *et al.*, 2015) and insulin secretion in the pancreatic beta-cells *via* an adenylyl cyclase/cAMP/ PKA-dependent pathway (Maczewsky *et al.*, 2019). The central roles of GLP-1 and insulin in carbohydrate

metabolism (Malik and Roohi, 2018) have given TGR5 agonists key consideration in the management of hyperglycemia and its associated diseases including type 2 diabetes, obesity, atherosclerosis, and fatty liver disease (Pellicciari *et al.*, 2009). Some of the agonists previously characterized include: pentacyclic triterpenoid (betulinic acid) (Lo *et al.*, 2016), 6 $\alpha$ -ethyl-23(S)-methyl-cholic acid (6-EMCA, INT-777) (Guo *et al.*, 2016, Li *et al.*, 2018), and 3-aryl-4-isoxazolecarboxamides (Duboc *et al.*, 2014). Based on the previous study which strongly suggests that CoF-induced GLP-1 gene expression and release in experimental rats (Omotuyi *et al.*, 2018) may also proceed via TGR5 activation but without any evidence for biophysical interaction, this research has the following objectives:

- \* Isolate the total flavonoid content of *C. odorata* (CoF).
- \* Monitor GLP-1 expression of the intestinal crypt, in response to flavonoid treatment.
- \* Monitor Insulin/PDX-1 expressions in the pancreas of diabetic Wistar rats treated with flavonoids isolated from *C. odorata*.
- \* Assess the gene expression levels of inflammatory and antioxidant genes associated with diabetes in the aorta and kidney as well as investigate the insulinotropic mechanisms of *C. odorata* in STZ-treated Wistar rats.
- \* Evaluate the histopathological changes in the Pancreas, Kidney, and aorta associated with flavonoid treatment in diabetic Wistar rats.
- \* Compare the performance of CoF with that of Metformin using gene expression techniques.

- \* Evaluate the No-observed adverse effect levels of flavonoids isolated from *C. odorata* using hematological (liver function and kidney function) tests and histological analysis.
- \* Investigate TGR5 interaction and activation by CoF using molecular docking and molecular dynamics simulation techniques.

## CHAPTER TWO

### 2.0 LITERATURE REVIEW

#### 2.1 OVERVIEW OF INSULIN SIGNALING PATHWAY

##### 2.1.1 INSULIN SECRETION

Insulin plays an important role in regulating blood glucose. Triggered by high amounts of glucose, this hormone is secreted into blood circulation by the pancreatic  $\beta$ -cells (PBCs). Glucose enters PBCs via the glucose transporter type 2 (GLUT-2), and once inside the cell, gets phosphorylated by glucokinase, the first step of glycolysis. Furthermore, glycolytic and oxidative metabolism of glucose eventually leads to an increase in the cytosolic ATP/ADP ratio, and binding to ATP-dependent-K<sup>+</sup>-channels, determines the closure of these channels, which in turn causes cells depolarization. This event provokes the activation of voltage-sensitive calcium channels, triggering a calcium influx, followed by insulin secretion (Kennedy *et al.*, 1999). Insulin facilitates the uptake of glucose, fatty acids and amino acids into the liver, adipose tissue and muscles, promoting the storage of these nutrients in the form of glycogen, lipids and protein, respectively. Failure to take up and store nutrients results in diabetes and its complications.

Insulin secretion is a complex mechanism with multiple points of regulation (Rorsman *et al.*, 2000). After insulin enters the bloodstream, it binds to a membrane-spanning glycoprotein receptor. The glycoprotein is embedded in the cellular membrane and has an extracellular receptor domain, made of two  $\alpha$ -subunits, and an intracellular catalytic domain, made up of two  $\beta$ -subunits. The  $\alpha$ -subunits acts as insulin receptors and the insulin molecule acts as a ligand, together forming a receptor-ligand complex. Binding of insulin to the  $\alpha$ -subunit results in conformational changes in the membrane-bound glycoprotein, which activates tyrosine kinase domains on each  $\beta$ -subunit. The tyrosine kinase activity causes an autophosphorylation of several tyrosine residues in the  $\beta$ -subunit. The

phosphorylation of 3 residues of tyrosine is necessary for the amplification of the kinase activity (Saini, 2010).

Tyrosine kinase, once activated on the insulin receptor, triggers the activation of the docking proteins, also called Insulin receptor substrates (IRS 1-4) that are important in the signaling pathway of Phosphatidylinositol-3-Kinase (PI3K). Activation of PI3K leads to crucial metabolic functions such as synthesis of lipids, proteins and glycogen. Most importantly, the PI3K pathway is responsible for the distribution of glucose for important cell functions. The activation of PI3K pathway leads to the activation of protein kinase B (PKB) that induces the impact of insulin on the liver. Hence, PKB possesses a crucial role in the linkage of glucose transporter (GLUT4) to the insulin signaling pathway (Fig 2.1) to the cell membrane and promotes the transportation of glucose into the intracellular medium (Saini, 2010).

The loss of glucose-stimulated insulin secretion is accompanied by marked alterations in beta cell phenotype and changes in gene and protein expressions (Laybutt *et al.*, 2002). As beta-cell function deteriorates over time, this creates a vicious cycle by which metabolic abnormalities impair insulin secretion, which further aggravates metabolic perturbations (Cnop *et al.*, 2007, Poitout *et al.*, 2010). As expected, the diabetic environment is enriched with high levels of glucose, advanced glycation end-products (AGEs), proinflammatory cytokines, free fatty acids, and other lipid intermediates (Robertson *et al.*, 2007; Robertson, 2009). These factors are toxic for beta-cells and might activate several stress response pathways, including oxidative and endoplasmic reticulum (ER) stress, mitochondrial dysfunction, apoptosis, and necrosis (Eizirik *et al.*, 2008).

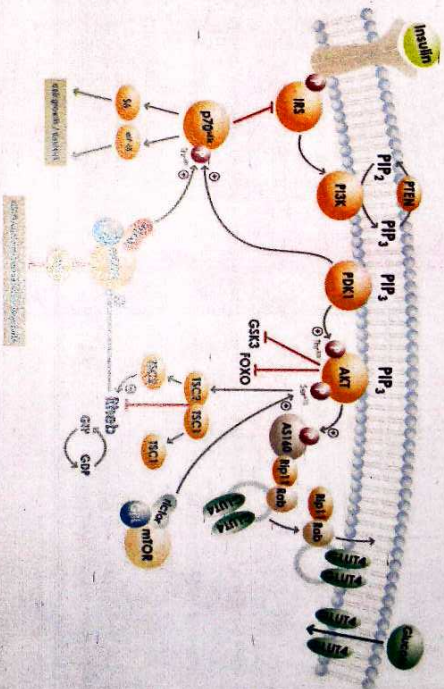


Figure 2.1: Insulin signal transduction pathway (May, 2008)

## 2.2 DIABETES MELLITUS

Diabetes mellitus (DM), commonly referred to as diabetes, is a metabolic disorder characterized by hyperglycemia as a result of insufficiency of secretion or action of endogenous insulin by the  $\beta$  cells (Maritim *et al.*, 2003), due to the abnormalities in carbohydrate, fat, and protein metabolisms, leading to severe complications (Buchanan, 2003). Persistent hyperglycemia is associated with significant morbidity and mortality due to microvascular (retinopathy, neuropathy, and nephropathy) and macrovascular (atherosclerosis) complications (Fowler, 2008).

Diabetes is considered one of the major problems and greatest challenges facing the health care system (Williams, 2009). The prevalence of diabetes in adults, according to International Diabetes Federation, was estimated to be 8.4% in 2017 with a projected rise to 9.9% in 2045 (Cho *et al.*, 2018) where majority (80%) live in low- and middle- income countries (Mendenhall *et al.*, 2014). This implies that an estimated 425 million people currently have diabetes worldwide; 5.5 million of this total population are Africans. These predictions, based on a larger number of studies than previous estimates, indicate a growing burden of diabetes, particularly in developing countries (Shaw *et al.*, 2010).

Nephropathy, retinopathy, cardiomyopathy and peripheral neuropathy are all recognized as major complications associated with 50% of diabetes mellitus (DM) patients, mostly due to a poor glycemic control or to an improper management of the pathology (Ghaed *et al.*, 2012; Baharvand-Ahmadi *et al.*, 2016). The exponential increase in the prevalence of diabetes mellitus has been linked to obesity and increasing sedentary behaviours, urbanization, modernization, genetics and family history as well as nutritional imbalance associated with consumption of high energy, fat and cholesterol rich diets among others (Ramachandran *et al.*, 2012).

## 2.3 TYPES OF DIABETES MELLITUS

There are two major types of diabetes, these include: Type 1 diabetes and Type 2 diabetes. They are both associated with loss of pancreatic beta cells (Buchanan, 2003; Stumvoll *et al.*, 2005; Eizirik *et al.*, 2009). Thus, halting the loss of insulin-producing  $\beta$  cells is a key tactic for contending with both types of the disease.

### 2.3.1 TYPE 1 DIABETES

Type 1 Diabetes (T1D), also called insulin dependent diabetes mellitus (IDDM), is caused by lack of insulin secretion by pancreatic beta cells. It is an autoimmune condition (Wilkinson *et al.*, 2011) characterized by the expansion of pathogenic T effector cells which cause the irreparable destruction of insulin producing  $\beta$  cells and thus limits insulin production and glucose homeostasis. Several features characterize T1D mellitus as an autoimmune disease. These include presence of immuno-competent and accessory cells in infiltrated pancreatic islets; association of susceptibility to disease with the class II (immune response) genes of the major histocompatibility complex (MHC; human leucocyte antigens HLA); presence of islet cell specific autoantibodies alterations of T cell mediated immunoregulation, in particular in CD4+ T cell compartment; the involvement of monokines and T-helper 1 (TH1) cells producing interleukins in the disease process; response to immunotherapy and; frequent occurrence of other organ specific auto-immune diseases in affected individuals or in their family members (Hussain, 2007). This may be due to genetic predisposition or a result of faulty beta cells in the pancreas that normally produce insulin. A number of medical risks are associated with T1D many of which stem from damage to the tiny blood vessels in the eyes (diabetic retinopathy), nerves (diabetic neuropathy) and kidneys (diabetic nephropathy), heart disease and stroke. Treatment for T1D involves taking insulin.

T1D occurring in genetically susceptible individuals may be precipitated by environmental factors. In a susceptible individual, the immune system is triggered to develop an autoimmune response against altered pancreatic beta cell antigens, or molecules in beta cells that resemble a viral protein. Approximately 85% of T1D patients have circulating islet cell antibodies, and the majority of patients also have detectable anti-insulin antibodies. Most islet cell antibodies are directed against glutamic acid decarboxylase (GAD) within pancreatic beta cells (Van Belle *et al.*, 2011).

Several scenarios for development of T1D have been put forth. In one model, an environmental trigger induces islet autoimmunity and beta-cell death in genetically susceptible individuals, leading to a sequence of prediabetic stages and eventually clinical onset of T1D (Eisenbarth, 2007). Other scenarios have been proposed to account for wide variations in the time between initiation of autoimmunity and clinical onset of T1D. For example, interactions between genetic factors and environmental challenges such as viral infections might contribute to fluctuations in beta-cell mass observed before onset of T1D (Chatenoud and Bluestone, 2007). Alternatively, T1D could be a relapsing-remitting disease, dependent on cyclical disruption and restoration of the balance between effector and regulatory T cells (Gomez-Tourino *et al.*, 2016).

### **2.3.2 TYPE 2 DIABETES**

Type 2 diabetes (T2D), also called non-insulin dependent diabetes mellitus (NIDDM), is caused by decreased sensitivity of target tissues (liver, muscle and adipose tissues) to insulin. This is the most prevalent form of diabetes accounting for 90% of cases in adults (Gonzalez, 2009), resulting from a combination of genetic susceptibility (Grarup *et al.*, 2014), environment, behaviour (calorie intake and physical activity), and as yet unexplained risk factors. Unlike patients with T1D, Individuals with T2D have detectable levels of circulating insulin. Development of T2D is characterized by two fundamental defects;

insulin resistance and impaired insulin secretion, which disrupt the delicate balance by which insulin target tissues communicate with the beta cells and vice versa. Insulin resistance and hyperinsulinemia eventually lead to impaired glucose tolerance. This insulin resistance or lack of sensitivity to insulin, happens primarily in fat, liver and muscle cells. Reduced sensitivity is caused by obesity (especially excess visceral adiposity), excess glucocorticoids (Cushing's syndrome or steroid therapy), excess growth hormone (acromegaly), pregnancy (gestational diabetes), polycystic ovary disease, lipodystrophy (acquired or genetic, associated with lipid accumulation in liver), auto antibodies to the insulin receptor, mutations of insulin receptor, mutations of the peroxisome proliferators' activator receptor  $\gamma$  (PPAR  $\gamma$ ), mutations that cause genetic obesity (e.g., melanocortin receptor mutations), hemochromatosis (a hereditary disease that causes tissue iron accumulation) (Guyton and Hall, 2006). Obesity, sedentary lifestyle, stress, as well as aging are known risk factors for T2D (Kaku, 2010).

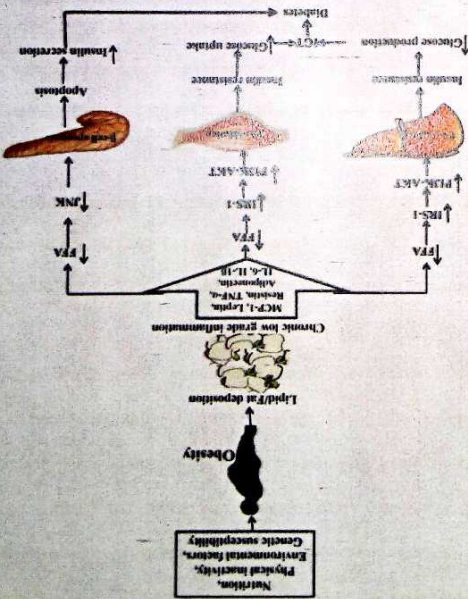
Older adults are at high risk for the development of T2D due to the combined effects of genetic, lifestyle, and aging factors. These factors contribute to hyperglycemia through effects on both  $\beta$ -cell insulin secretory capacity and on tissue sensitivity to insulin. The occurrence of T2D in an older person is complicated by the comorbidities and functional impairments associated with aging (Lee and Halter, 2017).

Hyperglycemia develops in type 2 diabetics when there is an imbalance of glucose production (i.e., hepatic glucose production during fasting) and glucose intake (i.e., food ingestion) as opposed to insulin-stimulated glucose uptake in target tissues, mainly skeletal muscle (Bajaj and DeFronzo, 2003).

Adipocytes are implicated in the link between obesity and diabetes (Figure 2.2). Macrophage infiltration is especially notable in the adipose tissue of obese individuals (Weisberg *et al.*, 2003; Xu *et al.*, 2003). The adipose tissue-derived monocyte-chemoattractant protein-1 (MCP-1), a  $\beta$ -chemokine, exhibiting chemotactic properties in

inflammatory cells, is a key factor for inducing macrophage infiltration into adipose tissue. Levels of MCP-1, released by adipocytes, was found to be higher in obese mice compared to non-obese mice, and the levels are distinctly increased when adipocytes are co-cultured with macrophages (Fain *et al.*, 2004; Bruun *et al.*, 2005; Yu *et al.*, 2006). MCP-1 triggers macrophage infiltration into adipose tissue and the subsequent release of inflammatory mediator tumor necrosis factor-alpha (TNF- $\alpha$ ) (Yu *et al.*, 2006), which hampers insulin signaling and stimulates fatty acid lipolysis in adipocytes. TNF- $\alpha$  and other pro-inflammatory cytokines including interleukin-6 (IL-6), interleukin-1  $\beta$  (IL-1 $\beta$ ), and C-reactive protein are involved in low-grade chronic inflammation and insulin resistance (Fain *et al.*, 2004; Maury *et al.*, 2007). The inflammatory cytokines inhibit triglyceride synthesis by downregulating peroxisome proliferator-associated receptor  $\gamma$  and its target gene, plasma lipoprotein lipase, as well as the glucose transporter, glucose transport type 4 (Fain *et al.*, 2004; Maury *et al.*, 2007). TNF- $\alpha$ , on the other hand, simultaneously downregulates the lipid droplet-associated protein perilipin, and enhances the cAMP pool, which increase free fatty acid (FFA) release (Guilherme *et al.*, 2008). Increased FFA reduces the expression of IRS-1, impairs the activation of PI3K-AKT (Khorami *et al.*, 2015) signaling in the liver and skeletal muscles, and increases the expression of c-Jun N-terminal kinase (JNK) signaling in the pancreas (Cheon *et al.*, 2010). Ultimately, the reduced expression of PI3K-AKT causes insulin resistance in the liver and skeletal muscles, and the increased expression of JNK aggravates apoptosis in the pancreas. Insulin resistance causes an increase in glucose production and a decrease in glucose uptake, leading to hyper-insulinemia. increased apoptosis of pancreatic beta cells results in a decrease of insulin secretion. Consequently, insulin resistance and beta cell apoptosis lead to diabetes (Guilherme *et al.*, 2008).

Figure 2. Molecular mechanisms of the link between obesity and diabetes (Hossain *et al.*, 2016)



## 2.4 DIABETES OXIDATIVE STRESS AND INFLAMMATION

Oxidative stress occurs when the production of free radicals overwhelms the detoxification capability of internal cellular antioxidant system bringing about biological damage (Halliwell, 2011). Involvement of oxidative stress in the pathogenesis of diabetes is suggested not only by the generation of free radicals, especially reactive oxygen species (ROS) but also because of non-enzymatic protein glycosylation, auto-oxidation of glucose, impaired glutathione metabolism, modification in antioxidant enzymes and lipid peroxides formation (Moghaddam *et al.*, 2015). On the other hand, oxidative stress induces overproduction of ROS, which activates several inflammatory signaling cascades that will contribute to inflammation (Samarghandian *et al.*, 2015).

Elevated levels of reactive oxygen species (ROS) in diabetes may be due to decrease in destruction and/or increase in the production by catalase (CAT-enzymatic/non-enzymatic), superoxide dismutase (SOD) and glutathione peroxidase (GPx-1). The variation in the levels of these enzymes makes the tissues susceptible to oxidative stress leading to the development of diabetic complications (Lipinski, 2001). Owing to their ability to directly oxidize and damage DNA, proteins, and lipids, free radicals are believed to play a key role in the onset and progression of diabetic complications (Rösen *et al.*, 2001). Where appropriate condensation by antioxidant defense networks are absent, increased oxidative stress leads to activation of stress-sensitive intracellular signaling pathways and formation of gene products that harm cells and contribute to diabetic complications.

In diabetes, ROS is thought to be generated through increased polyol pathway (Chung *et al.*, 2003), increased formation of advanced-glycation end products (AGEs) (Baynes and Thorpe, 1999) and activation of protein kinase C (PKC) (Inoguchi *et al.*, 2003). Oxidative stress can also accelerate AGE formation while AGE formation can also amplify the production of more ROS resulting in a vicious cycle of AGE formation and oxidative stress

(Ayepola *et al.*, 2014). AGEs mediate some of their effect via interaction with some receptors that bind to these chemical moieties. Among these receptors, Receptor for Advanced Glycation End products (RAGE) is the most extensively studied (Ramasamy *et al.*, 2005). Evidence from several studies suggest that AGEs are involved in a cycle of inflammation, generation of ROS and increased production of AGEs. Ligand RAGE interaction results in activation of pathways such as p21ras, erk1/2 (p44/p42), MAP kinases, p38 and SAPK/JNK MAP kinases (Yan *et al.*, 1994; Lander *et al.*, 1997; Goldin *et al.*, 2006). A consequence of the activation of these pathways is the translocation of Nuclear Factor Kappa B (NF-KB) to the nucleus, which in turn activates and increases the transcription of other proteins such as, vascular endothelial growth factor (VEGF), monocyte chemoattractant protein-1 (MCP-1), vascular cell adhesion molecule-1 (VCAM-1) and intracellular adhesion molecule-1 (ICAM-1) and pro-inflammatory cytokines such as interleukin (IL)-1 $\beta$ , IL-6, IL-18 and tumour necrosis factor (TNF)- $\alpha$  (Schiekofer *et al.*, 2003).

Both type I and type II diabetes are powerful and independent risk factors for coronary artery disease, stroke, and peripheral arterial disease (Schwartz *et al.*, 1992, American Diabetes Association, 1993, Orchard *et al.*, 2006). Diabetics are said to have a 2- to 4-fold higher risk for cardiovascular events (Ding and Triggle, 2005) and nearly 80% of diabetes-associated deaths are caused by cardiovascular disease (CVD) (Winer and Sowers, 2004). Atherosclerosis, (excessive accumulation of lipids, cholesterol, inflammatory cells, and connective tissue in the vessel wall) accounts for more than 80% of the CVD-associated death and disability (Epstein, and Ross, 1999, Libby *et al.*, 2011). Formation of atherosclerotic plaques can result in occlusion of the vessel lumen and a rapid cessation in blood flow to the target tissue (Funk *et al.*, 2012). Hyperglycemia, increased free fatty acids, and insulin resistance induces a large number of alterations at the cellular level that

contribute to vascular dysfunction and accelerate the atherosclerotic process. These include increased oxidative stress, decreased bioavailability of NO, disturbances of intracellular signal transduction and increased production of several prothrombotic factors (Funk *et al.*, 2012; Creager *et al.*, 2003).

It has been suggested that both conduit and resistance arteries such as aorta are dysfunctional in diabetes and impairment of endothelial function underlies both micro and macrovascular complications of diabetes (Sena *et al.*, 2013; Fowler, 2008). Changes in vascular responsiveness to vasoconstrictors and vasodilators are mainly responsible for development of some vascular complications of diabetics (Nasri *et al.*, 2011), most of which are due to increased serum glucose and augmented generation of reactive oxygen species that lead to endothelial dysfunction (Naito *et al.*, 2011). An interplay between high ROS generation and increased formation of advanced-glycation end products (AGEs) exists (Baynes and Thorpe, 1999), however, the underlying mechanisms between diabetes and atherosclerosis still remain unclear. Hence, it was suggested AGEs interact with receptor for advanced glycation end products (RAGE) and the oxidative stress results in the increased production of free-radicals (ROS). Oxidative stress can accelerate AGE formation while AGE formation in turn, can also amplify the production of more ROS resulting in a vicious cycle of AGE formation and oxidative stress (Ayepola *et al.*, 2014). AGEs can promote the atherosclerotic process by enhancing the oxidation of low-density lipoprotein (LDL) trapping LDL in the subendothelium and decreasing the recognition of AGE-modified LDL by LDL receptor; the process mediated by RAGE (Bucala *et al.*, 1994). AGE's are also involved in a vicious cycle of inflammation, generation of ROS and increased production of AGE's with the activation of pathways such as p21ras, erk1/2 (p44/p42), MAP kinases, p38 and SAPK/JNK MAP kinases (Goldin *et al.*, 2006), consequently activating Nuclear Factor Kappa B (NF-KB). Translocation of NF-KB to the nucleus increases the transcription of proteins such as, MCP-1, and pro-inflammatory cytokines such as interleukin (IL)-1 $\beta$ ,

IL-6, 1L-18 and TNF- $\alpha$  which are centrally involved in the endothelial recruitment of neutrophil and subsequent development or progression of atherosclerotic plaque (Goldin *et al.*, 2006, Schiekofer *et al.*, 2003).

## 2.5 MANAGEMENT OF DIABETES MELLITUS

The main goal of diabetes management is to maintain the blood glucose levels and blood pressure in order to prevent or delay microvascular and macrovascular complications (Kao *et al.*, 2000). Till date, there is no known cure for the disease; however, treatment modalities including lifestyle modifications, treatment of obesity, oral hypoglycemic agents and insulin sensitizers have been used to manage the disease (Olokoba *et al.*, 2012). Other goals of diabetes management are to prevent or treat the many complications that can result from the disease itself and from its treatment.

## 2.6 PHARMACOLOGICAL INTERVENTIONS

People with T1D are solely dependent on insulin injections given alone, or in combination with oral hypoglycemic agents. The general consensus on treatment of T2D is that lifestyle management is at the forefront of therapy options. In addition to exercise, weight control, and medical nutrition therapy, oral glucose-lowering drugs and injections of insulin are the conventional therapies. Since the most important pathological process during the development of diabetes involves three key organs, i.e., pancreatic islets, liver, and skeletal muscle (Lin and Sun, 2010), almost all anti-diabetic therapies are aimed at these organs. Pharmacological treatment is indicated when fasting glucose level exceeds 140 mg/dL, and post prandial glucose level exceeds 160 mg/dL.

Current drugs used in diabetes management can be categorized into three groups.

- Drugs used to increase endogenous insulin availability (Insulinotropic agents e.g insulin analogues, sulfonylureas, incretins).

- Drugs that enhance the sensitivity of insulin. These include the thiazolidinediones, which are agonists of the peroxisome proliferator- activated receptor gamma (PPAR $\gamma$ ) and the biguanide metformin. Insulin sensitizers address the core problem in T2D insulin resistance.
- Drugs that reduce the digestion of polysaccharides and their bioavailability which comprise the  $\alpha$ - glucosidase inhibitors such as acarbose (Chehade and Mooradian, 2000; Sheehan, 2003).

### 2.6.1 INSULIN THERAPIES

Insulin, a peptide hormone secreted by the pancreatic beta cells, is essential for glucose homeostasis. Patients who suffer from T1D are solely dependent on exogenous insulin therapies to maintain their blood glucose levels. The discovery of insulin as a therapeutic agent in 1922 marked a major breakthrough in medicine and therapy in patients with diabetes (Quianson and Cheikh, 2012) where the goal is to achieve glycemic status as near to normal as possible. Insulin therapy helps regulate glucose metabolism and is the most effective method of reducing hyperglycemia.

Insulin is usually administered to diabetic patients through subcutaneous injection. This mode of therapy has certain inherent disadvantages such as local pain, itching and insulin lipodystrophy around the injection site. Hence, pharmaceutical scientists have been trying to design an oral delivery system for insulin. Many challenges are associated with the oral delivery of insulin, relating to the physical and chemical stability of the hormone, and its absorption and metabolism in the human body (Gowthamarajan and Kulkarni, 2003).

### 2.6.2 SULFONYLUREAS

Sulfonylureas were the first widely used oral hypoglycemic medications and are the most widely used drugs for the treatment of T2D. They are insulin secretagogues, triggering insulin release by direct action on the K<sub>ATP</sub> channel of the pancreatic beta cells (Rendell,

### 2.6.3.1 GLP-1 - MEDIATED INSULIN PRODUCTION

In recent times, incretin-based therapies have shown promise and are widely used as treatment strategies for diabetes (Brubaker, 2007; Lovshin and Drucker, 2009). Studies have demonstrated that the G-protein coupled receptor, TGR5 (also known as GPR131, M-BAR or GPBAR1) signaling improves glucose homeostasis by inducing incretin secretion such as GLP-1 (Katsuma *et al.*, 2005; Thomas *et al.*, 2009). Activation of transmembrane bile acid receptor TGR5 stimulates insulin secretion in pancreatic cells (Kumar *et al.*, 2012), via GLP-1 activation. GLP-1 is a gut peptide hormone derived from the precursor, proglucagon, which is synthesized in the enteroendocrine L-cells of the intestinal epithelium (Baggio and Drucker, 2007; Nauck, 2009). GLP-1 has been shown to be a potent anti-hyperglycemic hormone, inducing glucose-dependent stimulation of insulin secretion while suppressing glucagon secretion (Holst, 2007). In addition to its insulinotropic effects, it inhibits gastric emptying, decreases food intake (Tang-Christensen *et al.*, 1998), inhibits glucagon secretion (Chelikani *et al.*, 2005), and slows the rate of endogenous glucose production (Prigeon *et al.*, 2003), all of which help to lower blood glucose in T2DM. GLP-1 has been shown to protect  $\beta$ -cells from apoptosis (Thomas *et al.*, 2008) as well as stimulate  $\beta$ -cell proliferation by up-regulation of the  $\beta$ -cell transcription factor pancreatic duodenal homeobox-1 protein (PDX-1) (Perfetti *et al.*, 2000), known to augment insulin gene transcription and up-regulate glucokinase and glucose transporter 2 (GLUT2) (Wang *et al.*, 2011). Continuous GLP-1 treatment in T2D is believed to normalize blood glucose, improve  $\beta$ -cell function, and restore first-phase insulin secretion and "glucose competence" to  $\beta$  cells (Zander *et al.*, 2002); hence, It is anticipated that therapies directly targeting intestinal L cells to stimulate GLP-1 secretion will have certain advantages (Zheng *et al.*, 2015).

Pancreas duodenum homeobox-1 (PDX-1) is a transcription factor that regulates the growth and differentiation of the pancreas, as well as the homeostatic mechanisms involved in

maintaining  $\beta$ -cell mass. In the absence of PDX1,  $\beta$ -cell death occurs by apoptosis, autophagy, and programmed necrosis (Kitamura, 2013). Activation of the GLP-1 receptor on the pancreas, triggers intracellular ATP accumulation, and favours  $\beta$ -cells survival through the improved expression of PDX-1 gene (Zheng *et al.*, 2016), and the binding of this factor to the insulin promoter, restores glucose homeostasis (Perfetti *et al.*, 2000).

#### 2.6.4 BIGUANIDES

These reduce hepatic glucose output and increase uptake of glucose by the periphery, including skeletal muscle. Metformin, an example of this class of drug, is approved by the U.S. Food and Drug Administration as a prescription medication to treat diabetes. This medication is used to decrease hepatic (liver) glucose production, to decrease gastrointestinal glucose absorption and to increase target cell insulin sensitivity. Metformin is mainly used in the treatment of T2D, especially in overweight people. In addition to suppressing hepatic glucose production, metformin increases insulin sensitivity, enhances peripheral glucose uptake (by phosphorylating GLUT-4 enhancer factor), increases fatty acid oxidation and decreases absorption of glucose from the gastrointestinal tract. Increased peripheral utilization of glucose may be due to improved insulin binding to insulin receptors (Collier *et al.*, 2006).

Metformin, a biguanide derivate, is mainly used as the first-line oral drug to treat patients with type T2D (Nathan *et al.*, 2009). Metformin works by decreasing intestinal glucose absorption, improving peripheral glucose uptake, lowering fasting plasma insulin levels and increasing insulin sensitivity, which result in a reduction of blood glucose concentrations without causing overt hypoglycemia (Grzybowska *et al.*, 2011).

### **2.6.5 THIAZOLIDINEDIONES**

The thiazolidinediones (pioglitazone, rosiglitazone, and troglitazone), also known as glitazones, are a class of drugs used in the treatment of T2D, which act by activating the group of nuclear receptors peroxisome proliferator-activated receptors (PPARs), with greatest specificity for PPAR $\gamma$  (Spiegelman, 1998). After activation, these receptors bind to DNA in complex with the retinoid X receptor, thus regulating transcription of several specific genes. The major clinical effect of thiazolidinediones is to improve insulin sensitivity of muscle and fat cells to exogenous and endogenous insulin, thereby increasing glucose uptake and reducing hepatic glucose output (Bell, 2003).

### **2.6.6 ALPHA-GLUCOSIDASE INHIBITORS**

These agents slow down the digestion of starch in the small intestines, so that glucose from starchy meal enters the blood stream more slowly, and can be matched more effectively by an impaired insulin response or insensitivity. Miglitol and acarbose are examples of alpha-glucosidase inhibitors and they are very effective in the treatment of T2D (Haffner *et al.*, 2007).

### **2.7 MEDICINAL PLANTS**

The search for natural products to cure diseases has received considerable attentions in which medicinal plants have been the most important source (Okwu, 2001). They are believed to be an essential source of new chemical substances with potential therapeutic effects (Kuhn and Winston, 2000), and due to the crucial role that plant-derived compounds have played in drug discovery and development for the treatment of several diseases, the isolation of new bioactive compounds from medicinal plants based on ethnomedicinal data appears to be a very promising approach (Newman, 2008).

It has been estimated that about 80-85 % of people, both in developed and developing countries rely on traditional medicine for their primary health care needs and it is assumed

effects associated with conventional hypoglycemic agents (Piero *et al.*, 2012). In fact, about 80% of the world population still rely on medicinal plants for treatment of diseases (Tiwari, 2008).

## 2.9 *Chromolaena odorata* (L.)

*Chromolaena odorata* (L.) is a tropical species of flowering shrub belonging to the sunflower family, Asteraceae (Chakraborty *et al.*, 2011). It is a fast-growing perennial and invasive weed native to America, but has also been dispersed to tropical regions of Asia, Africa and other parts of the world. It is an aggressive competitor that occupies different types of lands where it forms dense strands that prevent the establishment of other flora (Akinmoladun *et al.*, 2007). The plant is hairy and glandular and the leaves give off a pungent scent when crushed. The leaves are opposite, triangular to elliptical with serrated edges. Leaves are 4–10 cm long by 1–5 cm wide (up to 4 x 2 inches). They possess one-seeded fruits called achenes and are somewhat hairy. They are mostly spread by the wind, but can also cling to fur, clothes and machinery, enabling long distance dispersal. Seed production is about 80,000 to 90,000 per plant. Seeds need light to germinate. The plant can regenerate from the roots. In favorable conditions the plant can grow more than 3 cm per day (Lalith, 2009). It was earlier taxonomically classified under the genus *Eupatorium*, but is now considered more closely related to other genera.

*C. odorata* also goes by the common names Siam weed, Christmas bush, devil weed, camphor grass, and common floss flower (Lalith, 2009). In Nigeria, *C. odorata* is commonly called “*Ewe Akintola*” in Yoruba, “*triffi weed*” in Hausa and “*Obiraohu*”, in Igbo.

*C. odorata* can reproduce apomictically (Rambuda and Johnson, 2004) and is a prolific producer of light, wind dispersed seeds. A single shrub can produce as many as 80 000 seeds in one season. At the start of the wet season, established plants generate new shoots from the crown or from higher, undamaged auxiliary buds, while seeds in the soil, produced

during the previous dry season, germinate. Stems branch freely and a large plant may have up to 15 or more branches of varying size from a single rootstock. The plant can grow on many soil types, but prefers well-drained soils (Zachariades *et al.*, 2009).

*C. odorata* does not tolerate shade and flourish well in open areas. They can form dense stands and suppress the growth of other plants. This is due to the competition and allelopathic effects.



Figure 2.3: *Chromolaena odorata* (L.) leaves collected from Akungba-Akoko  
(7°28'58.64"N; 5°45'1.98"E)

### Scientific classification of *Chromolaena odorata* (L.)

- Kingdom:** Plantae  
**Subkingdom:** Tracheobionta  
**Superdivision:** Spermatophyta  
**Division:** Magnoliophyta  
**Class:** Magnoliopsida  
**Subclass:** Asteridae  
**Order:** Asterales  
**Family:** Asteraceae  
**Genus:** *Chromolaena*  
**Species:** *Chromolaena odorata*

#### 2.9.1 PHYTOCHEMICAL CONSTITUENTS OF *Chromolaena odorata* (L.)

##### LEAVES

Analyses of *C. odorata* have identified chemical constituents such as mono-terpenes, sesquiterpenes hydrocarbons, triterpenes/steroids, saponins, alkaloids and flavonoids (Akinmoladun *et al.*, 2007, Zhang *et al.*, 2012, Heiss *et al.*, 2014). The leaves, containing the highest concentration of allelochemicals isolated from a plant, are reported to be a rich source of flavonoids including quercetin, sinensetin, sakuranetin, padmatin, kaempferol and salvagenin (Torrenegra and Rodríguez, 2011, Akinmoladun *et al.*, 2007). Important bioactive compounds present in *C. odorata*, are stigmasterol, scutellarein tetramethyl ether (Scu; 4',5,6,7-tetramethoxy-flavone), flavonoids (Zhang *et al.*, 2012, Pandith *et al.*, 2013), and the phytoprostane compound chromomoric acid C-1 (Heiss *et al.*, 2014)

The crude ethanol extract of *C. odorata* contains phenolic acids (protocatechuic, p-hydroxybenzoic, p-coumaric, ferulic and vanillic acids) and complex mixtures of lipophilic flavonoid aglycones (flavanones, flavonols, flavones and chalcones) (Heiss *et al.*, 2014).

The aqueous extract of the leaves was reported to contain flavonoids (salvigenin, sakuranetin, isosakuranetin, kaempferide, betulenol, 2-5-7-3 tetra-*o*-methyl quercetagenin, tamarixetin, two chalcones and odoratin and its alcoholic compound), essential oils (geyren, bornyl acetate and  $\beta$ -eubeden), saponin triterpenoids, tannins, organic acids and numerous trace substances (Zhang *et al.*, 2012). The presence of saponins justifies the cholesterol lowering properties of *C. odorata*. Saponins are known to inhibit  $\text{Na}^+$  efflux leading to higher  $\text{Na}^+$  concentration in cells, thereby activating a  $\text{Na}^+$ - $\text{Ca}^{2+}$  antiport, this effect produces elevated cytosolic  $\text{Ca}^{2+}$  which strengthens the contraction of the heart muscle, reducing congestive heart failure (Anyasor *et al.*, 2011).

Other compounds isolated from this plant include 5 $\alpha$ ,6,9,9 $\beta$ ,10-pentahydro-10 $\beta$ -hydroxy-7-methylanthra[1,2-d] [1,3]dioxol-5-one, 1,2-methylenedioxy-6-methylanthraquinone, 3-hydroxy-1,2,4-trimethoxy-6-methyl anthraquinone, 3-hydroxy-1,2-dimethoxy-6-methylanthraquinone, 7-methoxy-7-epi-medioresinol, 3 $\beta$ -acetyloleanolic acid, ursolic acid, ombuin, 4,2'-dihydroxy-4',5',6'-trimethoxychalcone, (-)-pinoresinol, austrocortinin, tianshich acid, cleomiscosin D, (-)-medioresinol, (-)-syringaresinol, and cleomiscosin A (Zhang *et al.*, 2012)

## 2.9.2 BIOLOGICAL ACTIVITIES OF *Chromolaena odorata* (L.)

*C. odorata* is used as a source of medicine in traditional medicinal practice in West Africa and countries in Asia. The plant is known for its medicinal properties especially in the treatment of wounds (Phan *et al.*, 2001). Leaf extracts of *C. odorata* added with salt is used as gargle for sore throat and colds. *C. odorata* is used extensively in Nigeria for soil fertility improvement as well as for medicinal and ornamental purposes (Uyi *et al.*, 2014). Decoctions of this plant are popularly used for wound healing due to its antimicrobial properties (Odungbemi, 2006). Concentrations of 0.25 mg/mL and 0.125 mg/mL of ethanolic extract of *C. odorata* exhibited antimicrobial effects against some human

pathogens. Several researchers have reported the wider use of *C. odorata* as an effective therapy against diarrhea, malarial fever, tooth ache, diabetes, skin diseases, dysentery, and colitis (Odungbemi, 2006, Akinmoladun, 2007). It is also reported to have anthelmintic activity (Mishra *et al.*, 2010, Patel *et al.*, 2010), analgesic activity (Jena and Chakraborty, 2010), anti-inflammatory, antipyretic and antispasmodic properties (Taiwo *et al.*, 2000), anti-cancer (Adedapo *et al.*, 2016b), anti-inflammatory activity (Owoyele *et al.*, 2005), diuretic activity (Rejitha *et al.*, 2009), Cardioprotective effects (Ikewuchi and Ikewuchi, 2011), anti-oxidant effects on human dermal fibroblasts and epidermal keratinocytes (Thang *et al.*, 2001).

## 2.10 FLAVONOIDS

Flavonoids (FLVs) or bioflavonoids get their name from the Latin word *flavus*, meaning yellow. They are ubiquitous in plants and are the most abundant polyphenolic compounds in human diet (Prasad *et al.*, 2010; Castellarin and Gaspero, 2007). They are a diverse group of polyphenols (phenyl benzopyrans) which function as phytochemicals (Corradini *et al.*, 2011) possessing a 15-carbon skeleton containing two phenyl rings and a heterocyclic ring. FLVs are commonly found in fruits, vegetables, grains, bark, roots, stems, flowers, tea and wine. These natural products are well known for their beneficial effects on health, with multi-directional biological activities including anti-diabetic efficacy.

Experimental evidence has shown that flavonoids exhibit anti-inflammatory (Middleton *et al.*, 2000), anticarcinogenic (Batra and Sharma, 2013), antiviral (Selway, 1986) and antiallergic properties. These effects are generally associated with free radical scavenging activity of flavonoids. The antioxidant effects of flavonoids are enhanced by the number and position of hydroxyl groups in the molecule. The catechol structure, presence of unsaturation and 4-oxo function in the C-ring also contributes to their radical scavenging

activity (Rice-Evans *et al.*, 1996; Heim *et al.*, 2002). Flavonoids may be capable of binding the transition metal ions, which play a role in glycooxidation, thus preventing metal-catalysed formation of hydroxyl radicals or related species from hydrogen peroxide (Groot and Rauen, 1998). FLVs are now considered an indispensable component in a variety of nutraceutical, pharmaceutical, medicinal and cosmetic applications.

Based on several animal and some human studies, FLVs may play a role in many metabolic processes. They can modulate carbohydrate and lipid metabolism, hypoglycemia, dyslipidemia and insulin resistance, improve adipose tissue metabolism, and alleviate oxidative stress and stress-sensitive signaling pathways and inflammatory processes (Johnston *et al.*, 2005; Jung *et al.*, 2004). A number of studies have been carried out on properties of antioxidant in relation to different flavonoids and these studies emphasized that flavonoids can be used as potential drugs to prevent oxidative stresses (Hollman and Katan, 1998) caused by imbalance between oxidant antioxidant systems, which could result from elevated free radical generation and decreased activity of antioxidants. In addition to their specific pharmacological effect, the antioxidant potential of flavonoids renders them interesting molecular targets to induce therapeutic benefits while Fighting oxidative stress (Nicolle *et al.*, 2011).

### 2.10.1 STRUCTURE AND CLASSES OF FLAVONOIDS

Flavonoids can occur as aglycones, glycosides and methylated derivatives. Aglycones consists of a benzene ring (A) condensed with a six- membered ring (C), which in the carbon 2-position carries a phenyl ring (B) as a substituent (Fig 1). The six-member ring condensed with the benzene ring is either a  $\alpha$ -pyrone (flavonols and flavonones) or its dihydroderivative (flavanols and flavanones). The position of the benzenoid substituent divides the flavonoid class into flavonoids (2-position) and isoflavonoids (3-position).

Flavonols differ from flavonones by hydroxyl group the 3-position and a C2-C3 double bonds. Flavonoids are often hydroxylated at position 3, 5, 7, 2', 3', 4' and 5'. Methyl ethers and acetylestere of the alcohol group are known to occur in nature. When glycosides are formed, the glycosidic linkage is normally located in positions 3 or 7 and the carbohydrate can be L-rhamnose, D-glucose, glucor-hamnose, galactose or arabinose. (Narayana *et al.*, 2001)

Flavonoids are classified based on functional groups on the rings, generic structure of ring C, and connection position of ring B in relation to ring C, into: Flavones, Flavonols, Flavanones, Flavonols, Anthocyanidins and Isoflavonones

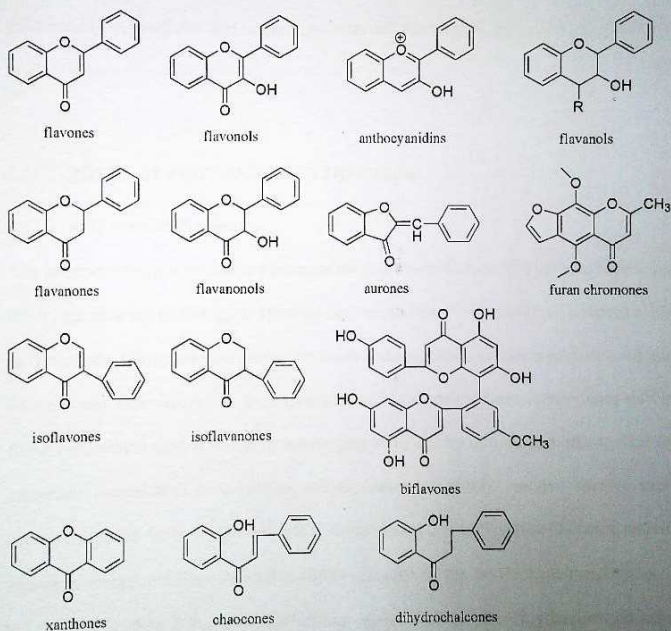


Figure 2.4: Structures of various flavonoid classes and subclasses (Wang *et al.*, 2018)

## 2.10.2 BIOSYNTHESIS OF FLAVONOIDS

Flavonoids are synthesized via the phenylpropanoid metabolic pathway transforming phenylalanine to 4-coumaroyl-CoA (Ferreya *et al.*, 2012). The metabolic pathway continues through a series of enzymatic modifications to yield flavanones → dihydroflavonols → anthocyanins. Although the central pathway for flavonoid biosynthesis is conserved in plants, depending on the species, a group of enzymes, such as isomerases, reductases, hydroxylases, and several Fe<sup>2+</sup>/2-oxoglutarate-dependent dioxygenases modify the basic flavonoid skeleton, leading to the different flavonoid subclasses (Martens *et al.*, 2010). Lastly, transferases modify the flavonoid backbone with sugars, methyl groups and/or acyl moieties, modulating the physiological activity of the resulting flavonoid by altering their solubility, reactivity and interaction with cellular targets (Bowles *et al.*, 2005; Ferrer *et al.*, 2008).

## 2.11 ROLES OF FLAVONOIDS IN DISEASES

### 2.11.1 Anti-oxidant Properties

The adverse effects of oxidative processes on organic molecules like carbohydrates, lipids, DNA and proteins in biological systems are reduced by a wide range of substances found in flavonoids. Flavonoids are present in fruits and vegetables as phytonutrients, containing flavones and catechins, which are important sources of antioxidants. Antioxidant activity of flavonoids exhibit double action by scavenging ROS and by inhibiting oxidases. One of the important antioxidants is quercetin, which scavenges highly reactive species such as peroxynitrite and the hydroxyl radicals (Unnikrishnan, 2014). The iron chelation activity of quercetin works to reduce oxidative injury induced in the erythrocyte membranes. This injury is induced by a number of oxidizing agents such as phenylhydrazine and acrolein

(Prochazkova *et al.*, 2011). Different diseases can be prevented by intake of antioxidants that are present in our food in the form of flavonoids in fruits and vegetables.

### **2.11.2 Antimicrobial Properties**

In several pharmaceuticals, plant parts and their extracts are used to improve human immune system against diseases (Atoui *et al.*, 2005). The antimicrobial properties of pure phenolic compounds and polyphenols of different wines against pathogens were investigated, and it was observed that bacterial species exhibited different sensitivities towards the different concentrations of phenolic compounds. (Vaquero *et al.*, 2007). Additionally, the antimicrobial activity of naringin and quercetin has also been established. Plants from different species rich in flavonoid are found exhibiting enhanced antibacterial activity (Mishra, 2009). Numerous flavonoids such as apigenin, galangin, glycosides, flavones, isoflavones, chalcones, flavanones, flavonol have shown effective antibacterial activity (Xu and Lee, 2001). Flavonoids that act as antibacterial agents possess different cell targets, as opposed to one particular site of activity. It has also been investigated that flavonoids which are lipophilic in nature may also disturb microbial membranes. Thus, such antimicrobial functions can be correlated to minimizing microbial adhesions, intracellular transport proteins etc. Study has depicted the use of flavonoids to Fight antibiotic resistant bacteria. (Xu and Lee, 2001).

### **2.11.3 Role in Cardiovascular Diseases**

Cardiovascular diseases are a major cause of mortality worldwide. Studies have supported the view that flavonoids and flavonoid-rich foods, contain cardiovascular protective properties (McCullough *et al.*, 2012; Feliciano *et al.*, 2015). Tea contains flavonoids which reduce levels of cholesterol in blood, damage caused by oxidative stress, lower blood pressure and inflammation. Studies suggest that flavonoids of tea also enhance functions of the endothelial cell (McCullough *et al.*, 2012). Similarly, bioactive compounds of flavonoids such as non-caloric, non-nutrient secondary metabolites, polyphenolic are found

mainly in cocoa, wine, tea, vegetables, nuts and fruits. These flavonoids may reduce LDL cholesterol and regulate anti-inflammatory and antioxidant activities (Stote *et al.*, 2012). A good source of quercetin is cranberries, which can help lower the blood pressure.

#### **2.11.4 Anti-inflammatory Properties**

Flavonoids are present in various plant parts and reportedly possess anti-inflammatory properties (Ginwala *et al.*, 2019). Apigenin, luteolin and fisetin are some of the flavonoids reported to have good anti-inflammatory properties (Funakoshi-Tago *et al.*, 2011).

#### **2.11.5 Anti-diabetic Properties**

Several lines of evidence suggest that flavonoids of plant origin such as shamimin, diadzein, epicatechin, myricetin, epigallocatechin, hesperidin, naringenin, hesperitin, chrysin, apigenin, genistein, kaempferol, luteolin, quercetin and rutin, have beneficial effects on diabetes by improving glycaemic control, lipid profile, and antioxidant status (Ghorbani, 2017). Flavonoids can restrain aldose reductase that converts sugars to sugar alcohols and are involved in diabetic intricacies, for example, neuropathy, cardiac disorder and retinopathy (Tadera *et al.*, 2006). Another mechanism, by which flavonoids are known to help reduce hyperglycemia, is by interrupting absorption of glucose from the intestine. The transport activity of sodium-dependent glucose transporter was markedly inhibited by green tea polyphenols (Kobayashi *et al.*, 2000).

### **2.12 FLAVONOIDS AND DIABETES**

Several studies have demonstrated the likely protective potential of flavonoids in the treatment of diabetes and they indicate the hypoglycaemic actions of flavonoids in different experimental models and treatments (Sabu *et al.*, 2002; Tsuneki *et al.*, 2004; Fukino *et al.*, 2005; MacKenzie *et al.*, 2007). Flavonoids have been shown to exert beneficial anti-diabetic effects on hyperglycaemia and prevent diabetic complications by enhancing altered glucose, oxidative and lipid metabolisms of diabetic states (Pinent *et al.*, 2004, Lee, 2006, Park *et al.*, 2006). Some flavonols, such as kaempferol, myricetin, rutin and its metabolite

quercetin, show hypoglycemic activity (Jang and Jeong, 2010, Kamalakkannan and Prince, 2006, Bhathena and Velasquez, 2002). In particular, oral administration of rutin to diabetic rats results in a plasma glucose levels reduction (Kamalakkannan and Prince, 2006). Several studies indicate that some flavonoids compete with glucose in several absorption mechanisms signifying that intestinal absorption reduction may represent one hypoglycemic effect. In fact, this action was observed in the intestinal brush border membrane vesicles of rabbits with a soybean extract which contains the two isoflavones genistein and daidzein (Bhathena and Velasquez, 2002).

Flavonoids have the ability to scavenge free radicals and chelate metals. Given the hypothesized relation between diabetes and inflammation and the potential of flavonoids to protect the body against free radicals and other pro-oxidative compounds (Duncan *et al.*, 2003; Rice-Evans *et al.*, 1996), it is biologically plausible that consumption of flavonoids or flavonoid-rich foods may reduce the risk of diabetes (Bahadoran *et al.*, 2013). New concepts have appeared with this trend, such as nutraceuticals, nutritional therapy, phytonutrients and phytotherapy. These functional foods and phytomedicines play positive roles in maintaining blood glucose levels, glucose uptake and insulin secretion and modulating immune function to prevent specific DM (Hanhineva *et al.*, 2010; Hajiaghaalipour *et al.*, 2015). Naturally occurring Flavonoids such as Diosmin, Fisetin, Morin, Isoflavones, Tangeretin, Quercetin and hesperedin have been reported to significantly lower plasma glucose levels (Prasath *et al.*, 2014), increased plasma insulin levels in diabetic rats by ameliorating oxidative stress (Srinivasan and Pari, 2012), improve diabetic associated complications (Jain *et al.*, 2014) decrease adipocytokines such as adiponectin, leptin, resistin, interleukin-6, and monocyte chemoattractant protein-1 (Miyata *et al.*, 2011; Kim *et al.*, 2012), stimulate  $\beta$ -cell proliferation and glucose-stimulated insulin secretion (Qin *et al.*, 2013; Sundaram *et al.*, 2014).

### 1.12.1 ROLE OF FLAVONOIDS IN STREPTOZOTOCIN-INDUCED DIABETES

STZ, a well-known toxic agent (Weiss, 1982) with pro-diabetic potency, causes hyperglycemia as a result of damaged PBC (Najafian *et al.*, 2010), induces nephropathy in the kidney (Wang *et al.*, 2015) and inflicts injury to epithelial cells of the aorta (Li *et al.*, 2016). PBCs function primarily in the transcription of the gene encoding insulin and secretion of insulin, in response to high glucose concentrations (Rorsman, 1997). Insulin production is dependent on the functionality of PBCs. T1D results, due to autoimmune-mediated destruction of PBCs and so little or no insulin is available to mop up excess glucose circulating in the blood. Similarly, in the case of T2D, increased glucotoxicity, lipotoxicity, endoplasmic reticulum-induced stress, and apoptosis lead to the progressive loss of beta cells (Petersen *et al.*, 2017).

The study by ElLatif *et al.* (2014) reported that oral administration of genistein to STZ-diabetic rats, increased insulin secretion from mouse pancreatic islets. The mechanism underlying this biological effect may have involved a rise in intracellular cAMP through the increase of adenylate cyclase activity and the activation of protein kinase A (PKA). Another study on the same flavonoid, genistein, suggests that it exerts its insulinotropic action through the activation of the cAMP/PKA signaling cascade (Liu *et al.*, 2006).

O-linked- $\beta$ -N-acetylglucosamine (O-GlcNAc) glycosylation (O-GlcNAcylation), which involves the covalent attachment of N-acetylglucosamine to serine or threonine residues of proteins, is a distinct post-translational modification (Vosseller *et al.*, 2002), which serves as a key regulator of nutrient and stress-induced signal transduction pathways and many other biological processes (Zeidan and Hart, 2010; Ma and Hart, 2013), and must remain within an optimal zone in the various fluctuations of cellular environments to preserve normal cellular functions (Yang and Qian, 2017). Protein O-GlcNAcylation is reversibly regulated by 2 enzymes – O-GlcNAc transferase (OGT) and  $\beta$ -N-Acetylglucosaminidase (OGA) – which catalyze the addition of a single UDP-GlcNAc moiety to the hydroxyl group

of serine and threonine residues and the hydrolytic cleavage of the *O*-linked sugar moiety from the protein, respectively. Aberrant O-GlcNAcylation has been implicated in the progression of diseases such as diabetes mellitus, cancer, and neurodegeneration (Banerjee *et al.*, 2016). Diabetes significantly elevates global O-GlcNAc levels in tissues such as the heart (Fricovsky *et al.*, 2012). The inhibitory effect of flavonoids on glycation, have been said in part to be due to their antioxidant properties (Wu and Yen, 2005).

### 2.13 TAKEDA G-PROTEIN RECEPTOR 5/ GLUCAGON-LIKE PEPTIDE-1 (TGR5/GLP-1) SIGNALING

TGR5 (also known as GPR131, M-BAR or GPBAR1) is a G-protein coupled receptor expressed in different body organs such as the pancreas, intestine, brain, skeletal muscle, brown and white adipose tissues and gallbladder, which is responsive by bile acids (BA). BAs can improve glycemic control so, they play an important role in glucose homeostasis (Zarrinpar and Loomba, 2012). When activated by BAs and potent TGR5 agonists (Pellicciari *et al.*, 2009, Wang *et al.*, 2017), TGR5 has been shown to promote GLP-1 secretion in murine enteroendocrine cell line STC-1 (Katsuma *et al.*, 2005). Activation of TGR5 by bile acids and TGR5 agonists in murine intestinal L-cells, elicit the release of GLP-1, an incretin with beneficial effects on glucose homeostasis, such as increased insulin secretion and thus improved glucose tolerance. (Katsuma *et al.*, 2005, Thomas *et al.*, 2009). Activated TGR5 also increases cyclic adenosine monophosphate (cAMP) (Lee and Jun, 2018) that may activate protein kinase A (PKA) and downstream signaling (Kawamata *et al.*, 2003, Lefkowitz, 2007). Glucagon-Like Peptide 1 (GLP-1), an incretin, typically augments glucose-stimulated insulin secretion in PBCs (MacDonald *et al.*, 2002). Some key functions of GLP-1 related to PBCs include - acting synergistically with glucose to promote insulin gene transcription, improve PBC proliferation (Brubaker and Drucker, 2004), improved glucose homeostasis (Thomas *et al.*, 2009), and counteract the detrimental effects of AGEs on PBCs, preserving both function and survival (Puddu *et al.*, 2010).

GLP-1 is a powerful physiological incretin, known to regulate glucose homeostasis (Malik and Roohi, 2018, Baggio and Drucker, 2007). GLP-1 augments insulin secretion after oral glucose administration and so plays a key role in diabetes treatment (Sonne *et al.*, 2014). GLP-1, when secreted in the intestines, binds to its receptor on the pancreas, stimulating insulin production. Activation of the GLP-1 receptor (GLP-1R) signaling pathway is a relevant strategy to repair deficient beta-cell mass and preserve beta-cell function (Portha *et al.*, 2011).

GLP-1 has been shown to stimulate insulin gene transcription and biosynthesis (Drucker *et al.*, 1987) via the insulin transcription factor pancreatic duodenal homeobox-1 (PDX-1), a key effector for the GLP-1R signaling pathway (Le Lay and Stein, 2006). GLP-1 causes PDX-1 protein translocation from the cytoplasm to the nucleus of pancreatic  $\beta$ -cells cyclic adenosine monophosphate/protein kinase A-dependent (cAMP/PKA) signaling, which activates insulin gene transcription and biosynthesis, as well as differentiation, proliferation, and survival of the beta cell (Wang *et al.*, 2001, Le Lay and Stein, 2006).

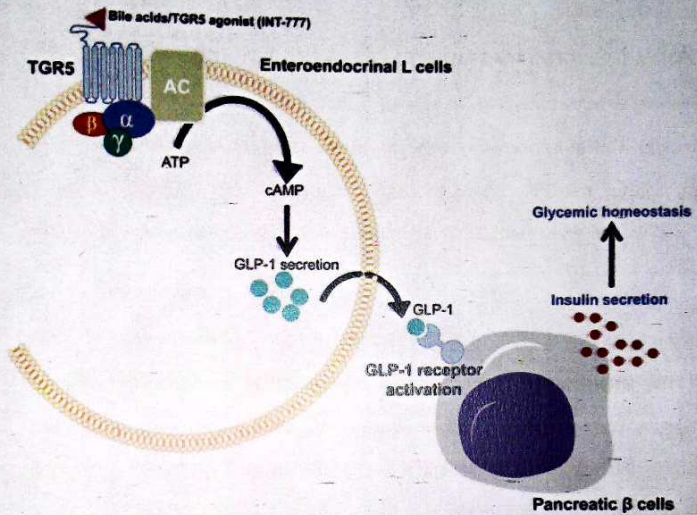


Figure 2.5: TGR-5-stimulated GLP-1 production in improved glycemic control (Kim and Fang, 2018)

## CHAPTER THREE

### 3.0 MATERIALS AND METHODS

#### 3.1 PLANT MATERIAL

Fresh *C. odorata* leaves were collected from Akungba-Akoko (7°28'58.64"N; 5°45'1.98"E). They were washed with clean tap water and macerated using a mortar and pestle.

##### 3.1.1. PREPARATION OF PLANT EXTRACT AND FLAVONOID ISOLATION

Total Flavonoid content (TFC) from fresh *C. odorata* leaves was extracted as previously documented (Omotuyi *et al.*, 2013). Briefly, the leaves were soaked in HCL (1%, v/v) overnight, filtered and concentrated with a rotary evaporator. TFC was purified using DOWEX-50 column (Raman *et al.*, 2004), resulting in *C. odorata* Flavonoid (CoF).

#### 3.2 EXPERIMENTAL ANIMALS

Thirty (30) male Wistar albino rats, weighing between 100 – 120 grams were purchased and maintained with a 12-hour light/12-hour dark cycle in the experimental animal unit of the Centre for Bio-Computing and Drug Development, Adekunle Ajasin University, Akungba-Akoko. They were allowed to acclimatize for two weeks and fed with commercial pelletized rat feed and water *ad libitum*. Protocols related to animal studies were approved by the Animal Ethics Committee of Centre for Research and Development (CRD), Adekunle Ajasin University, Akungba-Akoko.

##### 3.2.1 INDUCTION AND CONFIRMATION OF DIABETES IN EXPERIMENTAL ANIMALS

All chemicals used for experiments were of analytical grade. Streptozotocin (STZ) used in the induction of diabetes was prepared by dissolving in sodium citrate buffer (pH 4.5). Healthy male rats were first divided into two groups. Group C (n=5) served as the control,

while group S (n=25). Before diabetes induction, blood glucose (BG) levels were measured from the tail vein blood using an AccuChek Compact glucometer (Roche Diagnostics, Indianapolis, IN, USA). After an overnight fast, animals in group S were administered freshly prepared STZ solution (Furman, 2015) (40 mg/kg b.w., i.p.) once every other day for a total of three (3) times. Seven (7) days after the termination of STZ treatment, animals blood samples were drawn from the tail vein as previously described (Zou *et al.*, 2017) for BG determination. An animal should have the BG value of  $\geq 300$  mg/dL consistently for 14 days post STZ treatment, which confirms diabetes, to be used for the next experiment.

### 3.3 EXPERIMENTAL DESIGN

Fourteen (14) animals which were confirmed diabetic from group S above were further grouped into B (STZ, n=7) and C (STZ+CoF, n=7). CoF treatment (30 mg/kg b.w. oral) was performed once daily, for 60 days. Fasting Blood Glucose (FBG) was measured after fasting rats for 9 hours, once every seven (7) days after treatment commenced. At the end of the experiment, animals were sacrificed under light anesthesia and blood samples were drawn using venepuncture from each animal into properly labelled tubes for biochemical analysis, while the Pancreas, Kidneys and Aortas of the animals were harvested and immediately fixed in 10% neutral buffered formalin for histological studies. 100 $\mu$ g of Pancreas, Kidney, Aorta and the proximal end of the ileum, were also collected and immediately placed in 100 $\mu$ l TRIzol for gene expression analysis (Kakhki, 2014).

### 3.4 GENE EXPRESSION STUDIES

RNA was isolated from the Pancreas, Kidney, Aorta and the proximal end of the ileum, using TRIzol Reagent (ThermoFisher Scientific), following manufacturer's protocol. Purified RNA was quantified and converted to cDNA using ProtoScript® First Strand cDNA Synthesis Kit (NEB). PCR amplification was done using OneTaq® 2X Master Mix (NEB) using the following primer set:

**Table 3.1** Primer sequences for primers used to run RT-PCR

Gene	Forward Primer (5' - 3')	Reverse Primer (5' - 3')
INSULIN	AACCCCTAAGTGACCAGCTACAATCA	AAACCACGTTCCCCACACAC
PDX-1	GGAATTCGGGGGCGC	GGGTCTCTGATAGACTGT
GLP-1	TCCCAAAGGAGCTCCACCTG	TTCTCCTCCGTGCTTGAGGG
OGT	GCGGGGCACTTGATTGTAAC	TTCCCGATGTGCCAACTCAG
OGA	CAGTGGAAGAAGCTGAGCAAC	TGTGCATGTGCAAAAAGAACTGA
MCP-1	TGCCAAGTAGCCACATCCAG	CACAGTGTGAGCAACTGGGA
TNF- $\alpha$	CTCAAAACTCGAGTGACAAGC	CCGTGATGTCTAAGTACTTGG
IL-6	CATTCTGTCTCGAGCCACC	GCTGAAAAGTCTCTTGCGGAG
IL-1 $\beta$	TTGAGTCTGCACAGTTCCCC	TCCTGGGGAAAGCATTAGGA
CAT	CACAGTGTGAGCAACTGGGA	GAGGCCATAATCCGGATCTTC
GPx-1	CCGACCAGGGCATCAAAA	GAGGCCATAATCCGGATCTTC
KIM-1	GGTGCTGTGAGTAAATAGATCA	TAAACTTCAACTACCTTAAACACAATAAGATG
CYCLOPHILIN (control)	TGGAGAGCACCAAGACAGACA	TGCCGGAGTGCACAATGAT
$\beta$ -ACTIN (control):	GTCGAGTCCGCGTCCAC	AAACATGATCTGGGTCACTTTTCACG

Source: Primer synthesis report (Inquaba biotec)

### 3.4.1 PCR CONDITIONS

Initial denaturation – 94°C for 5mins

Denaturation – 94°C for 30 secs

Annealing – 55°C for 30 secs

Elongation – 74°C for 30 secs

Termination – 74°C for 10 mins

### **3.5 BLOOD UREA NITROGEN AND SERUM CREATINE ESTIMATION**

Blood samples were drawn as described earlier for blood urea nitrogen (BUN) and serum creatine (SC) estimations using commercial assay kits, following manufacturer's protocols.

### **3.6 NOAEL EXPERIMENTS**

#### **3.6.1 EXPERIMENTAL DESIGN**

Group 1 served as the control, Groups 2, 3, 4 and 5, were given (10, 30, 100 and 300) mg/kg body weight (bwt), CoF, respectively. Body weight was taken every 3 days, blood was drawn from the tail vein, every 7 days for a period of 28 days.

#### **3.6.2 LIVER FUNCTION TEST**

*in vitro* test for the quantitative determination of aspartate amino-transferase (AST) and alanine amino-transferase (ALT) in blood plasma were carried out using standard commercial assay kits, following manufacturer's protocols.

#### **3.6.3 KIDNEY FUNCTION TEST**

Enzymatic *in vitro* test for the quantitative determination of urea in blood plasma was carried out using standard kit.

### **3.7 HISTOLOGICAL EXAMINATION**

#### **Slide preparation protocol**

For histology specimens, the tissue pieces were first immersed in freshly prepared 10% formal saline solution, routinely processed and subsequently embedded in melted paraffin wax. The wax block was then cut on a microtome to yield thin 5  $\mu\text{m}$  slice sections of paraffin containing the tissue. The specimen slice was then applied to a microscope slide, air dried, and heated to cause the specimen to adhere to the glass slide. Residual paraffin was dissolved, followed by rinsing with an acid-alcohol followed by rinsing with water to remove the acid-alcohol. The slide was introduced into a concentrated hydrochloric acid solution to obtain a pH between 4 and 5 to turn the Hematoxylin blue. The bluing solution

was removed by rinsing with water. Other cytoplasmic elements were stained with an alcoholic solution of eosin Y, a red stain, and light green or fast green. Excess stain was removed and water by a series of sequential washes in a dehydrating reagent. Next, the slide was introduced into a chemical-clearing agent (toluene, xylene, or t-butanol) to remove residual dehydrating reagent remaining from the washing step. A cover-slip mountant and a cover-slip were applied after first removing the slide from the chemical-clearing agent. The clearing agent evaporates and the mountant hardens leaving a stained and mounted slide (Slaoui and Fiette, 2011)

Photomicrographs were taken at x100 and x400 magnifications with a Digital Microscope, VJ-2005 DN MODEL BIO-MICROSCOPE®. The morphometrical analyses was done using TS View CX Image® Software, File version 6.2.4.3 and Motic Image 2000 (China).

### **3.8 STATISTICAL ANALYSIS**

Gel electrophoresis images, Bowman's space thickness and Bowman's capsule diameter were quantified using Image J, and the values were plotted as mean  $\pm$  SEM as representative bar graphs. Statistical analysis was done by comparing differences between groups using one-way ANOVA nonparametric test ( $p < 0.05$ ) with GraphPad Prism Software, version 7.0a on a Mac OSX; 2015.

### **3.9 STARTING TGR5 MODEL FOR MOLECULAR DOCKING STUDIES**

Molecular simulations starting from active-state Beta-2 adrenergic receptor have been used to investigate structural ensembles preferentially sampled in activated receptor states and mechanism of activation in human adenosine A<sub>2A</sub> receptor bound to agonists starting from intermediate state conformation. Here, active-state evolution of TGR5 is intended starting from an intermediate state conformation therefore, the starting TGR5 (Accession: NP\_001308879.1) model was built on human adenosine A<sub>2A</sub> receptor (co-crystallized with adenosine) template (PDB ID: 2YDO, Sequence identity=19.12%, 0.82 coverage, human Adenosine receptor/TGR5 alignment using Biologics Suite (Biologics Suite 2017-4,

Schrödinger, LLC, New York, NY, 2017). Ramachandran plot as implemented on the RAM-PAGE web-service (<http://www-cryst.bioc.cam.ac.uk/rampage>) (Lovell *et al.*, 2003) was used for model quality assessment, where only 1.8% of the residues in outlier regions.

### 3.10 2D COORDINATES OF LIGANDS AND DOCKING PROTOCOLS

The 2D atomic coordinates of TRX (CID 5546), CoF (CID 5320438) and INT-777 (CID 45483949) were retrieved from PubChem repository and prepared using LigPrep scripts as implemented in Small-Molecule Drug Discovery Suite of Schrödinger. The ligands were docked into TGR5 model using Glide (Schrödinger Suite 2017-4 Induced Fit Docking protocol; Glide, Schrödinger, LLC, New York, NY, 2016; Prime, Schrödinger, LLC, New York, NY, 2017) extra-precision methods taking adenosine coordinate as the reference point.

### 3.11 BIOSYSTEMS SETUP AND MOLECULAR DYNAMICS (MD) SIMULATION

Hydrogen and semi-empirical AM1-bcc charges were added to the ligands using the UCSF Chimera tool (Lovell *et al.*, 2003) and parameterized using ParamChem web-service (<https://cgenff.paramchem.org>).

TGR5 (APO) and three complexes (TGR5+CoF, TGR5+INT-777 and TGR5+TRX) were prepared for simulation. For each complex, insertion into pre-equilibrated lipid (1-palmitoyl-2-oleoyl-sn-glycero-3-phosphocholine, POPC, 68 lipids per leaflet) and generation of topology files following CHARMM36 force field parameters (Lovell *et al.*, 2003) were done using High-Throughput Molecular Dynamics for Molecular Discovery (HTMD) python scripts (Pettersen *et al.*, 2004). The biosystems were solvated in TIP3P explicit water model and neutralized with 0.15M  $\text{Na}^+/\text{Cl}^-$ . Minimization at 0.5 kcal/mol/Å convergence threshold was performed on each complex using conjugate gradient method.

Equilibration molecular dynamics simulation was at 2fs time step, 10 Å cutoff for non-bonded interactions in a three-stage protocol. First, NVT ensemble was used to equilibrate lipid, water and ions as the fixed protein-ligand complex (heavy atoms) for 50 ns at 310K. Next, a 10 ns equilibration using NPT ensemble at 310K was performed with restraints on protein-ligand as described above. Finally, 40 ns equilibration simulations were performed on fully unrestrained biosystems using NPT protocols. NPT conditions were maintained by Berendsen equation for temperature and pressure coupling algorithms as implemented in GROMACS (ver. 5.0) (Huang and MacKerell, 2013). Two randomly selected biosystems were retrieved from fully unrestrained equilibration step for production MD simulations. Production MD simulations were run on ACEMD software (Doerr *et al.*, 2016) using parameters previously described (Van Der Spoel *et al.*, 2005) for 1000 ns each with snapshots saved every 1 ns. All MD simulation softwares were compiled on HPZ800 workstations with GPU (GTX-980, GTX680) cards.

### 3.12 POST-SIMULATION TRAJECTORY QUALITY ASSESSMENT

Prior to data analysis, convergence of the biosystems was confirmed using the stability of the protein C-alpha-backbone and lipid bilayer parameters. Root-mean-square deviation (RMSD) values (protein) and area-per-lipid/lipid bilayer thickness (Lipid bilayer) parameters were computed. At <200 ns, the protein C  $\alpha$ -backbone had stabilized around ~0.5 nm. The area-per-lipid represents an important parameter for assessing whether the lipid bilayer systems has achieved convergence in molecular simulations (Harvey *et al.*, 2009). Area-per-lipid of the POPC bilayer used in this study was maintained at an average of 82 Å<sup>2</sup> lipid bilayer thickness was maintained between 3~4 nm throughout the simulations, and the values remained consistent with previous studies.

### 3.13 DATA ANALYSIS

Atomic representations in this study were created using PyMol (Stanley *et al.*, 2016) and visual molecular dynamics (VMD) (Petrache *et al.*, 2000). All residues were numbered using the Ballesteros–Weinstein numbering system as reviewed. VMD (Volmap, Network Analysis Tools) and in-built GROMACS analysis (*gmx rms*, *gmx distance*, *gmx angle* ( $\chi^2$ ) *dihedral*, *gmx sham*) tools were used for post MD simulation analyses. MATHEMATICAL was used to draw the 3D surface plots; Volmap plugin (VMD) was used to generate intrahelical water density. Dynamical networks and community interaction between TMIII-TMVI during each trajectory was calculated using Network Analysis Tools in VMD. Line graphs were plotted using GraphPad prism (ver 6.0e, 2014) as the mean of two independent simulations

## CHAPTER FOUR

### 4.0 RESULTS

#### 4.1 CoF REVERSES STZ-INDUCED HYPERGLYCEMIA

Blood glucose levels of 70–99 mg/dl are said to be normal for non-diabetic subjects, while fasting blood glucose levels in diabetic state is given as 80–130 mg/dl. Healthy functional islets of the pancreas are able to produce insulin capable of maintaining blood glucose levels. The blood glucose levels of the animals were monitored by measuring fasting blood sugar levels, once every seven days, for the treatment period. STZ treatment evidently destroyed PBCs as recorded by high glucose levels in STZ-alone treated group. This is however reversed by CoF treatment (Fig 4.1 see pg 51).

#### 4.2 CoF REVERSES PANCREATIC BETA CELL DAMAGE IN STZ-INDUCED HYPERGLYCEMIA

It has been established that STZ treatment causes damage to PBCs. Damaged beta cells are unable to produce sufficient insulin to maintain glucose homeostasis. The results showed significant decreased insulin expression in the STZ-alone group (Fig 4.2 see pg. 52) and decreased islet cell density (Fig 4.4 see pg. 54), compared to control. CoF treated group however, shows increased (not significant,  $p < 0.05$ ) insulin production and islet cell density. PDX-1 (Fig 4.3 see pg. 53) and GLP-1 (Fig 4.6 see pg. 56) gene expressions in the CoF-treated group also show increased expression.

#### 4.3 STZ TREATMENT IS ASSOCIATED WITH ORGAN HISTO-STRUCTURAL DAMAGES IN THE PANCREAS; REVERSIBLE WITH CoF TREATMENT

Inside the substance of the pancreas are groups of specialized cells surrounded by connective tissue, which form the endocrine part of the gland and secrete hormones insulin and glucagon. These are the Islet of Langerhans, which are located among the acini cells

that form the gland's parenchyma. The pancreas has a thin cover of loose connective tissue from which septa pass into the gland, subdividing it into many small lobules which are also composed of rounded or tubular groups of pancreatic cells – these are the acini. Another important feature observed are the intercalated ducts (cuboidal epithelium) which receive secretions from the acini. The plate also showed the inter and intralobular ducts, found between and within the lobules, respectively, which represents the normal physiology of the pancreas (Plate 4.5 A see pg 55). In contrast, hyalinized islets, fatty droplets (FD) in the intralobular ducts, hyperplasia of intercalated duct cells was detected in the STZ group (Plate 4.5 B see pg 55). As seen in the CoF-treated group (Plate 4.5 C see pg 55), there is reduced FD, and regeneration of islet cells.

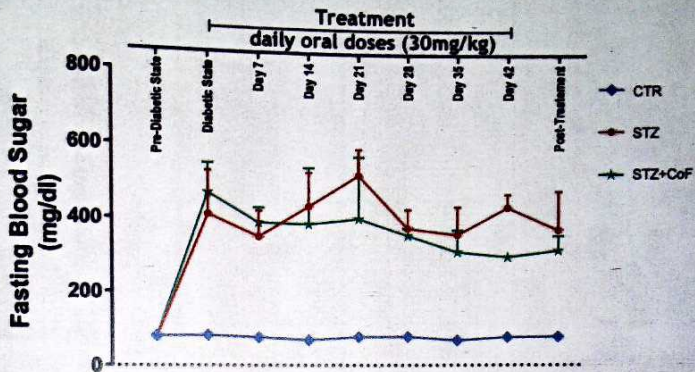
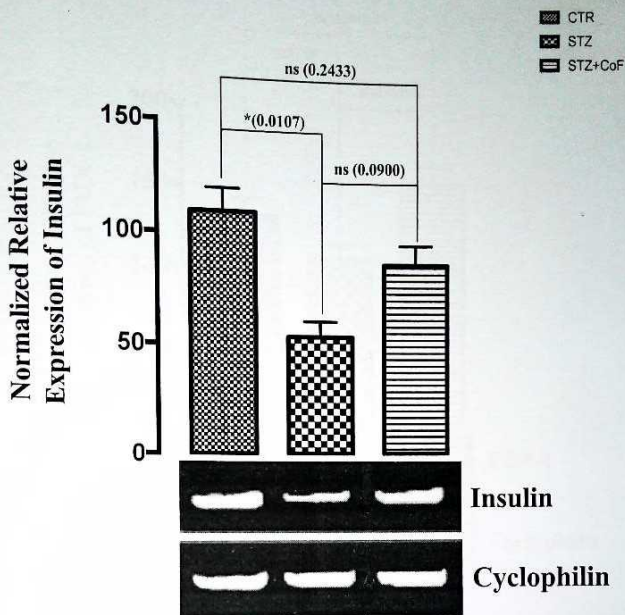
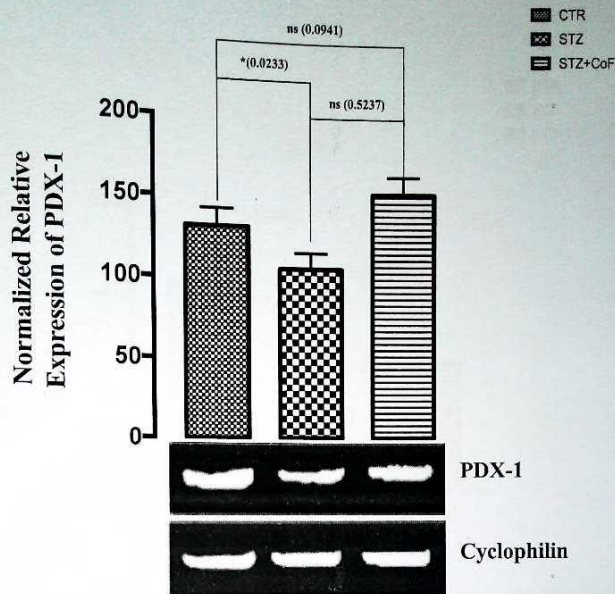


Figure 4.1: Fasting blood glucose levels of treatment and control groups.



**Figure 4.2:** Expression pattern of insulin gene in the pancreas of treatment and control groups. Bar graph represented mean and SEM values of quantified band from control and treatment groups. The gel image is the representative snapshot of the pooled samples. Each bar represented control normalized relative expression (gene/cyclophilin). Statistical comparison between groups was done at ( $p < 0.05$ ), the calculated p values are displayed. \* means significant difference compared to control, ns means not significant.



**Figure 4.3:** Expression pattern of pancreatic duodenal box - 1 (PDX-1) gene in the pancreas of treatment and control groups. Bar graph represented mean and SEM values of quantified band from control and treatment groups. The gel image is the representative snapshot of the pooled samples. Each bar represented control normalized relative expression (gene/cyclophilin). Statistical comparison between groups was done at ( $p < 0.05$ ), the calculated p values are displayed. \* means significant difference compared to control, ns means not significant.

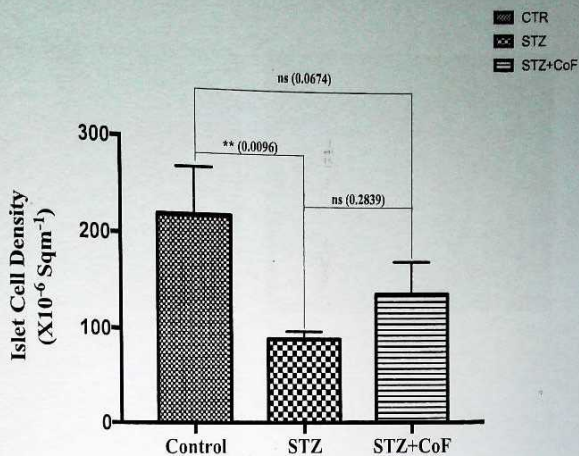


**Figure 4.4:** Islet cell density of pancreas. Bar graph represented mean and SEM values. Statistical comparison between groups was done at ( $p < 0.05$ ), the calculated p values are displayed. \*\* significant difference compared to control, ns means not significant.

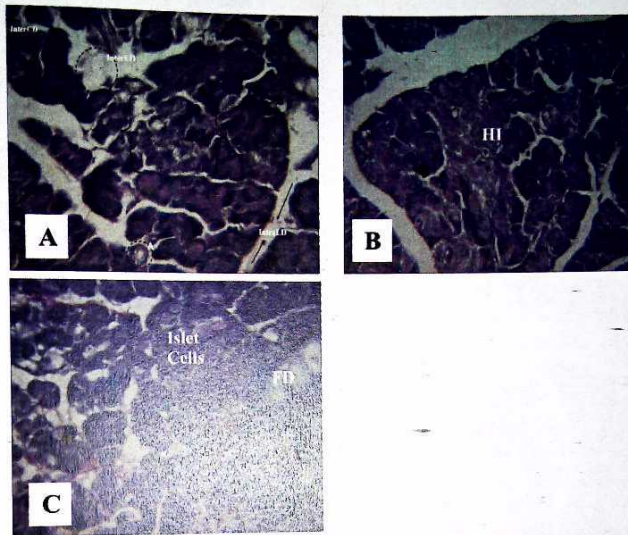


**Plate 4.5:** Representative Hematoxylin and Eosin stained photomicrograph (x400 objective) sections of pancreas. A-Control group; B-STZ group; C-STZ+CoF group. IntraLD: Intralobular duct; A: Acini; InterLD: Interlobular duct; InterCD: Intercalated duct; FD: Fatty droplets in the Intralobular ducts; HI: Hyalinized islets.

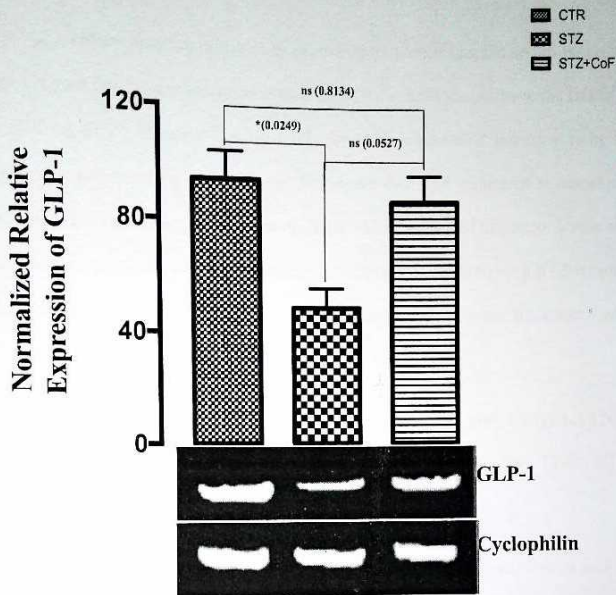


**Figure 4.6:** Expression pattern of glucagon-like peptide - 1 (GLP-1) gene in the intestinal crypt of treatment and control groups. Bar graph represented mean and SEM values of quantified band from control and treatment groups. The gel image is the representative snapshot of the pooled samples. Each bar represented control normalized relative expression (gene/cyclophilin). Statistical comparison between groups was done at ( $p < 0.05$ ), the calculated  $p$  values are displayed. \* means significant difference compared to control, ns means not significant.

#### **4.4 CoF RESTORES STZ-INDUCED LOSS OF KIDNEY FUNCTION IN EXPERIMENTAL NEPHROPATHY**

Routinely, kidney function is clinically examined by monitoring the serum levels of blood urea nitrogen (BUN) and serum creatinine (SC). An animal should have the BG/SC values of  $\geq 300$  mg/dL /  $\geq 80$  mmol/L consistently for 14 days post STZ treatment to be used for the next experiment. Fig. 4.7 (see pg. 59) shows that STZ treatment is associated with increased (not significant,  $p < 0.05$ ) serum BUN which is reduced to control levels with CoF intervention. Similarly, SC is statistically ( $p < 0.05$ ) increased following STZ treatment but not with CoF treatment. There is no significant difference between the control and STZ-CoF group.

#### **4.5 STZ TREATMENT IS ASSOCIATED WITH UP REGULATION OF ANTIOXIDANT AND PRO-INFLAMMATORY GENES IN THE KIDNEY; REVERSAL BY CoF**

Figures 4.9, 4.12 (see pgs. 61, 64) show significantly upregulated TNF- $\alpha$  and MCP-1, respectively in STZ group which is reversed by CoF treatment. TNF-R (Fig. 4.10 see pg. 62) and IL-10 (Fig. 4.11 see pg. 63) were both upregulated in STZ and STZ-CoF groups in comparison with basal control. Figures 4.13, 4.14 and 4.15 (see pgs. 65, 66, 67) show significantly upregulated GPx-1, CAT, and OCC-1, respectively, in STZ group. CoF treatment reverses these effects. KIM-1 (Fig. 4.16 see pg. 68) gene upregulation by STZ, on the other hand is completely reversed following CoF intervention.

#### 4.6 STZ TREATMENT IS ASSOCIATED WITH ORGAN HISTO- STRUCTURAL DAMAGES IN THE KIDNEY; REVERSIBLE WITH CoF TREATMENT

This kidney section (Plate 4.8A see pg 60) of the control group showed normal histology of the cortical part of the kidney, consisting the renal corpuscle, which is perhaps the most distinctive microscopic feature of the kidney; each of the renal corpuscle has Bowman's Capsule (BC) - the outer epithelial wall of the corpuscle, the Bowman's Space (BS) also called urinary space found lying within the BC, the Glomerulus (G), comprising Glomerular capillaries, Podocytes (P), and Mesangial cells (M). The Proximal Convoluted Tubules (PCT), which reabsorbs most minerals and other nutrients from the tubular fluid and passes them to the blood in the Peritubular Capillaries (PC), are also identified in this section. The PCT and corresponding Distal Convoluted Tubules are lined by simple cuboidal epithelium. Also, shown is the Macula densa (MD), a patch of densely-packed epithelial cell nuclei along the DCT, adjacent to the BC, which functions as a sensor for sodium and/or chlorine concentration as well as regulate blood pressure and the filtration rate of the glomerulus.

The kidney ultrastructure depicts various abnormal manifestations in the STZ-alone treated group (Plate 4.8B see pg 60), such as enlarged Bowman's space to thickened basement membrane to atrophied distal tubular epithelial cells and glomerulosclerosis, which are reversed in STZ-CoF group (Plate 4.8C see pg 60).

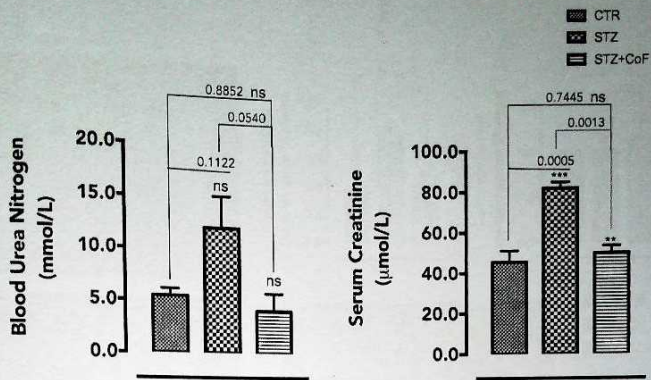


**Figure 4.7:** Kidney function tests: Bar graph representing mean and SEM values of Blood Urea Nitrogen and Serum Creatinine in control, STZ and STZ+CoF treatment groups. Statistical comparison between groups was done at ( $p < 0.05$ ). Calculated p values are displayed. \*\*\* means significant difference compared to control, \*\* means significant difference compared to STZ group, ns means not significant.

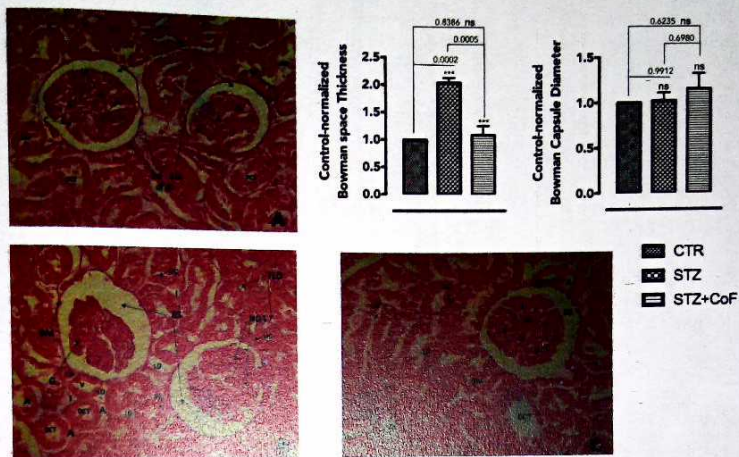


**Plate 4.8:** Haematoxylin and Eosin stained photomicrographs of kidney histomorphological presentations (x400) in Adult male Wistar rats across the various groups: A-Control; B-STZ; C-STZ+CoF. (BC – Bowman’s capsule, BS – Bowman’s Space, PCT – Proximal Convoluted Tubules, DCT – Distal Convoluted Tubules, G – Glomerulus, E – Erythrocytes in glomerular capillaries, MD – Macula densa, P – Podocytes, M – Mesengial cells, C – Capillaries, PC – Peritubular Capillaries, BM – Basement Membrane, I – Interstitial space between tubules, Atrophy – A, NGS - Nodules of Glomerular Scar, LD – Lipid deposits, Blue arrows – FSGS tip variant, TLD – Tubular Lipid Deposits, V – Vacoular modifications). \*\*\* means significant difference compared to control and STZ group, ns means not significant.

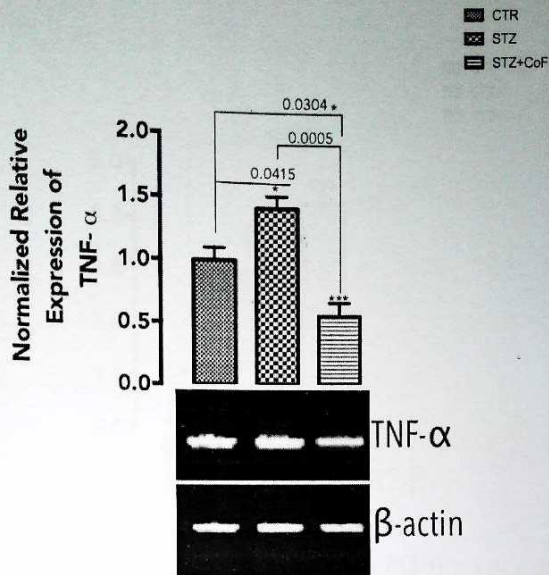


**Figure 4.9:** Expression pattern of inflammatory gene, tumor necrosis factor - alpha (TNF- $\alpha$ ), in kidney of treatment and control groups. Bar graph represented mean and SEM values of quantified band from each sample for specified inflammatory gene in control and treatment groups. The gel image is the representative snapshot of the pooled samples. Each bar represented control normalized relative expression (gene/ $\beta$ -actin). Statistical comparison between groups was done at ( $p < 0.05$ ), the calculated p values are displayed. \* significant compared to control; \*\*\* means significant difference compared to STZ group.

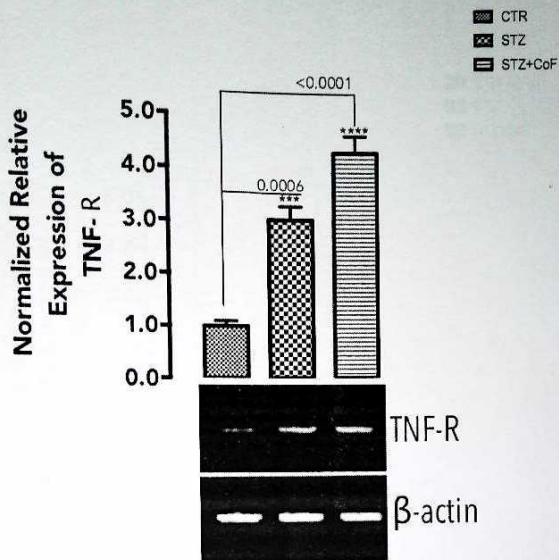


**Figure 4.10:** Expression pattern of inflammatory gene, tumor necrosis factor receptor (TNF-R), in kidney of treatment and control groups. Bar graph represented mean and SEM values of quantified band from each sample for specified inflammatory gene in control and treatment groups. The gel image is the representative snapshot of the pooled samples. Each bar represented control normalized relative expression (gene/ $\beta$ -actin). Statistical comparison between groups was done at ( $p < 0.05$ ), the calculated p values are displayed. \* means significant difference compared to control.

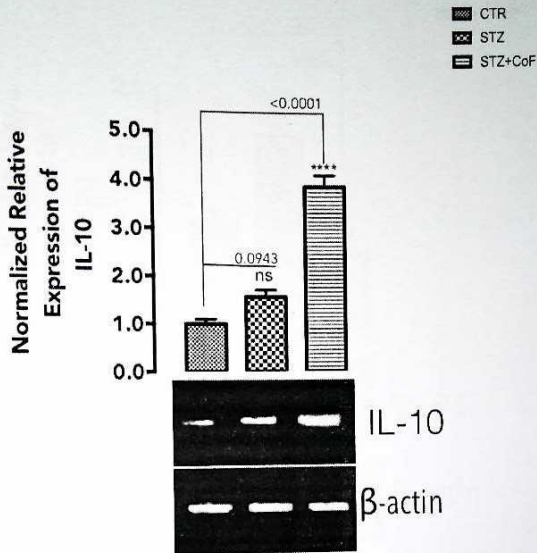


**Figure 4.11:** Expression pattern of inflammatory gene, interleukin -10 (IL-10), in kidney of treatment and control groups. Bar graph represented mean and SEM values of quantified band from each sample for specified inflammatory gene in control and treatment groups. The gel image is the representative snapshot of the pooled samples. Each bar represented control normalized relative expression (gene/ $\beta$ -actin). Statistical comparison between groups was done at ( $p < 0.05$ ), the calculated p values are displayed. \*\*\*\* means significant difference compared to control, ns means not significant.

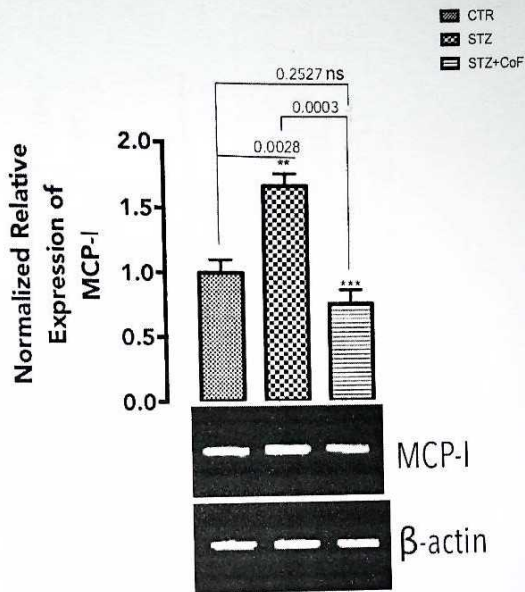


**Figure 4.12:** Expression pattern of inflammatory gene, monocyte chemoattractant protein-1 (MCP-1), in kidney of treatment and control groups. Bar graph represented mean and SEM values of quantified band from each sample for specified inflammatory gene in control and treatment groups. The gel image is the representative snapshot of the pooled samples. Each bar represented control normalized relative expression (gene/ $\beta$ -actin). Statistical comparison between groups was done at ( $p < 0.05$ ), the calculated p values are displayed. \*\* means significant difference compared to control, \*\*\* means significant difference compared to STZ group, ns means not significant.

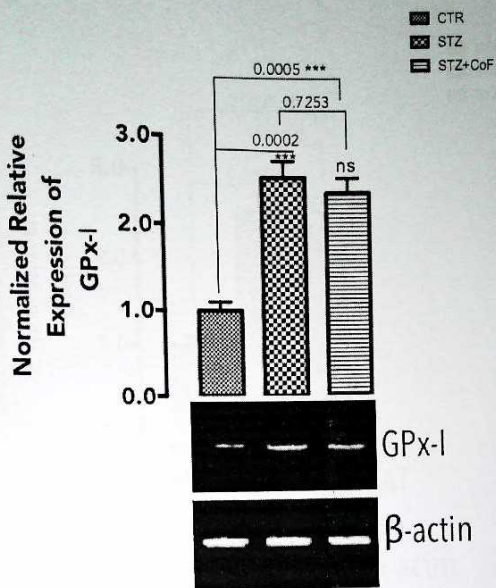


**Figure 4.13:** Expression pattern of antioxidant gene, glutathione peroxidase - 1 (GPx-1), in kidney of treatment and control groups. Bar graph represented mean and SEM values of quantified band from each sample for specified inflammatory gene in control and treatment groups. The gel image is the representative snapshot of the pooled samples. Each bar represented control normalized relative expression (gene/ $\beta$ -actin). Statistical comparison between groups was done at ( $p < 0.05$ ), the calculated p values are displayed. \*\*\* means significant difference compared to control, ns means not significant.

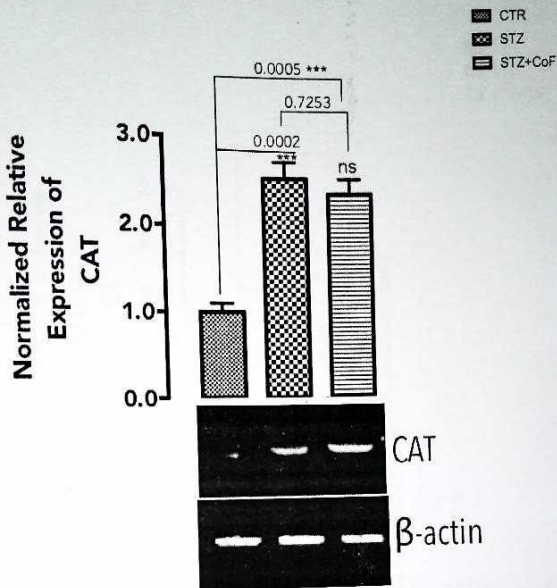


**Figure 4.14:** Expression pattern of antioxidant gene, catalase (CAT), in kidney of treatment and control groups. Bar graph represented mean and SEM values of quantified band from each sample for specified inflammatory gene in control and treatment groups. The gel image is the representative snapshot of the pooled samples. Each bar represented control normalized relative expression (gene/ $\beta$ -actin). Statistical comparison between groups was done at ( $p < 0.05$ ), the calculated p values are displayed. \*\*\* means significant difference compared to control, ns means not significant.

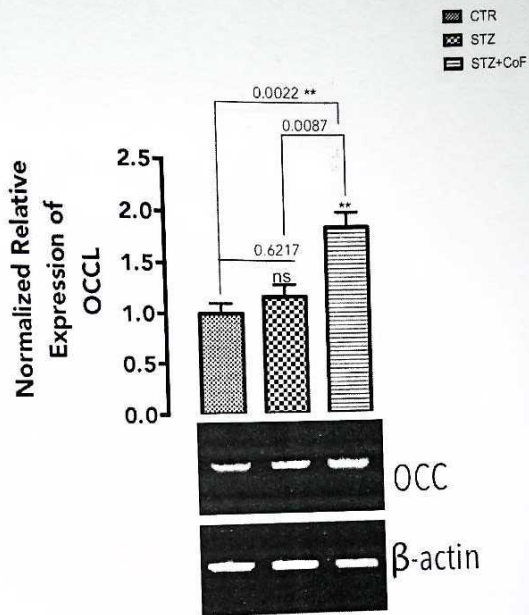


**Figure 4.15:** Expression pattern of occludin (OCC) in kidney of treatment and control groups. Bar graph represented mean and SEM values of quantified band from each sample for specified inflammatory gene in control and treatment groups. The gel image is representative snapshot of the pooled samples. Each bar represented control normalized relative expression (gene/ $\beta$ -actin). Statistical comparison between groups was done at ( $p < 0.05$ ), the calculated p values are displayed. \*\* means significant difference compared to control and STZ, ns means not significant.

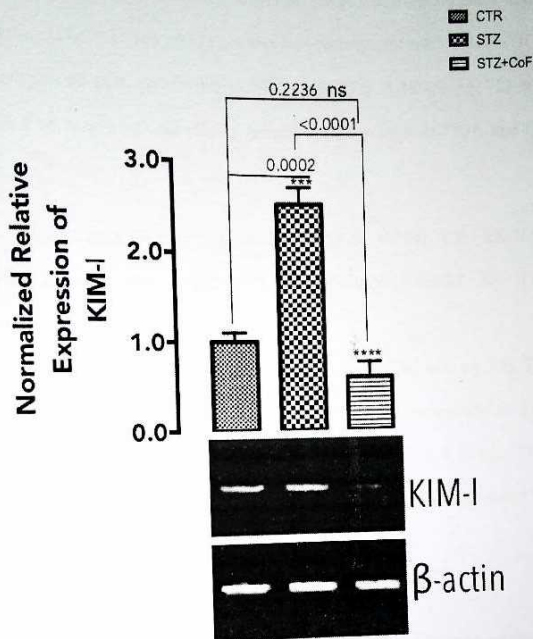


**Figure 4.16:** Expression pattern of kidney injury molecule - 1 (KIM-1) in kidney of treatment and control groups. Bar graph represented mean and SEM values of quantified band from each sample for specified inflammatory gene in control and treatment groups. The gel image is the representative snapshot of the pooled samples. Each bar represented normalized relative expression (gene/ $\beta$ -actin). Statistical comparison between control normalized relative expression ( $p < 0.05$ ), the calculated p values are displayed. \*\*\* means significant difference compared to control and \*\*\*\* means significant difference compared to STZ, ns means not significant.

#### **4.7 CoF RESTORES PROTEIN GLYCOSYLATION ENZYMES IN THE AORTA TO NORMAL LEVELS IN STZ-INDUCED RATS**

The results show that O-GlcNAc transferase (OGT) was significantly upregulated in the STZ group (Fig. 4.18 see pg. 71), while  $\beta$ -N-Acetylglucosaminidase (OGA) expression was upregulated (not significant) in STZ group (Fig. 4.19 see pg. 72) compared to the control. CoF treatment was able to reverse the expression of OGA and OGT to normal levels.

#### **4.8 STZ TREATMENT IS ASSOCIATED WITH UP REGULATION OF ANTIOXIDANT AND PRO-INFLAMMATORY GENES IN THE AORTA; REVERSAL BY CoF**

Pro-inflammatory genes, IL-6 (Fig. 4.20 pg. 73), IL-1 $\beta$  (Fig. 4.21 pg. 74), TNF- $\alpha$  (Fig. 4.22 pg. 75) and MCP-1 (Fig. 4.23 pg. 76) were significantly upregulated in STZ group which was reversed by CoF treatment. Antioxidant genes, CAT (Fig. 4.24 pg. 77) and GPx-1 (Fig. 4.25 pg. 78) which were downregulated as a result of STZ were restored to control levels with CoF treatment

#### **4.9 STZ TREATMENT IS ASSOCIATED WITH ORGAN HISTO-STRUCTURAL DAMAGES IN THE AORTA; REVERSIBLE WITH CoF TREATMENT**

From the histomorphological presentations of the aorta (Plate 4.26 see pg. 79), the control group (A) showed a normal aorta consisting of tunica intima, tunica media, tunica adventitia, and elastic fibers. The diabetic section (B) showed a significant increase in the thickness of tunica media, characterized mainly by compaction of proliferated muscle cells (myocytes) and atherosclerotic lesions (ASL). The CoF-treated group (C) showed reversal of the abnormalities induced by STZ

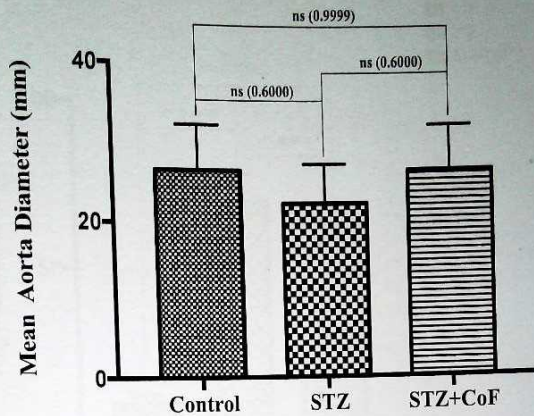


**Figure 4.17:** Aorta Diameter (mm) in treatment and control groups. Bar graph represented mean and SEM values of measured aorta diameters. Statistical comparison between groups was done at ( $p < 0.05$ ), the calculated p values are displayed. ns means not significant.

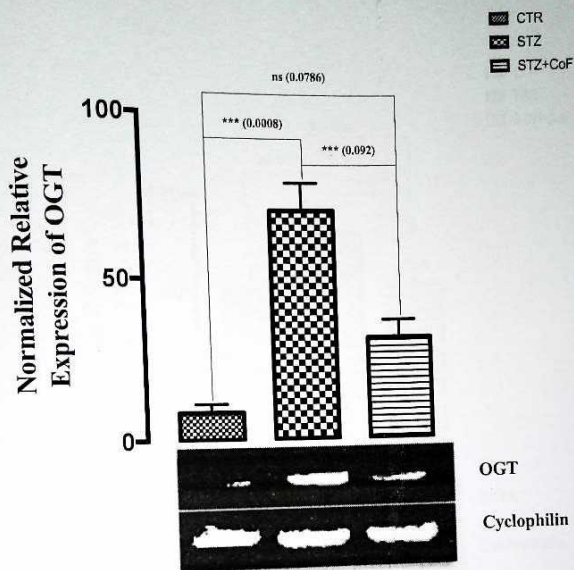


**Figure 4.18:** Expression pattern of protein glycosylation enzyme, O-GlcNAc transferase (OGT) gene in the aorta of treatment and control groups. Bar graph represented mean and SEM values of quantified band from control and treatment groups. The gel image is the representative snapshot of the pooled samples. Each bar represented control normalized relative expression (*gene/cyclophilin*). Statistical comparison between groups was done at ( $p < 0.05$ ), the calculated  $p$  values are displayed. \*\*\* means significant difference compared to control and STZ.

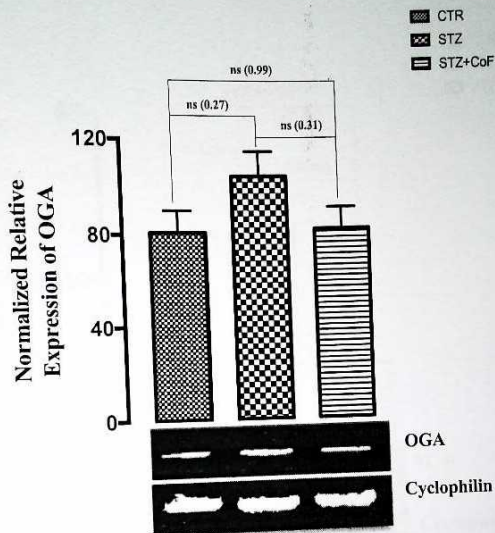


**Figure 4.19:** Expression pattern of protein glycosylation enzyme,  $\beta$ -N-Acetylglucosaminidase (OGA) gene in the aorta of treatment and control groups. Bar graph represented mean and SEM values of quantified band from control and treatment groups. The gel image is the representative snapshot of the pooled samples. Each bar represented control normalized relative expression (gene/cyclophilin). Statistical comparison between groups was done at ( $p < 0.05$ ), the calculated p values are displayed. ns means not significant

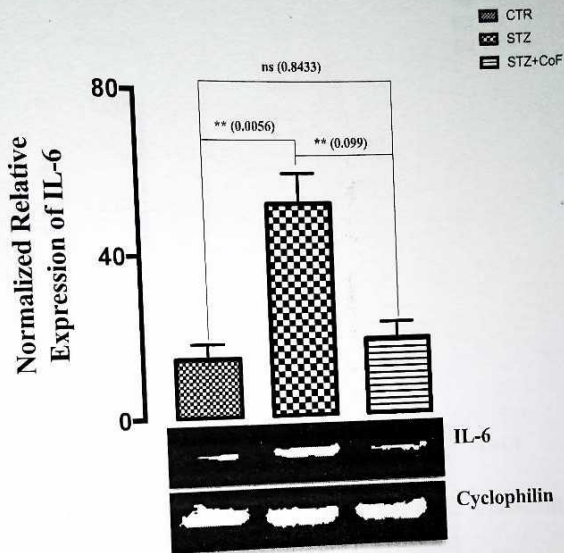


**Figure 4.20:** Expression pattern of inflammatory gene, interleukin 6 (IL-6), in the aorta of treatment and control groups. Bar graph represented mean and SEM values of quantified treatment and control groups. The gel image is the representative snapshot of the band from control and treatment groups. Each bar represented control normalized relative expression (gene/cyclophilin). Statistical comparison between groups was done at ( $p < 0.05$ ), the calculated p values are displayed. \*\* means significant difference compared to control and STZ.

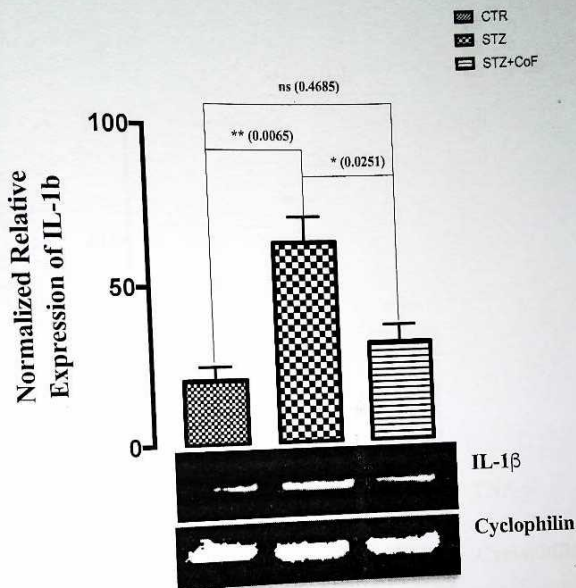


**Figure 4.21:** Expression pattern of inflammatory gene, interleukin -1 beta (IL-1 $\beta$ ), in the aorta of treatment and control groups. Bar graph represented mean and SEM values of quantified band from control and treatment groups. The gel image is the representative snapshot of the pooled samples. Each bar represented control normalized relative expression (gene/cyclophilin). Statistical comparison between groups was done at ( $p < 0.05$ ), the calculated p values are displayed. \*\* means significant difference compared to control and \* means significant difference compared to STZ.

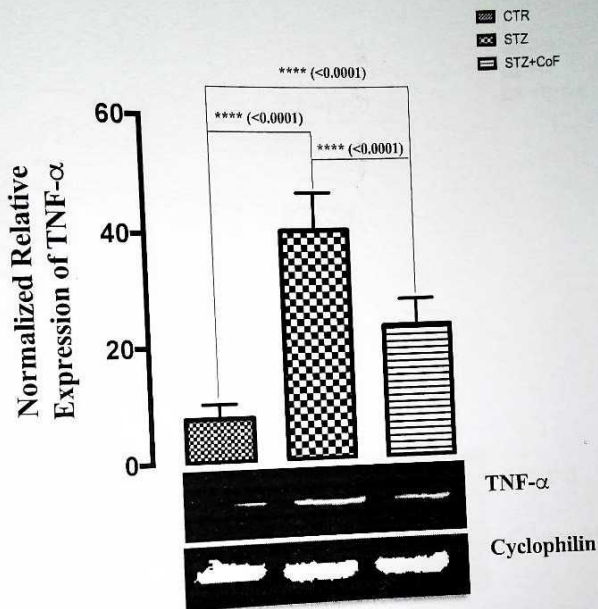


**Figure 4.22:** Expression pattern of inflammatory gene, tumor necrosis factor - alpha (TNF- $\alpha$ ), in the aorta of treatment and control groups. Bar graph represented mean and SEM values of quantified band from control and treatment groups. The gel image is the representative snapshot of the pooled samples. Each bar represented control normalized relative expression (gene/cyclophilin). Statistical comparison between groups was done at ( $p < 0.05$ ), the calculated p values are displayed. \*\*\*\* means significant difference compared to control and STZ.

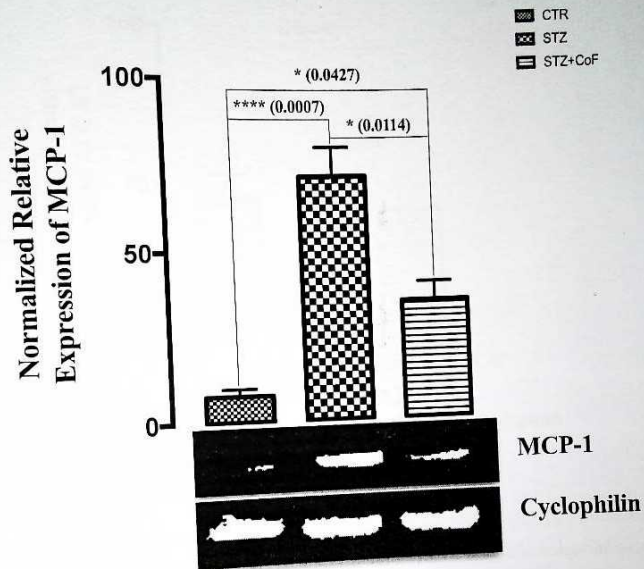


**Figure 4.23:** Expression pattern of inflammatory gene, monocyte chemoattractant protein - 1 (MCP-1), in the aorta of treatment and control groups. Bar graph represented mean and SEM values of quantified band from control and treatment groups. The gel image is the representative snapshot of the pooled samples. Each bar represented control normalized relative expression (gene/cyclophilin). Statistical comparison between groups was done at ( $p < 0.05$ ), the calculated  $p$  values are displayed. \* means significant difference.

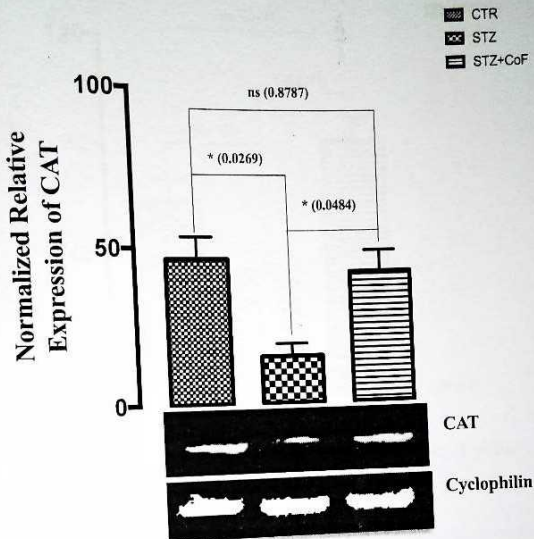


**Figure 4.24:** Expression pattern of antioxidant gene, catalase (CAT), in the aorta of treatment and control groups. Bar graph represented mean and SEM values of quantified pooled samples. Each bar represented control normalized relative expression (gene/cyclophilin). Statistical comparison between groups was done at ( $p < 0.05$ ), the calculated p values are displayed. \* means significant difference compared to control and STZ.

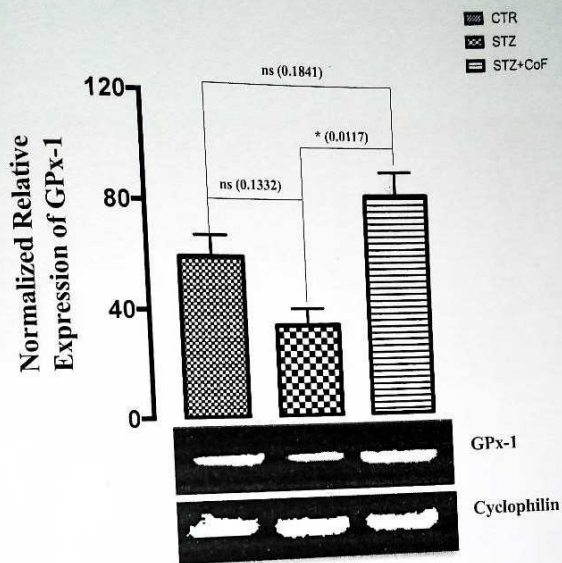


**Figure 4.25:** Expression pattern of antioxidant gene, glutathione peroxidase - 1 (GPx-1), in the aorta of treatment and control groups. Bar graph represented mean and SEM values of quantified band from control and treatment groups. The gel image is the representative snapshot of the pooled samples. Each bar represented control normalized relative expression (gene/cyclophilin). Statistical comparison between groups was done at ( $p < 0.05$ ), the calculated p values are displayed. \* means significant difference compared to STZ, ns means not significant.

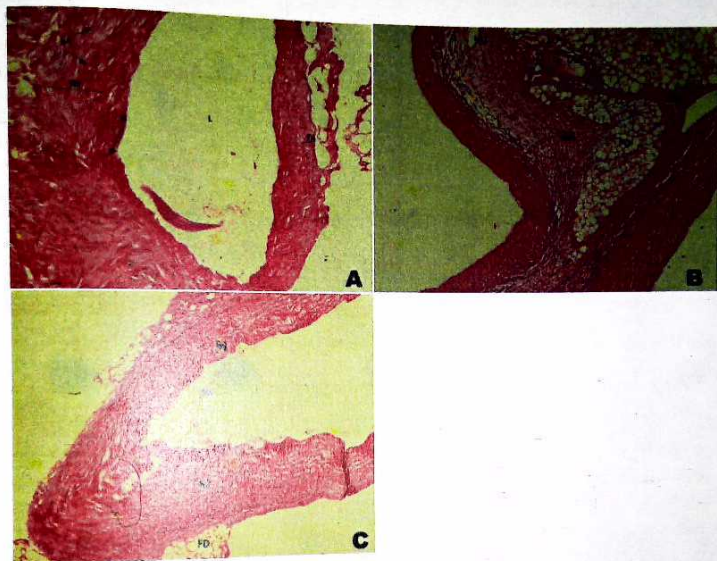


**Plate 4.26:** Photomicrographs showing panoramic views of aorta general histomorphological presentations (x100) in Adult male Wistar rats across the various groups: A-Control; B-STZ; C-STZ+CoF. TI – Tunica intima, TM – Tunica media, TA – Tunica adventitia, EF - Elastic fibers, FD – Fatty droplets, ASL – Artherosclerotic lesion, ULL – Ulcer-like lesion, H – Haemorrhage, M – Macrophages

#### 4.10 NO OBSERVED ADVERSE EFFECT LEVEL (NOAEL)

NOAEL results show that the body weight of the animals increased steadily across the different groups (Fig. 4.27 pg. 81). Urea concentrations (Fig. 4.28 pg. 82) were also within minimal ranges. Evaluation of serum enzymes alanine aminotransferase (Fig. 4.29 pg. 83) and aspartate aminotransferase (Fig. 4.29 pg. 83) levels, which is a biomarker of liver toxicity, showed that the trend was maintained across the groups. From the histomorphological presentation, the islet cells (Fig. 4.31 see pg 85) did not present observable lesions. In the kidney, no visible lesions were seen across groups one to four; group five, however, showed mild interstitial oedema (Fig. 4.32 see pg 86). The liver sections (Fig 4.33 see pg 87) showed mild diffuse vacuolar degeneration of hepatocytes in group 1, mild portal congestion (long arrow), with moderate diffuse vacuolar degeneration of the hepatocytes (short arrows) in group 2, groups 3 and 4 did not present any notable lesions, while very mild portal congestion (long arrows), with diffuse vacuolar degeneration of hepatocytes (short arrows) was observed in group 5.

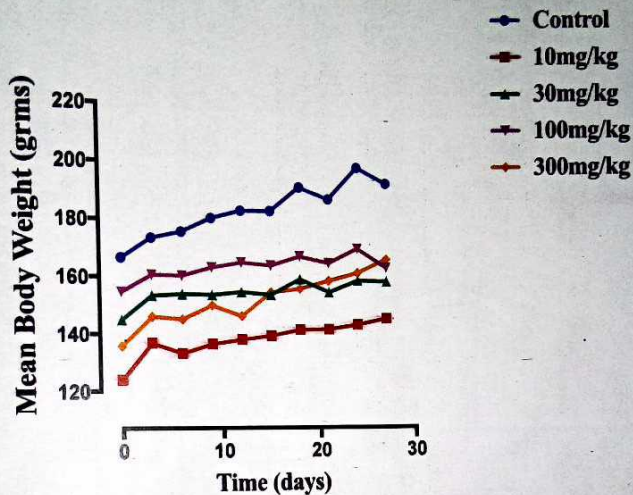
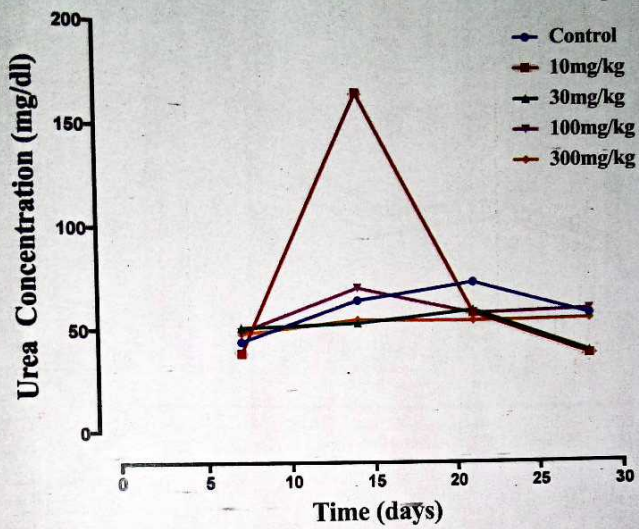


Figure 4.27: Graph of Mean Body Weight of control and treated groups for NOAEL Experiment



**Figure 4.28:** Graph of Urea Concentration in blood plasma of control and treated groups for NOAEL Experiment

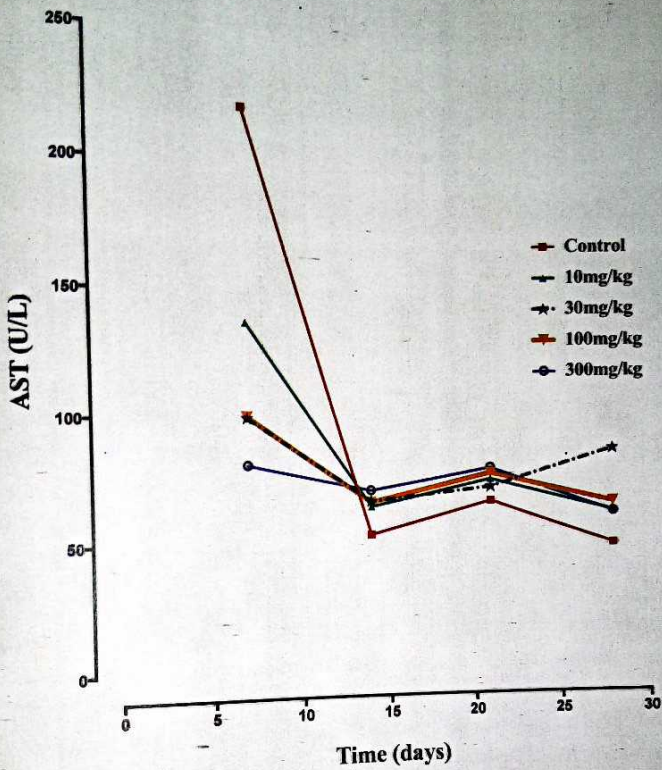
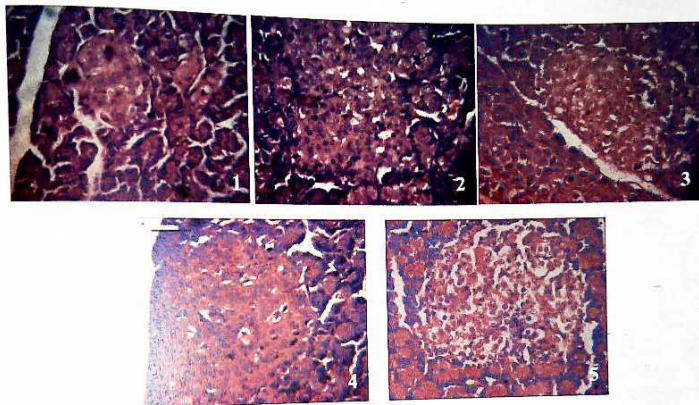
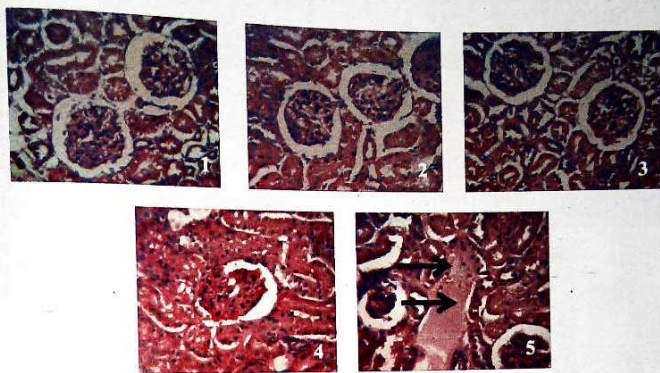


Figure 4.30: Graph of aspartate aminotransferase (AST) levels in blood plasma of control and treated groups for NOAEL Experiment



**Plate 4.31:** Photomicrographs showing panoramic views of pancreas for NOAEL experiment (x400). Group 1 served as the control; Group 2: 10mg/kg bwt.; Group 3: 30mg/kg bwt.; Group 4: 100mg/kg bwt.; Group 5: 300mg/kg bwt. The islets did not present observable lesions



**Plate 4.32:** Photomicrographs showing kidney sections for NOAEL experiment (x400). Group 1 served as the control; Group 2: 10mg/kg bwt.; Group 3: 30mg/kg bwt.; Group 4: 100mg/kg bwt.; Group 5: 300mg/kg bwt. The arrows indicated in group 5 shows pink staining oedema fluid in the interstitial space of the renal cortex (arrows), all other groups did not have lesions

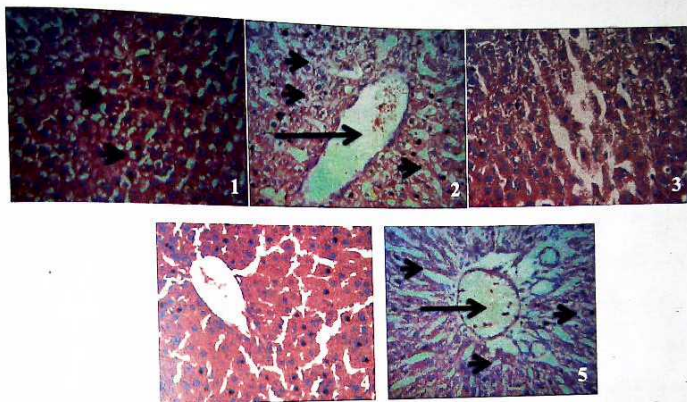


**Plate 4.33:** Photomicrographs showing liver sections for NOAEL experiment (x400): Group 1 served as the control; Group 2: 10mg/kg bwt.; Group 3: 30mg/kg bwt.; Group 4: 100mg/kg bwt.; Group 5: 300mg/kg bwt. The arrows indicated in the Figure show group 1-mild diffuse vacuolar degeneration of hepatocytes (short arrows); group 2-mild portal congestion (long arrow), with moderate diffuse vacuolar degeneration of the hepatocytes (short arrows); groups 3 and 4 did not present any notable lesions while group 5-very mild portal congestion (long arrows), with diffuse vacuolar degeneration of hepatocytes (short arrows).

#### 4.11 CoF ELICITS SIMILAR TGR5 INTERACTION AS KNOWN AGONIST IN MOLECULAR DOCKING STUDIES

The lack of 3D structure constitutes a major drawback to the development of novel drugs acting at TGR5. To circumvent this challenge, TGR5 model built on rhodopsin template (inactive state) has been used to identify key residues involved in ligand binding. This model explicitly explained the roles of Y89<sup>3,29</sup> and N93<sup>3,33</sup> in agonist binding but not E169<sup>5,43</sup>, whose roles have been established from mutagenesis studies. The apparent inability of rhodopsin-based model to account for all interactions may have instructed the choice of an active state model built on  $\beta$ 2 adrenergic receptor-Gs protein complex. Another model built on human adenosine A2A receptor (intermediate state) in adenosine (agonist)-bound state also accounted for the roles of Y89<sup>3,29</sup>, N93<sup>3,33</sup> and E169<sup>5,43</sup> when bound to 6 $\alpha$ -ethyl-3 $\alpha$ ,7 $\alpha$ -dihydroxy-24-nor-5 $\beta$ -cholan-23-yl-23-triethylammonium sulfate (INT-767) after taking full advantage of ligand mobility and side chain flexibility associated with MD simulation. In this study, rather than starting from the fully active conformation, an intermediate conformation was preferred in order to study the evolution associated with intermediate-active state transition. Therefore, the starting model was built on human adenosine A2A receptor (PDB ID: 2YDO) template. This model revealed that only Y89<sup>3,29</sup> and N93<sup>3,33</sup> interacted with atoms of 5,7-dihydroxyl-6,4-dimethoxyl flavanone (CoF) but not E169<sup>5,43</sup> (Fig. 4.34 A see pg. 89) and S270<sup>7,42</sup> as reported for bile acids (Fig. 4.34 B see pg. 89) in previous mutagenesis studies.

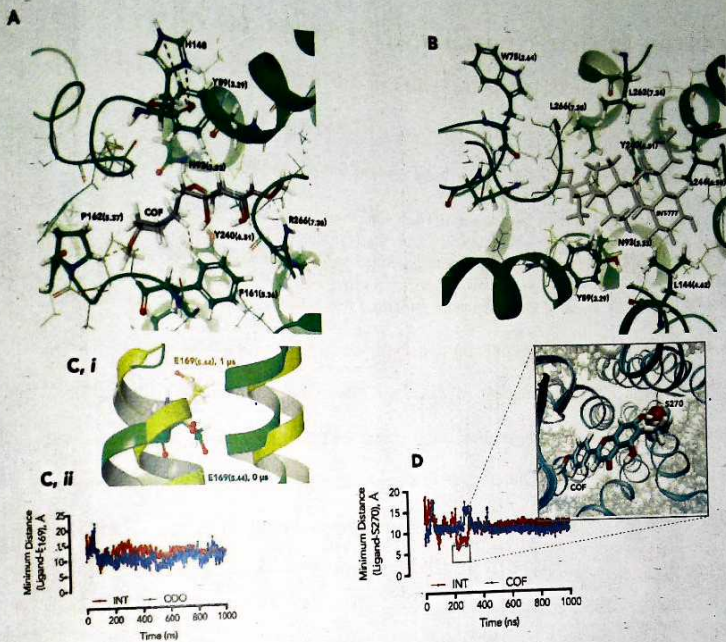


**Figure 4.34:** Binding pose of ligand within TGR5 orthosteric site. The docking pose of CoF (A) and INT-777 (B) within the orthosteric site of TGR5 showing proximity to residues (N93<sup>3.33</sup> and Y89<sup>3.29</sup>) previously identified in mutagenesis studies. (C): Molecular dynamics simulation shows the flipping of E169<sup>5.44</sup> into the helical core during the simulation. (D): Line graph showing the distance between S270<sup>7.42</sup> hydroxyl side chain and the atoms of CoF and INT-777 during the simulation.

#### 4.12 TGR5 IN CoF BOUND STATE ELICITS CONTINUOUS INTERNAL WATER PATHWAY THAT SINKS IN THE (E)-DRY MOTIF

Several G-protein-coupled receptors (GPCRs), whose 3D structures have been determined (crystallography) in agonist bound states, have shown highly ordered internal water molecules within the transmembrane helices. The functional role of the waters has been pinned to receptor activation using molecular dynamics simulations. NPxxY motif is shown to play a significant role in the water tunneling mechanism by Yuan et al. (2014) which is required for breaking the ionic lock contributed by the DRY-motif. In this study, TGR5 was investigated for such internal water pathways in the presence of CoF, INT-777 in comparison to an antagonist and apo state. In all the four complexes studied, no internal water tunnel was observed within the first 20 ns post equilibration (Fig. 4.35A see pg. 90). TGR5-bound CoF began to evolve continuous internal water patterns starting from 140 ns with an interesting pattern at 150 ns (Fig. 4.35B, *i*)

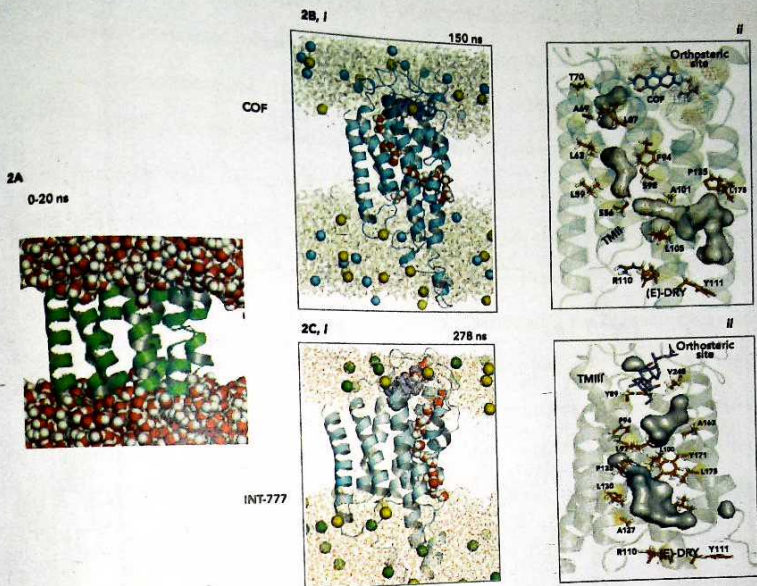


**Figure 4.35:** TGR5 evolves continuous internal water pathway in CoF and INT-777 bound states. (A) The average structure between 0 and 20ns showed no internal water pathway in states. (B, i) A representative snapshot of CoF-bound TGR5 showing highly ordered water pathway connecting the ligand to the TMIII-TMVI interface at 150 ns; (B, ii) Volumetric analysis of the water tunnel during the simulation. (C, i) A representative snapshot of INT-777-bound TGR5 showing highly ordered water pathway connecting the ligand to the TMIII-TMVI interface at 278 ns; (C, ii) Volumetric analysis of the water tunnel during the simulation. (TGR5 is presented as cartoon, water is represented as VMD, or surface plot).

#### 4.13 LIGAND-SENSITIVE TOGGLE SWITCHES IN TGR5

Aromatic Amino acids lining the crevice of the orthosteric site have been shown to play a key role in receptor activation. These aromatic amino acid clusters form a toggle switch *via* rotameric mechanisms. The rotameric mechanism has been well reported in adrenergic receptor-catecholamine bound state. Aromatic catechol ring in this complex influences the rotameric angles adoptable by W286<sup>6.48</sup> and F290<sup>6.52</sup> which ultimately promote a large conformational change around the transmembrane (TM) III and TMVI and rupturing of the ionic lock which keeps the receptor in the inactive state (Humphrey *et al.*, 1996). Agonist bound rhodopsin is another classical example of highlighting the key role of rotameric toggle switch in agonist-mediated activation. The side chain of W265<sup>6.48</sup> (TMVI) of rhodopsin protrudes into the ligand binding space in the apo state but retracts in the presence of an agonist; this movement significantly contributes to the disruption of the ionic lock formed between E113<sup>3.28</sup> (TMIII) and K296<sup>7.43</sup> (TMVII) thus, resulting in receptor activation (Fig. 4.36 see pg. 93).

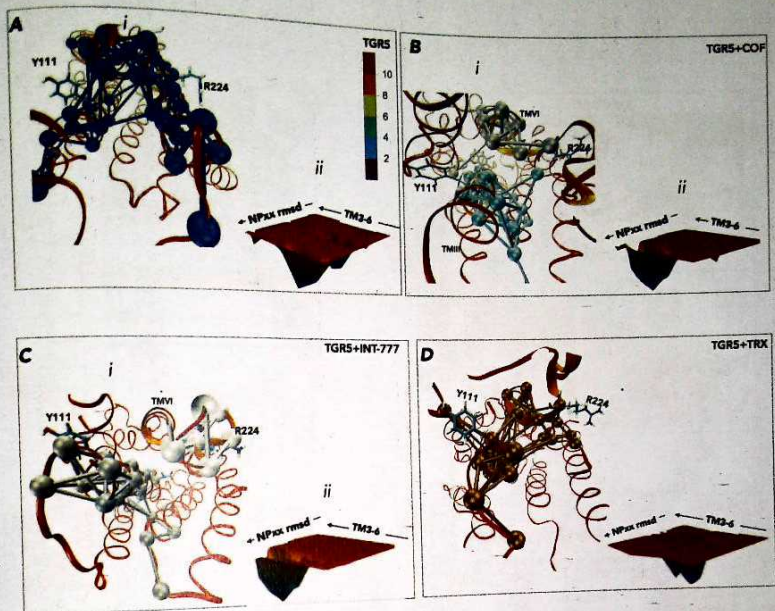


**Figure 4.36:** Dynamic network and free-energy surface plots. (A, *i*) Dynamic network between cytoplasmic ends of TMIII-TMVI in apo state and its free energy surface plots (*ii*) projected along TMIII-TMVI distance and NPxxY rmsd parameters. (B, *i*) Dynamic network between cytoplasmic ends of TMIII-TMVI in COF-bound state and its free energy surface plots (*ii*) projected along TMIII-TMVI distance and NPxxY rmsd parameters. (C, *i*) Dynamic network between cytoplasmic ends of TMIII-TMVI in INT-777-bound state and its free energy surface plots (*ii*) projected along TMIII-TMVI distance and NPxxY rmsd parameters. (D, *i*) Dynamic network between cytoplasmic ends of TMIII-TMVI in TRX-bound state and its free energy surface plots (*ii*) projected along TMIII-TMVI distance and NPxxY rmsd parameters.

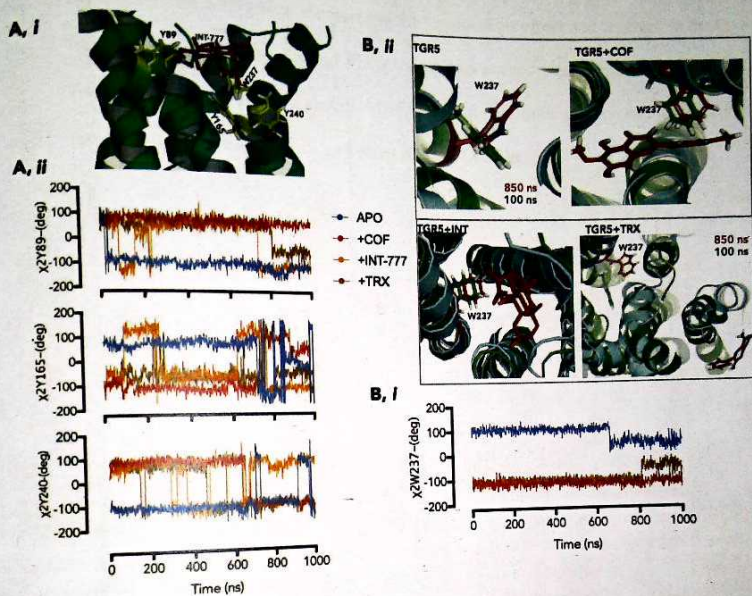


**Figure 4.37:** Rotameric Switch candidates in the orthosteric site of TGR5. (A, *i*) CoF (pink stick, without hydrogen) in TGR5 bound state showing proximal aromatic amino acids (Y89<sup>3.29</sup>, Y165<sup>5.40</sup>, Y240<sup>6.51</sup> and W237<sup>6.48</sup>) (A, *ii*) Line graph of +2-dihedral angle of Y89<sup>3.29</sup>, Y165<sup>5.40</sup>, and Y240<sup>6.51</sup> along the trajectories. (B, *i*) Line graph of +2-dihedral angle W237<sup>6.48</sup> along the trajectories (B, *ii*) Superposition of 100 ns (green cartoon) snapshot of TGR5 and 850 ns (cyan cartoon) showing W237 (stick) and the ligands (stick).

#### 4.14 PANCREATIC RESPONSE TO CoF AND METFORMIN

Insulin (Fig 4.38 see pg. 96) and PDX-1(Fig 4.39 see pg. 97) genes were significantly decreased in the STZ group, compared to the control. This effect was reversed in the CoF-treated group, where insulin and PDX-1 gene expressions were significantly increased compared to control and STZ groups. Metformin restored insulin gene expression to control levels, however, it did not have any effect on the PDX-1 gene.

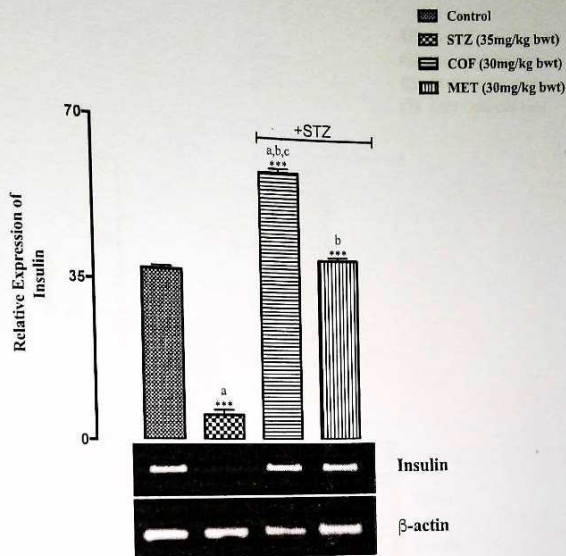


**Figure 4.38:** Expression pattern of insulin gene in the pancreas of treatment and control groups. Bar graph represented mean and SEM values of quantified band from control and treatment groups. The gel image is the representative snapshot of the pooled samples. Each bar represented control normalized relative expression (gene/ $\beta$ -actin). Statistical comparison between groups was done at ( $p < 0.05$ ), a is significant, compared to control group; b is significant, compared to STZ group; c is significant, compared to MET group.

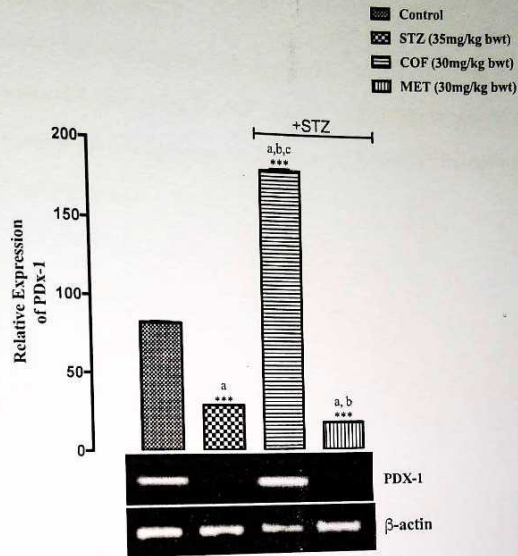


**Figure 4.39:** Expression pattern of pancreatic duodenal box-1 gene in the pancreas of treatment and control groups. Bar graph represented mean and SEM values of quantified band from control and treatment groups. The gel image is the representative snapshot of the pooled samples. Each bar represented control normalized relative expression (gene/ $\beta$ -actin). Statistical comparison between groups was done at ( $p < 0.05$ ), a is significant, compared to control group; b is significant, compared to STZ group; c is significant, compared to MET group.

#### 4.15 CoF, BUT NOT METFORMIN, MODULATES CIRCULATING GLP-1 AND GLP-2 IN INTESTINAL CRYPT

GLP-1 and GLP-2 gene expressions were significantly upregulated in the CoF-treated group, compared to all other groups (Fig 4.40 and 4.41, respectively see pgs. 99 and 100). Metformin treatment showed significant expression of GLP-1 and GLP-2 gene compared to the control and STZ groups.

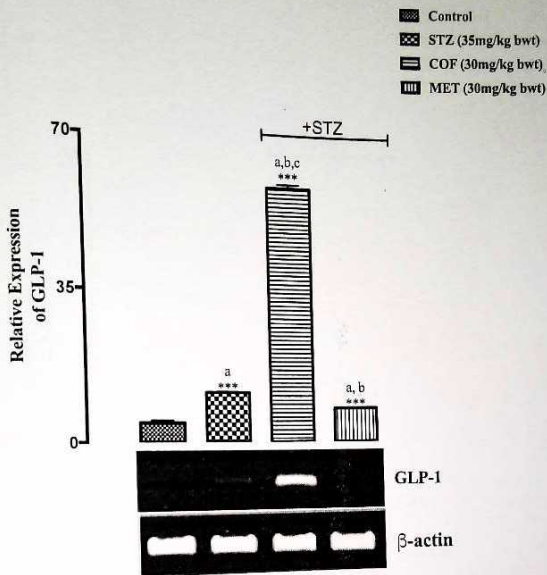


**Figure 4.40:** Expression pattern of glucagon-like peptide-1 gene in the intestinal crypt of treatment and control groups. Bar graph represented mean and SEM values of quantified band from control and treatment groups. The gel image is the representative snapshot of the pooled samples. Each bar represented control normalized relative expression (gene/ $\beta$ -actin). Statistical comparison between groups was done at ( $p < 0.05$ ), a is significant, compared to control group; b is significant, compared to STZ group; c is significant, compared to MET group.

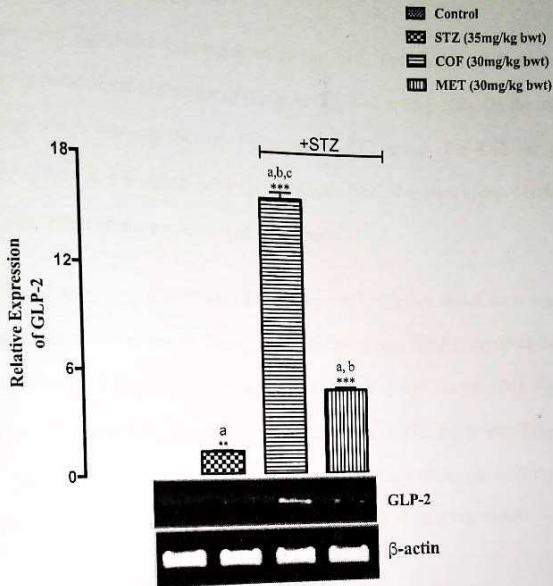


**Figure 4.41:** Expression pattern of glucagon-like peptide-2 gene in the intestinal crypt of treatment and control groups. Bar graph represented mean and SEM values of quantified pooled samples. Each bar represented control normalized relative expression (gene/ $\beta$ -actin). Statistical comparison between groups was done at ( $p < 0.05$ ), a is significant, compared to control group; b is significant, compared to STZ group; c is significant, compared to MET group.

#### 4.16 ACTION OF CoF AND METFORMIN ON THE AORTA OF EXPERIMENTAL ANIMALS

OGT gene was significantly upregulated in the STZ, CoF and metformin treatments significantly reduced the expression of this gene (Fig 4.42 see pg. 102). On the other hand, OGA gene which was significantly decreased in STZ group (Fig 4.43 see pg. 103), compared to control, was significantly upregulated in the CoF-treated group. Metformin did not have any effect on the expression of this gene.

GPx-1 (Fig. 4.44 see pg. 104) and CAT (4.45 see pg. 105) genes which were significantly downregulated in STZ group were upregulated in CoF group. Metformin upregulated GPx-1 but not CAT gene. Significantly upregulated TNF- $\alpha$  (Fig 4.46 see pg. 106), MCP-1 (Fig 4.47 see pg. 107) and IL-1 $\beta$  (Fig 4.48 see pg. 108) genes in STZ group were fully reversed with CoF and metformin treatments. CoF restored IL-6 (Fig 4.49 see pg. 109) even beyond control levels, but metformin treatment had no effect on IL-6 gene expression.

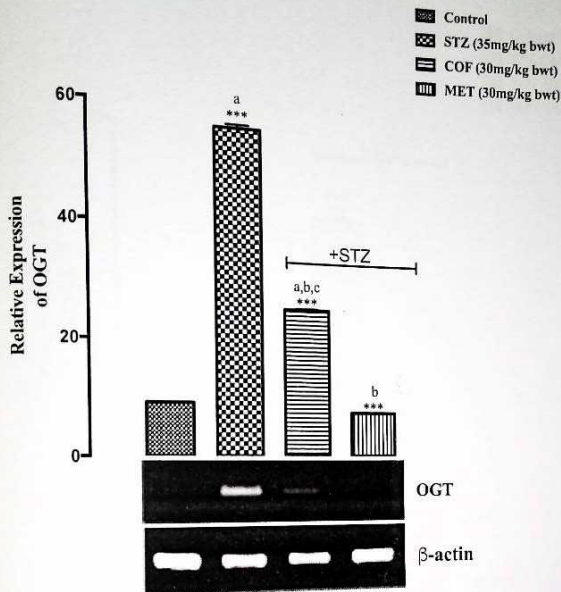


**Figure 4.42:** Expression pattern of O-GlcNAc transferase gene in the aorta of treatment and control groups. Bar graph represented mean and SEM values of quantified band from control and treatment groups. The gel image is the representative snapshot of the pooled samples. Each bar represented control normalized relative expression (gene/ $\beta$ -actin). Statistical comparison between groups was done at ( $p < 0.05$ ), a is significant, compared to control group; b is significant, compared to STZ group; c is significant, compared to MET group.

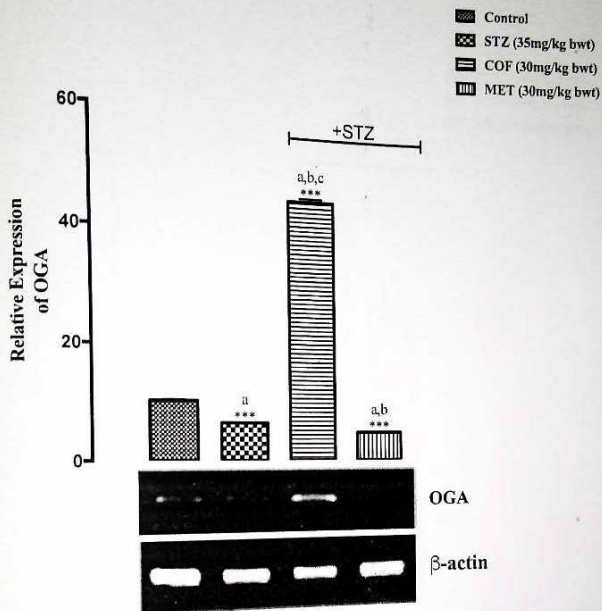


**Figure 4.43:** Expression pattern of  $\beta$ -N-Acetylglucosaminidase gene in the aorta of treatment and control groups. Bar graph represented mean and SEM values of quantified treatment and control groups. Bar graph represented mean and SEM values of quantified treatment and control groups. The gel image is the representative snapshot of the pooled samples. Each bar represented control normalized relative expression (gene/ $\beta$ -actin). Statistical comparison between groups was done at ( $p < 0.05$ ), a is significant, compared to control group; b is significant, compared to STZ group; c is significant, compared to MET group.

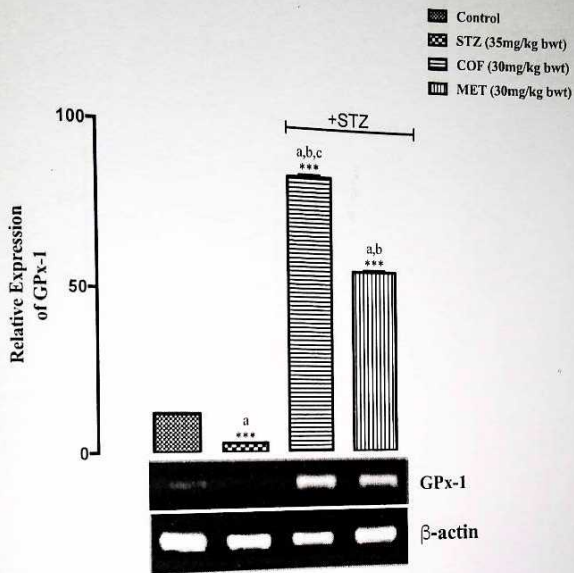


**Figure 4.44:** Expression pattern of glutathione peroxidase-1 in the aorta of treatment and control groups. Bar graph represented mean and SEM values of quantified band from control and treatment groups. The gel image is the representative snapshot of the pooled samples. Each bar represented control normalized relative expression (gene/ $\beta$ -actin). Statistical comparison between groups was done at ( $p < 0.05$ ), a is significant, compared to control group; b is significant, compared to STZ group; c is significant, compared to MET group.

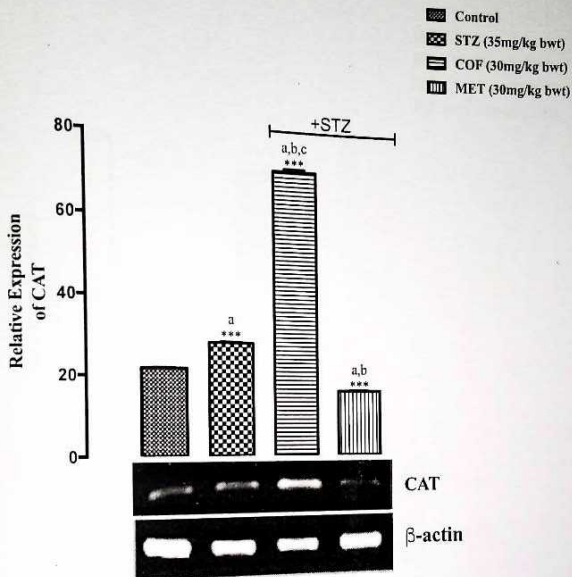


**Figure 4.45:** Expression pattern of catalase gene in the aorta of treatment and control groups. Bar graph represented mean and SEM values of quantified band from control and treatment groups. The gel image is the representative snapshot of the pooled samples. Each bar represented control normalized relative expression (gene/ $\beta$ -actin). Statistical comparison between groups was done at ( $p < 0.05$ ), a is significant, compared to control group; b is significant, compared to STZ group; c is significant, compared to MET group.

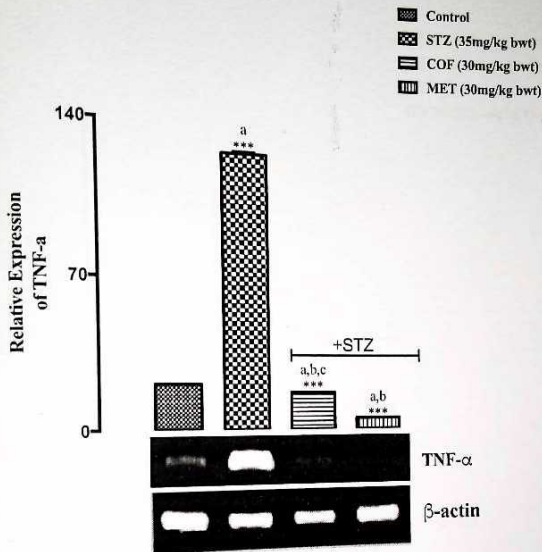


**Figure 4.46:** Expression pattern of tumor necrosis factor- $\alpha$  gene in the aorta of treatment and control groups. Bar graph represented mean and SEM values of quantified band from control and treatment groups. The gel image is the representative snapshot of the pooled samples. Each bar represented control normalized relative expression (gene/ $\beta$ -actin). Statistical comparison between groups was done at ( $p < 0.05$ ), a is significant, compared to control group; b is significant, compared to STZ group; c is significant, compared to MET group.

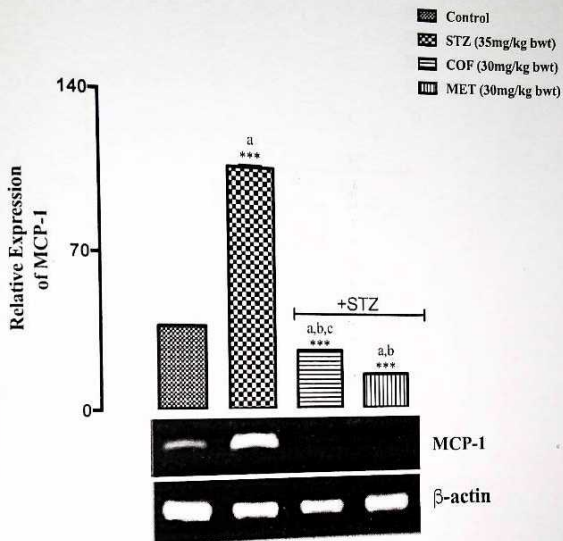


**Figure 4.47:** Expression pattern of monocyte chemoattractant protein-1 gene in the aorta of treatment and control groups. Bar graph represented mean and SEM values of quantified treatment and control groups. Bar graph represented mean and SEM values of quantified treatment and control groups. The gel image is the representative snapshot of the pooled samples. Each bar represented control normalized relative expression (gene/ $\beta$ -actin). Statistical comparison between groups was done at ( $p < 0.05$ ), a is significant, compared to control group; b is significant, compared to STZ group; c is significant, compared to MET group.

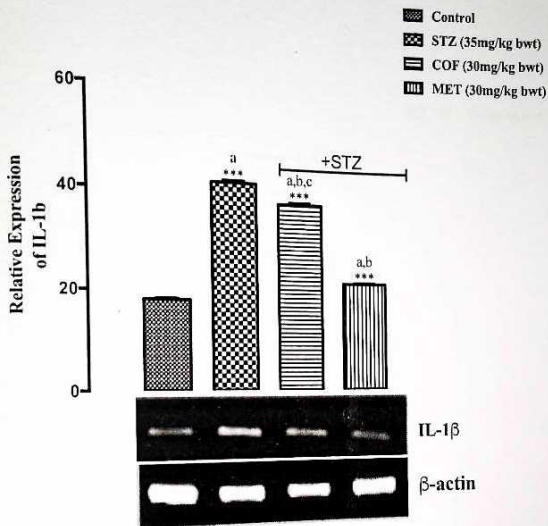


**Figure 4.48:** Expression pattern of Interleukin-1 beta gene in the aorta of treatment and control groups. Bar graph represented mean and SEM values of quantified band from control and treatment groups. The gel image is the representative snapshot of the pooled samples. Each bar represented control normalized relative expression (gene/ $\beta$ -actin). Statistical comparison between groups was done at ( $p < 0.05$ ), a is significant, compared to control group; b is significant, compared to STZ group; c is significant, compared to MET group.

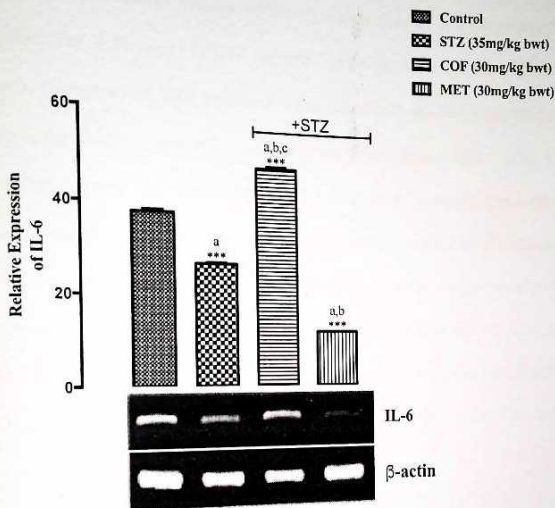


**Figure 4.49:** Expression pattern of Interleukin-6 gene in the aorta of treatment and control groups. Bar graph represented mean and SEM values of quantified band from control and treatment groups. The gel image is the representative snapshot of the pooled samples. Each bar represented control normalized relative expression (gene/ $\beta$ -actin). Statistical comparison between groups was done at ( $p < 0.05$ ), a is significant, compared to control group; b is significant, compared to STZ group; c is significant, compared to MET group.

#### 4.17 ACTION OF CoF AND METFORMIN ON THE KIDNEY OF EXPERIMENTAL ANIMALS

As expected, STZ caused damage to kidney which resulted to upregulated KIM-1 gene expression (Fig. 4.50 pg. 111). CoF and MET however, downregulated KIM-1 expression to normal control levels. STZ treatment is associated with decreased antioxidant activity as well as upregulation of pro-inflammatory genes in the kidney. GPx-1 (Fig. 4.51 pg. 112) gene expression was significantly decreased in STZ group, however, this is reversed in CoF and MET treated groups. Treatment with MET and CoF significantly decreased TNF- $\alpha$  (Fig. 4.52 pg. 113) and TNF-R (Fig. 4.53 pg. 114) genes. CoF also significantly decreased the expression of MCP-1 (Fig. 4.54 pg. 115) gene. MET however did not have any effect on MCP-1 gene. The expression of anti-inflammatory gene IL-10, was significantly decreased in STZ group, compared to the control, whereas, CoF and MET treatments upregulated the expression levels of IL-10 (Fig. 4.55 pg. 116).

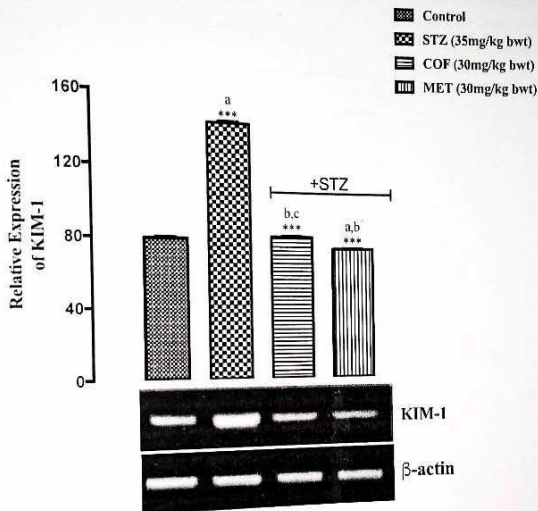


**Figure 4.50:** Expression pattern of kidney injury molecule-1 gene in kidney of treatment and control groups. Bar graph represented mean and SEM values of quantified band from control and treatment groups. The gel image is the representative snapshot of the pooled samples. Each bar represented control normalized relative expression (gene/ $\beta$ -actin). Statistical comparison between groups was done at ( $p < 0.05$ ), a is significant, compared to control group; b is significant, compared to STZ group; c is significant, compared to MET group.

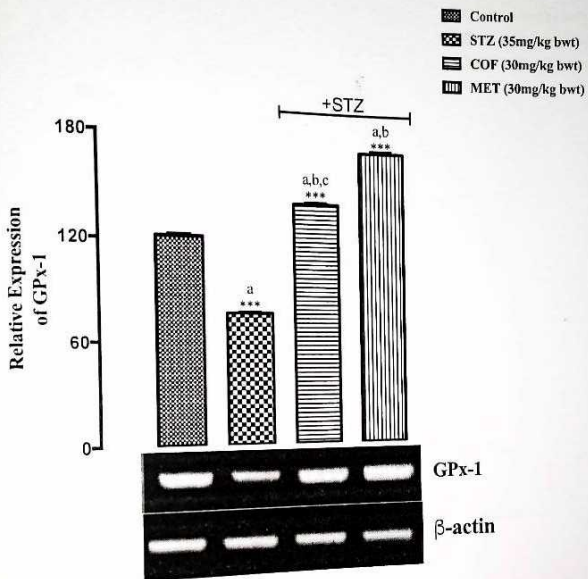


**Figure 4.51:** Expression pattern of glutathione peroxidase-1 gene in kidney of treatment and control groups. Bar graph represented mean and SEM values of quantified band from control and treatment groups. The gel image is the representative snapshot of the pooled samples. Each bar represented control normalized relative expression (gene/ $\beta$ -actin). Statistical comparison between groups was done at ( $p < 0.05$ ). a is significant, compared to control group; b is significant, compared to STZ group; c is significant, compared to MET group.

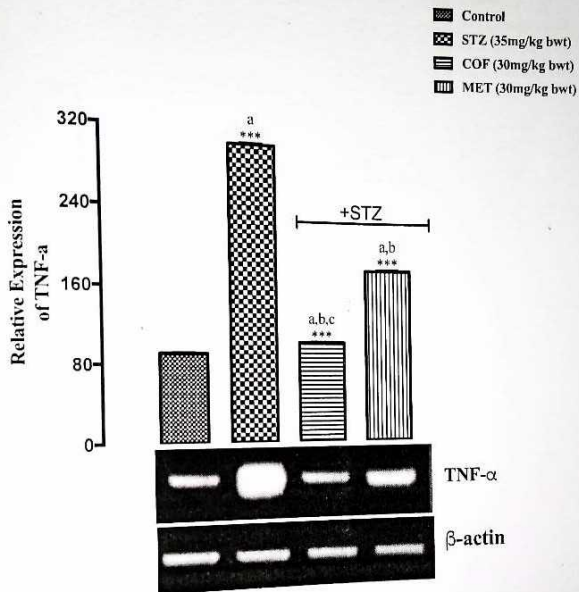


**Figure 4.52:** Expression pattern of tumor necrosis factor-alpha gene in kidney of treatment and control groups. Bar graph represented mean and SEM values of quantified band from control and treatment groups. The gel image is the representative snapshot of the pooled samples. Each bar represented control normalized relative expression (gene/ $\beta$ -actin). Statistical comparison between groups was done at ( $p < 0.05$ ), a is significant, compared to control group; b is significant, compared to STZ group; c is significant, compared to MET group.

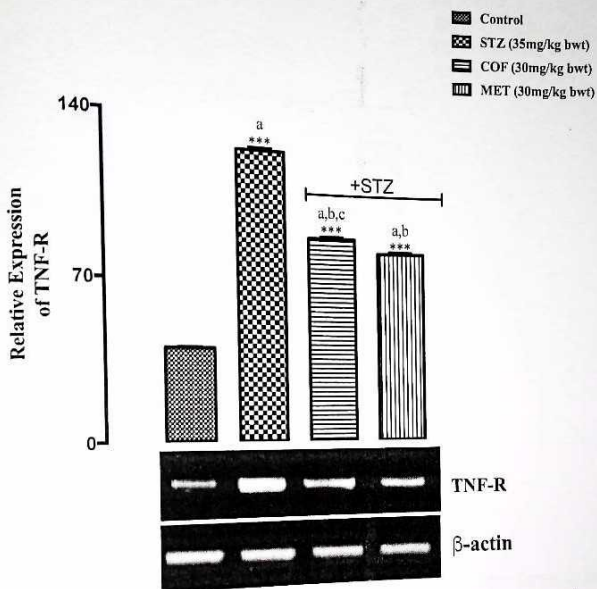


**Figure 4.53:** Expression pattern of tumor necrosis factor receptor gene in kidney of treatment and control groups. Bar graph represented mean and SEM values of quantified pooled samples. Each bar represented control normalized relative expression (gene/ $\beta$ -actin). Statistical comparison between groups was done at ( $p < 0.05$ ), a is significant, compared to control group; b is significant, compared to STZ group; c is significant, compared to MET group.

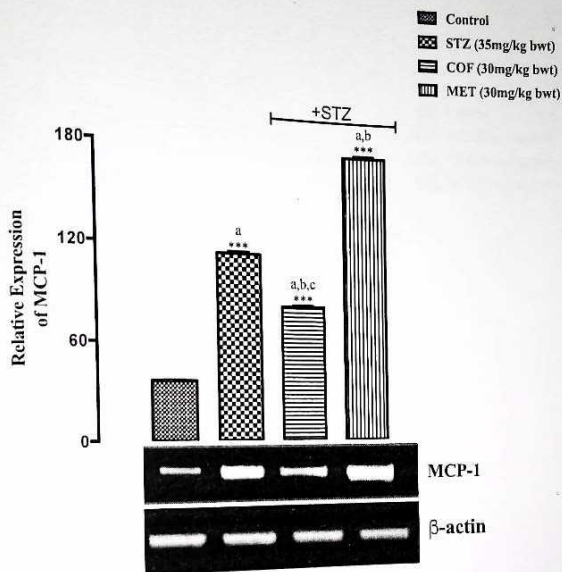


**Figure 4.54:** Expression pattern of monocyte chemoattractant protein-1 gene in kidney of treatment and control groups. Bar graph represented mean and SEM values of quantified treatment and control groups. The gel image is the representative snapshot of the pooled samples. Each bar represented control normalized relative expression (gene/ $\beta$ -actin). Statistical comparison between groups was done at ( $p < 0.05$ ), a is significant, compared to control group; b is significant, compared to STZ group; c is significant, compared to MET group.

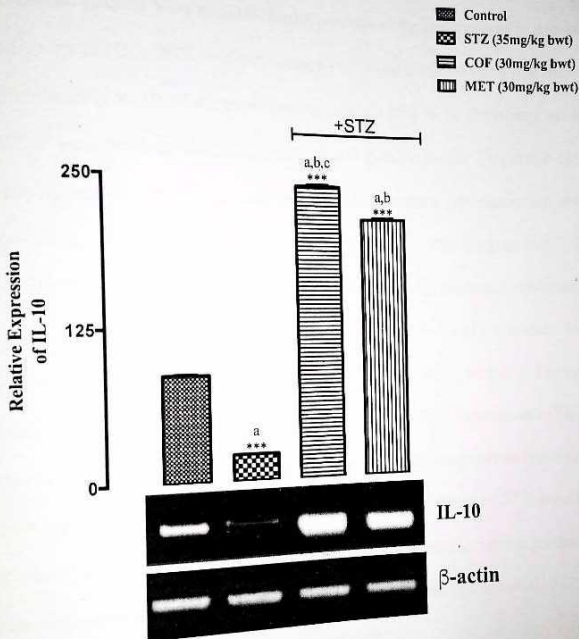


**Figure 4.55:** Expression pattern of Interleukin-10 gene in kidney of treatment and control groups. Bar graph represented mean and SEM values of quantified band from control and treatment groups. The gel image is the representative snapshot of the pooled samples. Each bar represented control normalized relative expression (gene/ $\beta$ -actin). Statistical comparison between groups was done at ( $p < 0.05$ ), a is significant, compared to control group; b is significant, compared to STZ group; c is significant, compared to MET group.

## CHAPTER FIVE

### 5.0 DISCUSSION

In this study, cardiovascular complications, nephropathy, and damage to pancreatic beta cells (PBCs) associated with STZ treatment and its challenge with CoF treatment in experimental animals were studied. Insulin production by the pancreas is dependent on the functionality of PBCs. STZ evidently caused PBC destruction, leading to a diabetic state as seen in the FBS levels of the experimental animals (Fig. 4.1). Treatment of diabetic rats with CoF was, however, able to lower the blood glucose levels. This result clearly shows the hypoglycemic properties of CoF. Increased insulin gene expression was also observed in the CoF-treated group compared to STZ group (Fig 4.2). This suggests that CoF treatment restored PBC integrity and function, which further validates the insulin-enhancing property of CoF. CoF possibly modulated the expression of GLP-1 and its release via TGR5 to produce increased insulin secretion via cAMP/PKA signaling pathway. Increased GLP-1 expression might have been responsible for increased PDX-1 expression (Fig 4.3) in the pancreas. PDX-1, in turn, might have acted to prevent PBC apoptosis and restore PBC mass, improving insulin production ultimately ameliorating the effects of STZ-induced diabetes. This result suggests that CoF support PBCs repair increasing insulin production, which agrees with reports that flavonoids influence insulin secretion (Soares *et al.*, 2017) as a result of upregulation of PDX-1 genes (Kaneto *et al.*, 2007).

Histological assessment of the pancreas shows normal histology of the pancreas in the control group (Fig. 4.5a). Treatment with STZ caused accumulation of fatty droplets in the intralobular ducts, hyalinized islets, and hyperplasia of intercalated duct cells (Fig. 4.5b). These observations are consistent with those reported by Coppieters and von Herrath, 2009 and Fujisawa *et al.*, 2012. Following treatment with CoF, reducing fatty droplets and less hyalinization in the islet of Langerhans were observed (Fig. 4.5c). Rifaai *et al.* 2012 and

Nurdiana *et al.*, 2017 reported a similar account to the present study: This suggests that CoF played a role in reversing PBC damage by reducing amyloid aggregation.

Diabetic nephropathy can result in a progressive decline in glomerular filtration rate characterized by glomerular hyperfiltration, glomerular and tubular epithelial hypertrophy, increased urinary albumin excretion, increased basement membrane thickness and mesangial expansion with the accumulation of extracellular matrix (ECM) proteins (Jain, 2012). The progression of renal injury often leads to end-stage renal disease, affecting 20%–40% of diabetic patients (Hakim and Pflueger, 2010). Acute kidney injury (AKI) development often results due to impaired renal perfusion, exposure to nephrotoxins, outflow obstruction, or intrinsic renal disease often from genetic mutation (Thomas *et al.*, 2015). AKI currently affects 8-16% of the global population (Balasubramanian, 2013) with serious economic implication thus, requiring urgent attention.

The effect of STZ treatment resulted in elevated serum levels of creatine and blood urea nitrogen which is suggestive of renal dysfunction but not necessarily structural renal disease (Baum *et al.*, 1975). Therefore, histological assessment of the renal tissues was done to establish that the SC and BUN data are predictors of renal failure. STZ treatment did cause negative ultrastructural changes in the kidney as revealed by the histopathology photomicrographs, but the underlying mechanism is unknown. Here, we propose oxidative and pro-inflammatory mechanisms. In the STZ-alone treated group, the kidney ultrastructure depicts various abnormal manifestations such as enlarged Bowman's space to thickened basement membrane to atrophied distal tubular epithelial cells and glomerulosclerosis. The abnormal increase in Bowman's space observed here is caused by an expansion of the Bowman's capsule and concurrent degeneration of the Glomerulus as reported by Yang *et al.* (2018), Xie *et al.* (2018) and Oskouei *et al.* (2019). Another abnormal feature observable in this group is glomerulosclerosis, characterised by the presence of nodules of glomerular scar (Kimmelstiel-Wilson nodules) in which the small

capillaries that filter blood are distorted or compressed by nodular scarring. This abnormality is usually also manifested in cases of nephrotic syndrome and characterized by mesangial cell expansion, with an increase in the matrix component of the mesangium; this has been identified as detected as early as 5-7 years after the onset of diabetes. Both mesangial expansion and basal membrane thickening are a consequence of extracellular matrix (ECM) accumulation, with increased deposition of the normal ECM local components of types IV and VI collagen, laminin, and fibronectin due to their increased production, decreased degradation or both. Furthermore, focal and segmental glomerulosclerosis (FSGS) tip variant, characterized by the presence of at least one segmental lesion involving the tip domain with either adhesion between the tuft and Bowman's capsule at the tubular lumen or neck, or confluence of podocytes with parietal or tubular epithelial cells at the tubular lumen or neck is also observable following STZ treatment. These features characterize renal failure (Eardley *et al.*, 2008).

Interestingly, just as CoF treatment reversed elevated levels of SC and BUN, all histological features characterizing renal failure in the STZ group were markedly reduced in CoF treated group. CoF treatment shows an essential "repair-in-progress" state, showing a remarkable reduction in the Bowman's space, less thickened basement membrane and repair in the glomerulus of the renal corpuscle, with normal podocytes, mesangial cells, and glomerular capillaries. This shows that CoF may contribute to the reduction and development of diabetic nephropathy. Puerarin, another flavonoid, also displayed some of these properties (Mao and Gu, 2005).

To understand the underlying mechanism of action of CoF, two plausible mechanisms were proposed: anti-oxidant and anti-inflammatory mechanisms, as a related study indicated that flavonoids from *Moringa oleifera* reduced kidney histopathological damage and expression of TNF- $\alpha$  (Tang *et al.*, 2017) indicating the contribution of inflammatory mechanism in renal damage also noting that inflammation is, an underlying consequence of ROS

accumulation (Reuter *et al.*, 2010). In the kidney, reactive oxygen species build-up triggers nuclear factor-erythroid 2-related factor 2 (Nrf2) translocation and antioxidant response element activation (ARE). Within the oxidatively charged nephron, infiltration of macrophage (Ye *et al.*, 2015) and other inflammatory cells (Takaori and Yanagita, 2016) via monocyte chemoattractant protein 1 (MCP-1) (Ismail *et al.*, 2016), is a precondition for the generation of pro-inflammatory cytokines such as IL-10, TNF- $\alpha$  and its cognate receptor. One of the genes upregulated by ARE is glutathione peroxidase (GPx-1) (Chen *et al.*, 2006). The STZ-treated group exhibited significantly high expressions of TNF- $\alpha$ , MCP-1 and GPx-1, which account for injury observed in the kidney histology in the current study. CoF significantly downregulated TNF- $\alpha$  and MCP-1 and upregulated TNF-R and IL-10 similar to previous findings of Ye *et al.* (2015) where flavonoid-rich preparations from traditional Chinese medicine inhibited the production of TNF- $\alpha$  and MCP-1 but enhanced IL-10 production in serum and tissues.

Catalase (CAT) and GPx-1 are part of the battery of antioxidant enzymes used by the body for detoxifying hydrogen peroxide generated during macrophage infiltration to Fight ROS accumulation via NRSF/ARE mechanisms (Chen *et al.*, 2006). Since the expression of GPX-1 and CAT is insensitive to CoF treatment, it may seem that once STZ initiates ROS build-up, the cellular mechanism at detoxification is initiated regardless of the presence of CoF. The overall health of the kidney is also monitored by the expression pattern of occludin (OCC) and Kidney Injury Molecule-1 (KIM-1). OCC is an important protein of the tight junction and renal tubule (Gonzalez-Mariscal *et al.*, 2000) while KIM-1, a known epithelial cell adhesion molecule, is up-regulated in renal cell injury (Ichimura *et al.*, 1998). CoF is beneficial as the tight junction molecules such as occludin is being reassembled as shown by the increased expression levels and more importantly, the injury is being resolved as

KIM-1 expression levels are declining; these are key indicators of renal epithelial cell regeneration (Pennemans *et al.*, 2012)

Diabetes is an important risk factor for the development of cardiovascular complications and vascular diseases, which are considered the leading cause of mortality in individuals with diabetes (Paneni *et al.*, 2013). Inflammatory cytokines, such as TNF- $\alpha$  and IL-6 are considered important contributors to endothelial dysfunction in obesity and T2D. They have been shown to increase stress, resulting in coronary endothelial dysfunction in T2D mice (Lee *et al.*, 2017). Oxidative stress, on the other hand, results from damage to biological macromolecules due to overproduction of ROS, which activates several inflammatory signaling cascades that will contribute to inflammation (Samarghandian *et al.*, 2015) and overwhelms the detoxification capacity of intercellular antioxidant system (Halliwell, 2011). The results of this study show that STZ treatment caused significant increase in IL-6 (Fig. 4.20), IL-1 $\beta$  (Fig. 4.21), TNF- $\alpha$  (Fig. 4.22) and MCP-1 (Fig. 4.23) genes in the aorta, as a result of STZ treatment, which is reversed following CoF treatment which shows downregulation of these genes. This result is in line with a study by Barari *et al.* (2012) who reported that the antioxidant property of the flavonoid, silymarin, a substance in milk thistle (*Silybum marianum*), reduced inflammatory agents such as TNF- $\alpha$  and IL-6. Hyperglycemia-induced glucotoxicity is associated with endothelial dysfunction as a result of increased ROS production (Capellini *et al.*, 2010). As expected, STZ treatment, which causes cellular stress, resulted in the down-regulation of CAT and GPX-1 genes in the aorta. CoF treatment was able to restore these antioxidant enzymes to normal levels, which might have been due to their free radical scavenging ability as flavonoids. Observed improvements might be due to increased endothelial nitric oxide synthase (eNOS) phosphorylation leading to greater nitric oxide production. This result is in line with another study where the flavonoid Puerarin, was reported to improve diabetic Aorta injury by inhibiting NADPH

oxidase-derived oxidative stress in STZ-induced diabetic rats (Li *et al.*, 2016). CoF might have also exerted its effects via inhibition of NADPH oxidase.

Expressions of OGT and OGA genes were upregulated compared to control, following STZ treatment. This is expected as excess expression of OGT has been shown to alter GlcNAcylation, impairing calcium cycling, which is a contributing factor to cardiac dysfunction, and increased OGlcNAcylation is directly linked to hyperglycaemia-induced glucose toxicity, a hallmark of diabetic complications. This is in line with a study carried out by Lunde *et al.* (2012), where OGT, OGA mRNA levels were increased as a result of pressure overload. Treatment with CoF significantly ( $p < 0.05$ ) decreased OGT expression. The results exhibited by the CoF-treated group might be due to alteration of UDP-GlcNAc amounts available via the HBP, as a result of enzyme inhibition.

From the histomorphological presentations of the aorta (Fig 4.26), the control group (A) shows a normal aorta consisting of tunica intima, tunica media, tunica adventitia, and elastic fibers. It is worthy of note that the tunica intima layer has been reported to constitute one-fourth of the entire aortic wall, with the media layer being the thickest (Aymen, 2000). The diabetic section (B) shows a significant increase in the thickness of tunica media, characterized mainly by compaction of proliferated muscle cells (myocytes). Atherosclerotic lesions (ASL) were also observed. These findings are consistent with the earlier work which mentioned the smooth muscle cells proliferation in the tunica intima and tunica media layer of the ascending aorta, which are consistent with the effect of STZ-induced diabetes in the cardiomyocytes of the heart (Balkis *et al.*, 2009; Thent *et al.*, 2012). Prolonged hyperglycaemia itself could induce the development of premature atherosclerotic lesions (Aronson and Rayfield, 2002). In this section, Atherosclerotic lesions were observed with numerous fatty deposits and macrophages with foam cell formation in the tunica intima layer and smooth muscle cells proliferation in medial layer, suggesting that diabetes may present lipid build-up within the vessels, which could form atherosclerotic plaques,

obstructing the lumen, thus blocking the free flow of blood. These observations are consistent with previous studies reported by Wald et al. (2002) and Kerkeni et al. (2006). The CoF-treated group (C) showed tremendous healing as revealed by a reduction in fatty droplets, with a complete repair in the lumen and remarkable reduction in the surrounding vessel. This suggests that CoF exhibit vascular protective potential possibly via anti-atherogenic and anti-lipidemic properties. CoF treatment additionally reduced plaque formation, keeping the lumen thin and localized. It is, therefore, safe to say that flavonoid compounds could reduce the risk of developing coronary heart disease by decreasing the LDL oxidation. The results of this study were seen to be in line with another research carried out to study the effects of total flavonoids of astragalus on atherosclerosis formation (Wang et al., 2012). The results showed that these flavonoids can significantly reduce plasma total cholesterol levels, fatty streak area, aortic arch total cholesterol content, and the ratio of plaque intima/media thickness. Several studies have shown that the main mechanism by which flavonoids inhibit the development of fatty streak lesions in atherosclerosis was a reduction in LDL oxidation. Furthermore, Fuhrman et al. (2000) reported that macrophages without foamy appearance were observed as well as macrophage enrichment with polyphenolic flavonoids in vitro or in vivo reduced the macrophage oxidative state and subsequently cell-mediated oxidation of LDL. With respect to the thickness in tunica media, the present study showed less compaction of cells with slightly reduced proliferation. The hypolipidemic components of flavonoids such as boswellic acid, ellagic acid, quercetin, and rutin, have been documented (Jadhav and Puchchakayala, 2012). Studies have suggested that pro-inflammatory cytokines such as IL-1 $\beta$  and TNF- $\alpha$  play a critical role in the pathogenesis of diabetes, consequently, control of the inflammatory response is a potential option for influencing the disease. To further explore the molecular mechanisms involved in metformin-mediated protective effects on the aorta and kidney, this researcher investigated the effect on the expression of oxidative stress mediated genes and

pro-inflammatory genes. The results show that metformin lowered the expressions of pro-inflammatory genes and modulated anti-oxidant genes in the aorta and kidney of experimental animals, which is consistent with previous studies where metformin alleviated oxidative stress and inflammatory response as well as improved endothelial cell function (Isoda *et al.*, 2006, Alhaider *et al.*, 2011, Wan *et al.*, 2013).

Based on the performance of CoF in ameliorating complications associated with STZ-induced diabetes, this served as an indication that it could be a good drug candidate. For this reason, the No Observed Adverse Effect level (NOAEL) was investigated in order to gather preclinical data for CoF drug development. The NOAEL results revealed that pure CoF fraction did not impair liver and kidney functions and were safe up to levels of 100mg/kg bwt.

The application of computational techniques such as molecular docking and molecular dynamics simulation in the drug discovery pipeline is a vital tool which currently provides insight to protein-ligand interactions. In this study, atomistic simulation was deployed to study active-state signatures in TGR5 complexed with CoF and compared with a well reported agonist 6- $\alpha$ -ethyl-23-(S)-methyl-cholic acid (S-EMCA, also known as INT-777). The results were compared with those evolved in antagonist (triamterene, TRX) bound and apo-states in 1 microsecond trajectories. The results obtained strongly indicate CoF as a TGR5 agonist as active-state consistent signatures evolved its trajectories. The TGR5 starting model in this study revealed that the E169<sup>5,43</sup> side chain carboxylic functional group is orientated outwards from the helical core without the possibility of making contacts with the ligands. When the trajectories were viewed, E169<sup>5,43</sup> side chain flipped into the helical core (Fig. 4.34C, i) and resided within approximately 5.2 Å from CoF, thus, underscoring the importance of E169<sup>5,43</sup> in TGR5 activation subject to mutagenesis experiments. Similarly, in INT-777 bound TGR5, E169 side chain carboxylic functional group also flipped into the helical core and resides within < 8 Å from the INT-777 during the simulation

(Fig. 4.34C, *ii*). This result is consistent with the loss of agonist mediated receptor activation in cells expressing TGR5-E169<sup>S43A</sup> mutant thus, underscoring the importance of E169 in agonist-activated TGR5. Next, the interaction between CoF and S270<sup>7.42</sup> was probed using the distance parameter. From the starting coordinate, the side chain hydroxyl group of S270<sup>7.42</sup> is oriented towards the core of the helix but placed too deep into TMVII to make contacts with the ligand, however, along the trajectories; starting at 200 ns through 300 ns, 6-hydroxyl substituent on ring A moved at a distance of ~ 5 Å from the hydroxyl side chain of S270<sup>7.42</sup> (Fig. 4.34D). These data provided key structural insight into the agonist's property of flavonoids acting at TGR5.

From Fig 4.35B *i*, the C4 hydroxyl of ring A links 12 water molecules from the orthosteric site to the DRY motif through a curved ring of hydrophobic residues contributed by TMII (T70<sup>2.59</sup>, A67<sup>2.56</sup>, L63<sup>2.52</sup>, L59<sup>2.48</sup>, S56<sup>2.45</sup>), TMIII (L87<sup>3.27</sup>, F94<sup>3.34</sup>, S98<sup>3.38</sup>, A101<sup>3.41</sup>, L105<sup>3.45</sup>, and the (E)-DRY motif, TMIV (P135<sup>4.53</sup>), and TMV (L175<sup>5.49</sup>) (Fig. 4.35B, *ii*). This water tunneling pattern is consistent with previous findings that it may play a significant role in breaking the DRY ionic lock, which results in receptor activation and in some cases, when the ionic lock is interrupted, antagonists are turned into super agonists.

Next, INT-777, a highly selective and potent

TGR5 agonist when simulated in complex with TGR5 also elicited (dis)-continuous internal water pathway as observed for CoF/TGR5 complex. Starting from 250 ns (Fig. 4.35C, *i*), water is tunneled through hydrophobic residues lining TMIII (Y89<sup>3.29</sup>, F94<sup>3.34</sup>), (E)-DRY motif, TMIV (A127<sup>4.45</sup>, L130<sup>4.48</sup>, P135<sup>4.53</sup>) and TMV (Y171<sup>5.46</sup>, L175<sup>5.49</sup>) (Fig. 4.35C, *ii*). Both water tunnels tend to terminate at the (E)-DRY motif, thus, suggesting a key role in receptor activation. Such structured internal water is not observed in antagonist bound and apo states.

Class A GPCR activation is characterized by structural signatures such as: active-state kinking of conserved NPxxY motif at the TMVII (DeLano, 2002), rotameric switches in

orthosteric aromatic residue, rupturing of the ionic lock formed between TMIII and TMVI, and most recently, the formation of an internal water pathway within the helices. Salt-bridge formation between R3.50 (TGR5, TMIII, R110) and E6.30 (TGR5, TMVI, T219) restrains most GPCRs in an inactive state referred to as "ionic lock". Clearly, this interaction is further reinforced by the strength of interaction between TMIII-TMVI residues. Therefore, inter-residue network and community formation (network analysis) around TMIII and TMVI was investigated for the complexes and apo state. The network analysis was developed based on a mathematical model, which decomposes atomic interaction between protein residues into nodes (amino acid residues) and edges (weighted strength of interaction between node centers). Here, an edge is defined as an atomic contact between the nodes at a cut-off distance of 4.0 Å occurring more than 85% of the period of simulation. Similarly, when the ionic lock is ruptured, conformational transition around NPxxY motif located on TMVII prevents the reformation of ionic lock, thus the projection of TMIII-TMVI distance and NPxxY root mean square deviation (*rmsd*) along the free energy surface has been used to identify conformations sampling, active state, inactive state and meta-states in MD simulation trajectories and delineation of GPCR activation mechanisms. (E)-DRY motif (residues L104<sup>3.44</sup>-Y111<sup>3.51</sup>, TMIII) and those of TMVI (residues R221<sup>6.32</sup>-A227<sup>6.38</sup>) show strong interaction (edges) and assemble into a single interacting community in apo TGR5 (Fig. 4.36A, i). Next, TMIII-TMVI distance along the trajectory and *rmsd* of V-276<sup>7.49</sup>PVAM-280<sup>7.53</sup> (corresponding to NPxxY motif) calculated from inactive state (TGR5 built on adenosine receptor bound to antagonist (PDB ID: 3EML) (Lovell *et al.*, 2003) were projected along the free energy surface (Fig.4.36A, ii). Two major conformations have been observed, in both cases, TMIII-TMVI ionic lock appeared unbroken but NPxxY motif resonated between the active (*increased rmsd*) and inactive (*low rmsd*) conformations. In the presence of CoF (Fig. 4.36B, i) and INT (Fig. 4.36C, i), TMIII-TMVI network in TGR5 is broken. Intra-helical but not inter-helical communities form

between TMIII and TMVI in these complexes. Furthermore, the free energy surface plots in both complexes reveal complete disruption of the ionic lock ( $\Delta G \sim 0$  kcal/mol, high TMIII/TMVI values) coupled with NPxxY-motif conformation away from the inactive state (Fig. 4.36B, *ii* and Fig. 4.36C, *ii*), thus, CoF and INT behave like classical TGR5 agonists by evolving patterns previously reported in atomistic simulation involving LPA1 receptor in agonist-bound states which had been experimentally validated. TGR5 in TRX bound state equally evolved an inactive state conformation with the formation of TMIII-TMVI ionic lock (Fig. 4.36D, *i*) shown as inter-helical residue community formation. The evidence for this is more obvious in the free energy surface plot as inactive conformation is preferentially sampled during the trajectories (Fig. 4.36D, *ii*).

TGR5 was also examined for possible rotameric signature(s) that can distinguish between apo, agonist and antagonist bound states. Y89<sup>3,29</sup>, Y165<sup>5,40</sup>, Y240<sup>6,51</sup> and W237<sup>6,48</sup> (Fig. 4.37A, *i*) 2 angles were monitored along the trajectories. The data here did not show a clear ligand-dependent rotameric pattern for Y89<sup>3,29</sup>, Y165<sup>5,40</sup> and Y240<sup>6,51</sup> (Fig. 4.37A, *ii*) but W237<sup>6,48</sup> 2 angles indicated ligand-dependent pattern. In the presence of a ligand, the indole moiety of W237<sup>6,48</sup> adopts  $\sim 100^\circ$  in the presence of a ligand but  $\sim +100^\circ$  in the apo state (Fig. 4.37B *ii*, TGR5). Another piece of data that supports this observation is that in TRX (antagonist) bound TGR5, W237<sup>6,48</sup> indole moiety maintained  $\sim 100^\circ$  until the dissociation of TRX at  $\sim 800$  ns (snapshot, TGR5+TRX, red stick) causing a change in rotameric angle to  $-50^\circ$  (Fig. 4.37B, *i*). Whilst W237<sup>6,48</sup> may predict the presence of a ligand within the orthosteric site, it could not differentiate between an antagonist and an agonist (Fig. 4.37B, *ii*, TGR5+CoF, TGR5+INT).

## CHAPTER SIX

### 6.0 CONCLUSION, RECOMMENDATION AND CONTRIBUTIONS TO KNOWLEDGE

#### 6.1 CONCLUSION

This study investigated the putative anti-diabetic principle in *C. odorata* and its underlying mechanisms using *in silico* and *in vivo* experiments. Comorbidities associated with STZ treatment in experimental animals were challenged by CoF. The study demonstrated that these comorbidities are reversible by CoF administration in experimental animals via countering of oxidative and inflammatory processes. TGR5 is suggested as the putative receptor, resulting in GLP-1 release and insulin stimulation via PDX-1 expression and ultimate reversal of hyperglycemia. Tyrosine-89 (Y<sup>89</sup>), Asparagine-93 (N<sup>93</sup>), Glutamic acid-169 (E<sup>169</sup>) and Serine-270 (S<sup>270</sup>) are key residues involved in ligand binding based on the results obtained from molecular dynamics simulation studies where TGR5 evolved active state conformation in CoF-bound state. CoF exhibited comparable properties to the drug Metformin. NOAEL experiments reveal that there are no adverse effects on the organs and it is relatively safe to consume up to 100mg/kg body weight in experimental animals. The findings from this study clearly show that CoF possesses anti-diabetic properties thus, it may represent an emerging bioresource and new management option in diabetes treatment.

#### 6.2 RECOMMENDATION

Given the anti-diabetic properties displayed by CoF, and its low adverse effect on experimental animals, it is recommended that further human clinical trials be carried out to ascertain these reported effects in human subjects.

### 6.3 CONTRIBUTIONS TO KNOWLEDGE

The following contributions to knowledge were made from this research

1. The study suggested Takeda G-protein receptor-5 as the plausible receptor for binding of flavonoids isolated from *C. odorata*.
2. The study identified key residues involved in flavonoids binding to TGR5 at the active site.
3. The plausible insulinotropic mechanisms of action of CoF in STZ-treated Wistar rats might be via GLP-1/Insulin/PDX-1 signaling pathway.
4. The study presents the gene expression profiles of genes involved with diabetes and changes associated with CoF treatment, in the pancreas, aorta, kidney and ileum.
5. Histopathological changes in the Pancreas, Kidney and Aorta associated with STZ- and CoF treatment in diabetic Wistar rats are now available.
6. The study has pre-clinical data from No-observed adverse effect levels suggesting that flavonoids isolated from *C. odorata* are safe up to doses of 100mg/kg bwt.

## REFERENCES

- Abdel-Azim, N.S., Shams, K.A., Shahat, A. A. A., El-Missiry, M. M., Ismail, S. I. and Hammouda, F. M. (2011). Egyptian Herbal Drug Industry: Challenges and Future Prospects. *Research Journal of Medicinal Plant*, 5: 136-144.
- Adedapo, A. A., Ogunmiluyi, I. O., Adeoye, A. T., Ofuegbe, S. O. and Emikpe, B. O. (2016a). Evaluation of the Medicinal Potential of the Methanol Leaf Extract of *Chromolaena odorata* in Some Laboratory Animals. *Journal of Medicinal Plants*, 4: 29-37.
- Adedapo, A. A., Oyagbemi, A. A., Fagbohun, O. A., Omobowale, T. O. and Yakubu, M. A. (2016b). Evaluation of the Anticancer Properties of the Methanol Leaf Extract of *Chromolaena odorata* on HT29 Lung Cancer Cell Line. *The FASEB Journal*, 30 (1 supplement), 1193-6.
- Akinmoladun, A. C., Ibukun, E. O. and Don-Ologe, I. A. (2007). Phytochemicals Constituents and Antioxidant Properties of Extracts from the Leaves of *C. odorata*. *Scientific Research and Essay*, 2 (6): 191-194.
- Alhaider, A. A., Korashy, H. M., Sayed-Ahmed, M. M., Mobark, M., Kfoury, H. and Mansour, M. A. (2011). Metformin Attenuates Streptozotocin-Induced Diabetic Nephropathy in rats through Modulation of Oxidative Stress Genes Expression. *Chemico-biological interactions*, 192(3), 233-242.
- American Diabetes association. Consensus Statement, 1993. Role of Cardiovascular Risk Factors in Prevention and Treatment of Macrovascular Disease in Diabetes. *Diabetes Care*, 16:72-78.
- Andersen, O. M. and Markham, K. R. (2005). *Flavonoids: Chemistry, Biochemistry and Applications*. 1<sup>st</sup> Edition, CRC press, Boca Raton, 2005, 1256.
- Anyasor, G. N., Aina, D. A., Olushola, M. and Aniyikawe, A. F. (2011). Phytochemical Constituents, Proximate Analysis, Antioxidants, Anti-bacterial and Wound Healing Properties of leaf extracts of *Chromolaena odorata*. *Annals of Biological Research*, 2: 441-451.
- Aronson, D. and Rayfield, E. J. (2002). How Hyperglycemia Promotes Atherosclerosis: Molecular Mechanisms. *Cardiovascular Diabetology*, 1(1): 1.
- Atkinson, M. A. (2012). The Pathogenesis and Natural History of Type 1 Diabetes. *Cold Spring Harbor Perspectives in Medicine*, 2(11), a007641.
- Atoui, A. K., Mansouri, A., Boskou, G. and Kefalas, P. (2005). Tea and Herbal Infusions: their Antioxidant Activity and Phenolic Profile. *Food Chemistry*, 89(1), 27-36.
- Ayepola, O. R., Brooks, N. L. and Oguntibeju, O. O. (2014). Oxidative Stress and Diabetic Complications: the Role of Antioxidant Vitamins and Flavonoids. In *Antioxidant- Agents and Human Health*. IntechOpen <http://dx.doi.org/10.5772/57282>.
- Aymen, M. G. (2000). Introduction to Functional and Clinical Histology, Text and Atlas, Part I, 4th ed. Giza, Egypt. 193-196.
- Baena-Díez, J. M., Peñafiel, J., Subirana, I., Ramos, R., Elosua, R., Marín-Ibañez, A., Guembe, M. J., Rigo, F., Tormo-Díaz, M. J., Moreno-Iribas, C. and Cabré, J. J. (2016). Risk of Cause-Specific Death in Individuals with Diabetes: A Competing Risks Analysis. *Diabetes Care*, 39(11): 1987-1995 <https://doi.org/10.2337/dcl16-0614>.
- Baggio, L. L. and Drucker, D. J. (2007). Biology of Incretins: GLP-1 and GIP. *Gastroenterology*, 132: 2131-2157.
- Bahadoran, Z., Mirmiran, P. and Azizi, F. (2013). Dietary Polyphenols as Potential Nutraceuticals in Management of Diabetes: A review. *Journal of Diabetes and Metabolic Disorders*, 12: 43.

- Baharvand-Ahmadi, B., Bahmani, M., Tajeddini, P., Naghdi, N. and Rafieian-Kopaei, M. (2016). An Ethno-medicinal Study of Medicinal Plants used for the Treatment of Diabetes. *Journal of Nephropathology*, 5(1); 44-50.
- Bahmani, M., Golshahi, H., Saki, K., Rafieian-Kopaei, M., Delfan, B. and Mohammadi, T. (2014). Medicinal Plants and Secondary Metabolites for Diabetes Mellitus Control. *Asian Pacific Journal of Tropical Disease*, 4, S687-S692.
- Bajaj, M. and DeFronzo, R. A. (2003). Metabolic and Molecular Basis of Insulin Resistance. *Journal of Nuclear Cardiology*, 10(3), 311-323.
- Balasubramanian, S. (2013). Progression of Chronic Kidney Disease: Mechanisms and Interventions in Retardation. *Apollo Medicine*, 10(1): 19-28.
- Balkis, B. S., Othman, F., Louis, S. R., Abu Bakar M., Radzi, M., Osman, K., Das, S. and Mohamed, J. (2009). Effect of Alpha Lipoic Acid on Oxidative Stress and Vascular Wall of Diabetic Rats. *Romanian Journal of Morphology and Embryology*, 50(1): 23-30.
- Banerjee, P. S., Lagerloef, O. and Hart, G. W. (2016). Roles of O-GlcNAc in Chronic Diseases of Aging. *Molecular Aspects of Medicine*, 51: 1-15.
- Barari, A. R., Alavi, S. H., Shirali, S. and Ghazalian, F. (2012). Effect of Short-term Endurance Training and Silymarin Consumption on some of Pro Inflammatory Cytokines, Growth Mediators and Immune System Performance. *Annals of Biological Research*, 3(6): 2933-7. <https://doi.org/00.0000>.
- Batra, P. and Sharma, A. K. (2013). Anti-Cancer Potential of Flavonoids: Recent Trends and Future Perspectives. *3 Biotechnology*. DOI 10.1007/s13205-013-0117-5.
- Baum, N., Dichoso, C. C. and Carlton, C. E. (1975). Blood Urea Nitrogen and Serum Creatinine: Physiology and Interpretations. *Urology*, 5(5): 583-588.
- Baynes, J. W. and Thorpe, S. R. (1999). Role of Oxidative Stress in Diabetic Complications: A New Perspective on an Old Paradigm. *Diabetes*, 48(1): 1-9.
- Bell, D. S. (2003). Beneficial Effects Resulting from Thiazolidinediones for Treatment of Type 2 Diabetes Mellitus. *Postgraduate Medicine*, (Spec No): 35-44.
- Bhathena, S. J. and Velasquez, M. T. (2002). Beneficial Role of Dietary Phytoestrogens in Obesity and Diabetes. *American Journal of Clinical Nutrition*, 76: 1191-1201.
- Bhattacharya, S. and Chirangeebee, B. (2006). Dose-Dependent Effects of Fenugreek Composite in Diabetes with Dyslipidaemia. *Internet Journal of Food Safety*, 8: 49-55.
- Bowles, D., Isayenkova, J., Lim, E. K. and Poppenberger, B. (2005). Glycosyltransferases: Managers of Small Molecules. *Current Opinion in Plant Biology*, 8(3), 254-263.
- Brighton, C. A., Rievaj, J., Kuhre, R. E., Glass, L. L., Schoonjans, K., Holst, J. J., Gribble, F.M. and Reimann, F. (2015). Bile Acids Trigger GLP-1 Release Predominantly by Accessing Basolaterally Located G Protein-Coupled Bile Acid Receptors. *Endocrinology*, 156(11): 3961-3970. <http://dx.doi.org/10.1210/en.2015-1321>.
- Brubaker, P. L. (2007). Incretin-Based Therapies: Mimetics Versus Protease Inhibitors. *Trends in Endocrinology and Metabolism*, 18: 240-245.
- Brubaker, P. L. and Drucker, D. J. (2004). "Minireview: Glucagon-Like Peptides Regulate Cell Proliferation and Apoptosis in the Pancreas, Gut, and Central Nervous System," *Endocrinology*, 145(6): 2653-2659.
- Bruun, J. M., Lihn, A. S., Pedersen, S. B. and Richelsen, B. (2005). Monocyte Chemoattractant Protein-1 Release is Higher in Visceral than Subcutaneous Human Adipose Tissue (AT): Implication of Macrophages Resident in the AT. *The Journal of Clinical Endocrinology and Metabolism*, 90(4): 2282-2289.
- Bucala, R., Makita, Z., Vega, G., Grundy, S., Koschinsky, T., Cerami, A. and Vlassara, H. (1994). Modification of Low Density Lipoprotein by Advanced Glycation End

- Products Contributes to the Dyslipidemia of Diabetes and Renal Insufficiency. *Proceedings of the National Academy of Sciences*, 91(20): 9441-9445.
- Buchanan, T. A. (2003). Pancreatic Beta-Cell Loss and Preservation in Type 2 Diabetes. *Clinical Therapeutics*, 25: B32-B46.
- Capellini, V. K., Celotto, A. C., Baldo, C. F., Olivon, V. C., Viaro, F., Rodrigues, A. J. and Evora, R. B. P. (2010). Diabetes and Vascular Disease: Basic Concepts of Nitric Oxide Physiology, Endothelial Dysfunction, Oxidative Stress and Therapeutic Possibilities. *Current Vascular Pharmacology*, 8: 526-544.
- Castellarin, S. D. and Gaspero, G. D. (2007). Transcriptional Control of Anthocyanin Biosynthetic Genes in Extreme Phenotypes for Berry Pigmentation of Naturally Occurring Grape Vines. *BMC Plant Biology*, 7: 46.
- Chakraborty, A. K., Rambhade, S. and Patil, U. K. (2011). *Chromolaena odorata* (L.): An Overview. *Journal of Pharmaceutical Research*, 4(3), 573-576.
- Chatenoud, L. and Bluestone, J. A. (2007). CD3-Specific Antibodies: A Portal to the Treatment of Autoimmunity. *Nature Reviews Immunology*, 7: 622-32.
- Chelikani, P. K., Haver, A. C. and Reidelberger, R. D. (2005). Intravenous Infusion of Glucagon-Like Peptide-1 Potently Inhibits Food Intake, Sham Feeding, and Gastric Emptying in Rats. *American Journal of Physiology-Regulatory, Integrative and Comparative Physiology*, 288(6): R1695-R1706.
- Chen, X. L., Dodd, G., Thomas, S., Zhang, X., Wasserman, M. A., Rovin, B. H. and Kunsch, C. (2006). Activation of Nrf2/ARE Pathway Protects Endothelial Cells from Oxidant Injury and Inhibits Inflammatory Gene Expression. *American Journal of Physiology-Heart and Circulatory Physiology*, 290(5): H1862-H1870.
- Chehade, J. and Mooradian, A. (2000). A Rational Approach to Drug Therapy of Type 2 Diabetes Mellitus. *Drugs*, 60: 95-113.
- Cheon, H., Cho, J. M., Kim, S., Baek, S. H., Lee, M. K., Kim, K. W., Yu, S. W., Solinas, G., Kim, S. S. and Lee, M. S. (2010). Role of JNK Activation In Pancreatic Beta-Cell Death by Streptozotocin. *Molecular and Cellular Endocrinology*, 321: 131-137.
- Cho, N. H., Shaw, J. E., Karuranga, S., Huang, Y., da Rocha Fernandes, J. D., Ohlrogge, A. W. and Malanda, B. (2018). IDF Diabetes Atlas: Global Estimates of Diabetes Prevalence for 2017 and Projections for 2045. *Diabetes Research and Clinical Practice*, 138, 271-281.
- Chung, S. S., Ho, E. C., Lam, K. S. and Chung, S. K. (2003). Contribution of Polyol Pathway to Diabetes-Induced Oxidative Stress. *Journal of the American Society of Nephrology*, 14 (suppl 3): S233-S236.
- Cnop, M., Vidal, J., Hull, R. L., Utzschneider, K. M., Carr, D. B., Schraw, T., Scherer, P.E., Boyko, E.J., Fujimoto, W.Y. and Kahn, S. E. (2007). Progressive Loss of  $\beta$ -cell Function Leads to Worsening Glucose Tolerance in First-Degree Relatives of Subjects with Type 2 Diabetes. *Diabetes Care*, 30(3): 677-682.
- Collier, C. A., Bruce, C. R., Smith, A. C., Lopaschuk, G. and Dyck, D. J. (2006). Metformin Counters the Insulin-Induced Suppression of Fatty Acid Oxidation and Stimulation of Triacylglycerol Storage in Rodent Skeletal Muscle. *The American Journal of Physiology-Endocrinology and Metabolism*, 291(1): 182-189.
- Coppieters, K. T. and von Herrath, M. G. (2009). Histopathology of Type 1 Diabetes: Old Paradigms and New Insights. *The Review of Diabetic Studies: RDS*, 6(2), 85-96.
- Corradini, E., Foglia, P., Giansanti, P., Gubbio, R., Samperi, R. and Lagana, A. (2011). Flavonoids: Chemical Properties and Analytical Methodologies of Identification and Quantitation in Foods and Plants. *Natural Products Research*, 25(5): 469-495.

- Creager, M. A., Lüscher, T. F., Cosentino, F. and Beckman, J. A. (2003). Diabetes and Vascular Disease Pathophysiology, Clinical Consequences, and Medical Therapy: Part I. *Circulation*, 108(12): 1527-1532.
- DeLano, W. L. (2002). Pymol: An Open-Source Molecular Graphics Tool. *CCP4 Newsletter on Protein Crystallography*, 40(1), 82-92.
- Ding, H. and Triggle, C. R. (2005). Endothelial Cell Dysfunction and the Vascular Complications Associated with Type 2 Diabetes: Assessing the Health of the Endothelium. *Vascular Health and Risk Management*, 1(1): 55.
- Dirks, J. H. (2004). The Drumbeat of Renal Failure: Symbiosis of Prevention and Renal Replacement Therapy. *Blood Purification*, 22: 6-8.
- Doerr, S., Harvey, M. J., Noé, F. and De Fabritiis, G. (2016). HTMD: High-Throughput Molecular Dynamics for Molecular Discovery. *Journal of Chemical Theory and Computation*, 12(4), 1845-1852.
- Drucker, D. J., Philippe, J., Mojsov, S., Chick, W. L. and Habener, J. F. (1987). Glucagon-Like Peptide 1 Stimulates Insulin Gene Expression and Increases Cyclic AMP levels in a Rat Islet Cell Line. *Proceedings of the National Academy of Sciences*, 84(10): 3434-3438.
- Drucker, D. J. (2003). Glucagon-Like Peptide-1 and the Islet  $\beta$ -Cell: Augmentation of Cell Proliferation and Inhibition of Apoptosis. *Endocrinology*, 144(12): 5145-5148.
- Duboc, H., Taché, Y. and Hofmann, A. F. (2014). The Bile Acid TGR5 Membrane Receptor: from Basic Research to Clinical Application. *Digestive and Liver Disease*, 46(4): 302-312.
- Duncan, B. B., Schmidt, M. I., Pankow, J. S., Ballantyne, C. M., Couper, D., Vigo, A., Hoogeveen, R., Folsom, A. R. and Heiss, G. (2003). Low-Grade Systemic Inflammation and the Development of Type 2 Diabetes: The Atherosclerosis Risk in Communities Study. *Diabetes*, 52(7): 1799-1805.
- Eardley, K. S., Kubal, C., Zehnder, D., Quinkler, M., Lepenies, J., Savage, C. O., Howie, A. J., Kaur, K., Cooper, M. S., Adu, D. and Cockwell, P. (2008). The Role of Capillary Density, Macrophage Infiltration and Interstitial Scarring in the Pathogenesis of Human Chronic Kidney Disease. *Kidney International*, 74(4): 495-504.
- Ebrahimi, E., Shirali, S. and Afrisham, R. (2017). Effect and Mechanism of Herbal Ingredients in Improving Diabetes Mellitus Complications. *Jundishapur Journal of Natural Pharmaceutical Products*, 12(1): e31657. doi:10.5812/jjnpp.31657.
- Eddouks, M., Maghrani, M., Lemhadri, A., Ouahidi, M. L. and Jouad, H. (2002). Ethno Pharmacological Survey of Medicinal Plants Used for the Treatment of Diabetes Mellitus, Hypertension and Cardiac Diseases in the South-East Region of Morocco. *Journal of Ethnopharmacology*, 82: 97-103.
- Eidi, A., Eidi, M. and Sokhth, M. (2007). Effect of Fenugreek (*Trigonella foenum-graecum* L) Seeds on Serum Parameters in Normal and Streptozotocin-Induced Diabetic Rats. *Nutrition Research*, 27(11): 728-33.
- Eisenbarth, G. S. (2007). Type 1 Diabetes Mellitus. A Chronic Autoimmune Disease. *The New England Journal of Medicine*, 314: 1360-8.
- Eizirik, D. L., Cardozo, A. K. and Cnop, M. (2008). "The Role for Endoplasmic Reticulum Stress in Diabetes Mellitus," *Endocrine Reviews*, 29(1): 42-61.
- Eizirik, D. L., Colli, M. L. and Ortis, F. (2009). The Role of Inflammation in Insulinitis and  $\beta$ -cell Loss in Type 1 Diabetes. *Nature Reviews Endocrinology*, 5(4): 219.
- ElLatif, M. A. A., Mohamed, N. H., Zaki, N. L., Abbas, M. S. and Sobhy, H. M. (2014). Effects of Soy Bean Isoflavone on Lipid Profiles and Antioxidant Enzyme Activity in Streptozotocin-Induced Diabetic Rats. *Global Journal of Pharmacology*, 8: 378-384.

- Epstein, F. H. and Ross, R. (1999). Atherosclerosis - an Inflammatory Disease. *The New England Journal of Medicine*, 340(2): 115-126.
- Eurich, D. T., McAlister, F. A. and Blackburn, D. F. (2007). Benefits and Harms of Anti-Diabetic Agents in Patients with Diabetics and Heart Failure. *Systematic Reviews*, 335(7618): 497-499.
- Fain, J. N., Madan, A. K., Hiler, M. L., Cheema, P. and Bahouth, S. W. (2004). Comparison of the Release of Adipokines by Adipose Tissue, Adipose Tissue Matrix, and Adipocytes from Visceral and Subcutaneous Abdominal Adipose Tissues of Obese Humans. *Endocrinology*, 145: 2273-2282.
- Feliciano, R. P., Pritzel, S., Heiss, C. and Rodriguez-Mateos, A. (2015). Flavonoid Intake and Cardiovascular Disease Risk. *Current Opinion in Food Science*, 2, 92-99.
- Ferrer, J. L., Austin, M. B., Stewart Jr., C. and Noel, J. P. (2008). Structure and Function of Enzymes Involved in the Biosynthesis of Phenylpropanoids. *Plant Physiology and Biochemistry*, 46(3), 356-370.
- Ferreira, M. L. F., Rius, S. and Casati, P. (2012). Flavonoids: Biosynthesis, Biological Functions, and Biotechnological Applications. *Frontiers in Plant Science*, 3, 222.
- Frantisek, S. (1991). The National Guide to Medicinal Herbs and Plants. *Tiger Barks Inst. Twickenham, UK Pp1-8*.
- Fricovsky, E. S., Suarez, J., Ihm, S. H., Scott, B. T., Suarez-Ramirez, J. A., Banerjee, L., Torres-Gonzalez, M., Wang, H., Ellrott, I., Maya-Ramos, L. and Villarreal, F. (2012). Excess Protein O-GlcNAcylation and the Progression of Diabetic Cardiomyopathy. *American Journal of Physiology-Regulatory, Integrative and Comparative Physiology*, 303(7): R689-R699.
- Fowler, M. J. 2008. Microvascular and Macrovascular Complications of Diabetes. *Clinical Diabetes*, 26(2): 77-82.
- Fuhrman, B., Rosenblat, M., Hayek, T., Coleman, R. and Aviram, M. (2000). Ginger Extract Consumption Reduces Plasma Cholesterol, Inhibits LDL Oxidation and Attenuates Development of Atherosclerosis in Atherosclerotic, Apolipoprotein E-Deficient Mice. *Journal of Nutrition*, 130(5): 1124-1131.
- Furman, B. L. (2015). Streptozotocin-Induced Diabetic Models in Mice and Rats. *Current Protocols in Pharmacology*, 70(1), 5-47.
- Fujisawa, H., Zhang, Z., Sun, W., Huang, M., Kobayashi, J., Yasuda, H., Kinoshita, Y., Ando, R., and Tamura, K. (2012). Histopathological Changes in the Pancreas from a Spontaneous Hyperglycemic Cynomolgus Monkey. *Journal of Toxicologic Pathology*, 25(3): 215-9.
- Fukino, Y., Shimbo, M., Aoki, N., Okubo, T. and Iso, H. (2005). Randomized Controlled Trial for an Effect of Green Tea Consumption on Insulin Resistance and Inflammation Markers. *Journal of Nutritional Science and Vitaminology*, 51: 335-342.
- Funakoshi-Tago, M., Nakamura, K., Tago, K., Mashino, T. and Kasahara, T. (2011). Anti-Inflammatory Activity of Structurally Related Flavonoids, Apigenin, Luteolin and Fisetin. *International Immunopharmacology*, 11(9), 1150-1159.
- Funk, S. D., Yurdagul, A. and Orr, A. W. (2012). Hyperglycemia and Endothelial Dysfunction in Atherosclerosis: Lessons from Type 1 Diabetes. *International Journal of Vascular Medicine*, 2012: 1-19.
- Ghaed, F., Rafeian-Kopaei, M., Nematbakhsh, M., Baradaran, A. and Nasri, H. (2012). Ameliorative Effects of Metformin on Renal Histologic and Biochemical Alterations of Gentamicin-Induced Renal Toxicity in Wistar Rats. *Journal of Research in Medical Sciences*, 17(7): 621-625.
- Ghorbani, A. (2017). Mechanisms of Antidiabetic Effects of Flavonoid Rutin. *Biomedicine and Pharmacotherapy*, 96, 305-312.

- Ginwala, R., Bhavsar, R., Chigbu, D. G. I., Jain, P. and Khan, Z. K. (2019). Potential Role of Flavonoids in Treating Chronic Inflammatory Diseases with a Special Focus on the Anti-Inflammatory Activity of Apigenin. *Antioxidants*, 8(2), 35.
- Goldin, A., Beckman, J. A., Schmidt, A. M. and Creager, M. A. (2006). Advanced Glycation End Products Sparking the Development of Diabetic Vascular Injury. *Circulation*, 114(6): 597-605.
- Gomez-Tourino, I., Arif, S., Eichmann, M. and Peakman, M. (2016). T Cells in Type 1 Diabetes: Instructors, Regulators and Effectors: A Comprehensive Review. *Journal of Autoimmunity*, 66, 7-16.
- Gonzalez-Mariscal, L., Namorado, M. C., Martin, D., Luna, J., Alarcon, L., Islas, S., Valencia, L., Muriel, P., Ponce, L. and Reyes, J. L. (2000). Tight Junction Proteins ZO-1, ZO-2, and Occludin along Isolated Renal Tubules 1. *Kidney International*, 57(6): 2386-2402.
- González, E. L., Johansson, S., Wallander, M. A. and Rodriguez, L. A. (2009). Trends in the Prevalence and Incidence of Diabetes in the UK: 1996 – 2005. *Journal of Epidemiology and Community Health*, 63: 332-336
- Gowthamarajan, K. and Kulkarni, G. T. (2003). Oral Insulin—Fact or Fiction? *Resonance*, 8(5), 38-46.
- Grarup, N., Sandholt, C. H., Hansen, T. and Pedersen, O. (2014). Genetic Susceptibility to Type 2 Diabetes and Obesity: from Genome-Wide Association Studies to Rare Variants and Beyond. *Diabetologia*, 57(8), 1528-1541.
- Groot, H. D. and Rauven, U. (1998). Tissue Injury by Reactive Oxygen Species and the Protective Effects of Flavonoids. *Fundamental and Clinical Pharmacology*, 12(3): 249-255.
- Grzybowska, M., Bober, J. and Olszewska, M. (2011). Metformin—Mechanisms of Action and use for the Treatment of Type 2 Diabetes Mellitus. *Advances in Hygiene and Experimental Medicine*, 65, 277-285. DOI: [10.5604/17322693.941655](https://doi.org/10.5604/17322693.941655)
- Guilherme, A., Virbasius, J. V., Puri, V. and Czech, M. P. (2008). Adipocyte Dysfunctions Linking Obesity to Insulin Resistance and Type 2 Diabetes. *Nature Reviews Molecular Cell Biology*, 9: 367-377.
- Guo, C., Chen, W. D. and Wang, Y. D. (2016). TGR5, Not Only A Metabolic Regulator. *Frontiers in Physiology*, 7: 646. <http://dx.doi.org/10.3389/fphys.2016.00646>
- Guyton, A. C., and Hall, J. E. (2006). Dietary Balances; Regulation of Feeding; Obesity and Starvation; Vitamins and Minerals. *Textbook of Medical Physiology (Guyton AC, Hall JE, eds)*. Elsevier Saunders Inc. Philadelphia, PN, 876.
- Habbu, P. V., Mahadevan, K. M., Kulkarni, V. H., Marietta, P., Pratap, V., Thippeswamy, B. S., and Veerapur, V. P. (2010). Antidiabetic Activity of *Argyrea speciosa* (sweet) (Burm.F.)Boj. in Normoglycemic and Streptozotocin-Induced Diabetic Rats. *Oriental Pharmacy and Experimental Medicine*, 10: 90-102.
- Haffner, S. M., Kahn, S. E., Zinman, B., Holman, R. R., Viberti, G. F., Herman, W. H., Lachin, J. M., Kravitz, B. G. and Heise, M. A. (2007). Greater Reductions in C-Reactive Protein with Rosiglitazone than with Glyburide or Metformin Despite Greater Weight Gain. *Journal of Medicinal Plants Research*, 50 (1): S502.
- Hajiaghaalipour, F., Khalilpourfarshbafi, M. and Arya, A. (2015). Modulation of Glucose Transporter Protein by Dietary Flavonoids in Type 2 Diabetes Mellitus. *International Journal of Biological Science*, 11: 508-524.
- Hakim, F. A. and Pflueger, A. (2010). Role of Oxidative Stress in Diabetic Kidney Disease. *Medical Science Monitor*, 16(2), RA37-RA48.
- Halliwell, B. 2011. Free Radicals and Antioxidants. *Trends in Pharmacological Science*, 32(3): 125-130.

- Hanhineva, K., Törrönen, R., Bondia-Pons, I., Pekkinen, J., Kolehmainen, M. and Mykkänen, H. (2010). Impact of Dietary Polyphenols on Carbohydrate Metabolism. *International Journal of Molecular Science*, 11: 1365-1402.
- Haq, J. (2004). Safety of Medicinal Plants. *Pakistan Journal of Medical Research*, 43: 8-15.
- Harvey, M. J., Giupponi, G. and Fabritiis, G. D. (2009). ACEMD: Accelerating Biomolecular Dynamics in the Microsecond Time Scale. *Journal of Chemical Theory and Computation*, 5(6), 1632-1639.
- Huang, J. and MacKerell Jr, A. D. (2013). CHARMM36 All-Atom Additive Protein Force Field: Validation Based on Comparison to NMR Data. *Journal of Computational Chemistry*, 34(25), 2135-2145.
- Heim, K. E., Tagliaferro, A. R. and Bobilya, D. J. (2002). Flavonoid Antioxidants: Chemistry, Metabolism and Structure-Activity Relationships. *The Journal of Nutritional Biochemistry*, 13(10), 572-584.
- Heiss, E. H., Tran, T. V., Zimmermann, K., Schwaiger, S., Vouk, C., Mayerhofer, B., Malainer, C., Atanasov, A. G., Stuppner, H. and Dirsch, V. M. (2014). Identification of Chromomoric Acid C-I as an Nrf2 Activator in *Chromolaena odorata*. *Journal of Natural Products*, 77: 503-508.
- Hollman, P. C. and Katan, M. B. (1998). Bioavailability and Health Effects of Dietary Flavonols in Man. *Diversification in Toxicology—Man and Environment*, 237-248.
- Holst, J. J. (2007). The Physiology of Glucagon-Like Peptide 1. *Physiological Reviews*, 87: 1409-1439.
- Hossain, M. K., Dayem, A. A., Han, J., Yin, Y., Kim, K., Saha, S. K., Yang, G., Choi, H. Y. and Cho, S. (2016). Molecular Mechanisms of the Anti-Obesity and Anti-Diabetic Properties of Flavonoids. *International Journal of Molecular Sciences*, 17: 569. doi:10.3390/ijms17040569.
- Humphrey, W., Dalke, A. and Schulten, K. (1996). VMD: Visual Molecular Dynamics. *Journal of Molecular Graphics*, 14(1), 33-38.
- Hussain, S. A. R. (2007). Silymarin as an Adjunct to Glibenclamide Therapy Improves Long-Term and Postprandial Glycemic Control and Body Mass Index in Type 2 Diabetes. *Journal of Medicinal Food*, 10(3), 543-547.
- Hussein, R. A. and El-Anssary, A. A. (2019). Plants Secondary Metabolites: The Key Drivers of the Pharmacological Actions of Medicinal Plants. *Herbal Medicine*, 1, 13.
- Ichimura, T., Bonventre J. V., Bailly, V., Wei, H., Hession, C. A., Cate, R. L. and Sanicola, M. (1998). Kidney injury molecule-1 (KIM-1), A Putative Epithelial Cell Adhesion Molecule Containing A Novel Immunoglobulin Domain, is Up-regulated in Renal Cells After Injury. *Journal of Biological Chemistry*, 273(7): 4135-4142.
- Ignacimuthu, S., Ayyanar, M. and Sivaraman, S. K. (2006). "Ethnobotanical Investigations Among Tribes in Madurai District of Tamil Nadu (India)". *Journal of Ethnobiology and Ethnomedicine*, 2: 1-7.
- Ikwewuchi, J. C. and Ikwewuchi, C. C. (2011). Anti-Cholesterolemic Effect of Aqueous Extract of the Leaves of *Chromolaena odorata* (L) King and Robinson (Asteraceae): Potential for the Reduction of Cardiovascular Risk. *The Pacific Journal of Science and Technology*, 12(2), 385-391.
- Inoguchi, T., Sonta, T., Tsubouchi, H., Etoh, T., Kakimoto, M., Sonoda, N., Sato, N., Sekiguchi, N., Kobayashi, K. and Sumimoto, H. (2003). Protein Kinase C-Dependent Increase in Reactive Oxygen Species (ROS) Production in Vascular Tissues of Diabetes: Role of Vascular NAD(P)H Oxidase. *Clinical Journal of the American Society of Nephrology*, 14(suppl 3): S227-S232.

- Ismail, N. A., El Baky, A. N., Ragab, S., Hamed, M., Hashish, M. A. and Shehata, A. (2016). Monocyte Chemoattractant Protein 1 And Macrophage Migration Inhibitory Factor in Children with Type 1 Diabetes. *Journal of Pediatric Endocrinology and Metabolism*, 29(6):641-5.
- Isoda, K., Young, J. L., Zirlik, A., MacFarlane, L. A., Tsuboi, N., Gerdes, N., Schonbeck, U. and Libby, P. (2006). Metformin Inhibits Proinflammatory Responses and Nuclear Factor- $\kappa$ B in Human Vascular Wall Cells. *Arteriosclerosis, Thrombosis, and Vascular Biology*, 26(3), 611-617.
- Jadhav, R. and Puchchakayala, G. (2012). Hypoglycemic and Antidiabetic Activity of Flavonoids: Boswellic Acid, Ellagic Acid, Quercetin, Rutin on Streptozotocin-Nicotinamide Induced Type 2 Diabetic Rats. *International Journal of Pharmacy and Pharmaceutical Sciences*, 4(2): 251-256.
- Jain, M. (2012). Histopathological Changes in Diabetic Kidney Disease. *Clinical Queries Nephrology*, 102, 127-133.
- Jain, D., Bansal, M. K., Dalvi, R., Uppanlawar, A. and Somani, R. (2014). Protective Effect of Diosmin Against Diabetic Neuropathy in Experimental Rats. *Journal of Integrative Medicine*, 12: 35-41.
- Jang, J. S. and Jeong, J. C. (2010). Anti-Adipogenic Effect of Kaempferol, A Component of Polygonatirrhizoma. *Journal of Korean Oriental Medicine*, 31: 158-166.
- Jena, P. K. and Chakraborty, A. K. (2010). Evaluation of Analgesic Activity Studies of Various Extracts of Leaves of *Eupatorium odoratum* Lim. *International Journal of Pharmacy and Technology*, 2(3): 612-616.
- Johnston, K., Sharp, P., Clifford, M. and Morgan, L. (2005). Dietary Polyphenols Decrease Glucose Uptake by Human Intestinal Caco-2 Cells. *FEBS letters*, 579(7): 1653-1657.
- Jung, U. J., Lee, M. K., Jeong, K. S. and Choi, M. S. (2004). The Hypoglycemic Effects of Hesperidin and Naringin are Partly Mediated by Hepatic Glucose-Regulating Enzymes in C57BL/KsJ-db/db Mice. *The Journal of Nutrition*, 134(10): 2499-2503.
- Kahn, S. E. (2001). The Importance of  $\beta$ -cell Failure in the Development and Progression of Type 2 Diabetes. *The Journal of Clinical Endocrinology and Metabolism*, 86(9): 4047-4058.
- Kaku, K. 2010. Pathophysiology of Type 2 Diabetes and its Treatment Policy. *Japan Medical Association Journal*, 53(1): 41-46.
- Kamalakkannan, N. and Prince, P. S. M. (2006). Anti-Hyperglycaemic and Antioxidant Effect of Rutin, A Polyphenolic Flavonoid, in Streptozotocin-Induced Diabetic Wistar Rats. *Basic Clinical Pharmacology and Toxicology*, 98: 97-103.
- Kaneto, H., Miyatsuka, T., Kawamori, D. and Matsuoka, T. A. (2007). Pleiotropic Roles of PDX-1 in the Pancreas. *The review of diabetic studies: RDS*, 4(4), 209.
- Kao, P. C., Wu, T. J., Ho, L. L. and Li, X. J. (2000). Current Trends and New Approaches in the Management of Diabetes Mellitus. *Annals of Clinical and Laboratory Science*, 30(4): 339-345.
- Katsuma, S., Hirasawa, A. and Tsujimoto, G. (2005). Bile Acids Promote Glucagon-Like Peptide-1 Secretion Through TGR5 in a Murine Enteroendocrine Cell Line STC-1. *Biochemical and biophysical research communications*, 329(1): 386-390.
- Kawamata, Y., Fujii, R., Hosoya, M., Harada, M., Yoshida, H., Miwa, M., Fukusumi, S., Habata, Y., Itoh, T., Shintani, Y., Hinuma, S., Fujisawa, Y., Fujino, M. (2003). A G Protein- Coupled Receptor Responsive to Bile Acids. *Journal of Biological Chemistry*, 278(11): 9435-9440.
- Kennedy, H. J., Pouli, A. E., Ainscow, E. K., Jouaville, L. S., Rizzuto, R. and Rutter, G. A. (1999). Glucose Generates Sub-Plasma Membrane ATP Microdomains in Single

- Islet  $\beta$ -Cells Potential Role for Strategically Located Mitochondria. *Journal of Biological Chemistry*, 274: 13281–13291.
- Kerkeni, M., Addad, F., Chauffert, M., Chuniaud, L., Miled, A., Trivin, F. and Maaroufi, K. (2006). Hyperhomocysteinemia, Paraoxonase Activity and Risk of Coronary Artery Disease. *Clinical Biochemistry*, 39(8):821-5.
- Khorami, S. A. H., Movahedi, A. and Sokhini, A. M. M. (2015). Review Article; PI3K/AKT Pathway in Modulating Glucose Homeostasis and its Alteration in Diabetes. *Annals of Medical and Biomedical Sciences*, 1(2): 46–55.
- Kim, M. J., Ryu, G. R., Chung, J. S., Sim, S. S., Min, D. S., Rhie, D. J., Yoon, S. H., Hahn, S. J., Kim, M. S. and Jo, Y. H. (2003). Protective Effects of Epicatechin Against the Toxic Effects of Streptozotocin on Rat Pancreatic Islets: *in vivo* and *in vitro*. *Pancreas*, 26: 292-299
- Kim, M. S., Hur, H. J., Kwon, D. Y. and Hwang, J. T. (2012). Tangeretin Stimulates Glucose Uptake Via Regulation of AMPK Signalling Pathways in C2C12 Myotubes and Improves Glucose Tolerance in High-Fat Diet-Induced Obese Mice. *Molecular Cell Endocrinology*, 358: 127–134.
- Kim, H. and Fang, S. (2018). Crosstalk Between FXR and TGR5 Controls Glucagon-Like Peptide 1 Secretion to Maintain Glycemic Homeostasis. *Laboratory Animal Research*, 34(4): 140-146.
- Kitamura, T. (2013). The Role of FOXO1 in  $\beta$ -cell Failure and Type 2 Diabetes Mellitus. *Nature Reviews Endocrinology*, 9(10): 615.
- Kobayashi, Y., Suzuki, M., Satsu, H., Arai, S., Hara, Y., Suzuki, K., Miyamoto, Y. and Shimizu, M. (2000). Green Tea Polyphenols Inhibit the Sodium-Dependent Glucose Transporter of Intestinal Epithelial Cells by A Competitive Mechanism. *Journal of Agricultural and Food Chemistry*, 48(11), 5618-5623.
- Krentz, A. J., Ferner, R. E. and Bailey, C. J. (1994). Comparative Tolerability Profiles of Oral Antidiabetic Agents. *Drug Safety*, 11(4), 223-241.
- Kuhn, M. and Winston, D. (2000). Herbal Therapy and Supplements: A Scientific and Traditional Approach. New York: Lippincott and Wilkins, 347-350.
- Kumar, D. P., Rajagopal, S., Mahavadi, S., Mirshahi, F., Grider, J. R., Murthy, K. S., and Sanyal, A. J. (2012). Activation of Transmembrane Bile Acid Receptor TGR5 Stimulates Insulin Secretion in Pancreatic Cells. *Biochemical and Biophysical Research Communications*, 427: 600-605.
- Lander, H. M., Tauras, J. M., Ogiste, J. S., Hori, O., Moss, R. A. and Schmidt, A. M. (1997). Activation of the Receptor for Advanced Glycation End Products Triggers A p21 Ras-Dependent Mitogen-Activated Protein Kinase Pathway Regulated by Oxidant Stress. *Journal of Biological Chemistry*, 272(28): 17810-17814.
- Lalith, G. (2009). Invasive Plants: A Guide to the Identification of the Most Invasive Plants of Sri Lanka, Colombo.
- Laybutt, D. R., Kaneto, H., Hasenkamp, W., Grey, S., Jonas, J. C., Sgroi, D. C., Groff, A., Ferran, C., Bonner-Weir, S., Sharma, A. and Weir, G. C. (2002). "Increased Expression of Antioxidant and Antiapoptotic Genes in Islets that may Contribute to  $\beta$ -cell Survival During Chronic Hyperglycemia". *Diabetes*, 51(2): 413-423.
- Le Lay, J. and Stein, R. (2006). Involvement of PDX-1 in Activation of Human Insulin Gene Transcription. *Journal of Endocrinology*, 188(2): 287–294.
- Lee, J. S. (2006). Effects of Soy Protein and Genistein on Blood Glucose, Antioxidant Enzyme Activities, and Lipid Profile in Streptozotocin-Induced Diabetic Rats. *Life Sciences*, 79: 1578–1584.
- Lee, J., Lee, S., Zhang, H., Hill, M. A., Zhang, C. and Park, Y. (2017). Interaction of IL-6 and TNF- $\alpha$  Contributes to Endothelial Dysfunction in Type 2 Diabetic Mouse Hearts. *PLoS One*, 12(11), e0187189.

- Lee, Y. and Jun, H. (2018). Glucagon-Like peptide-1 Receptor Agonist and Glucagon Increase Glucose-Stimulated Insulin Secretion in Beta Cells via Distinct Adenylyl Cyclases. *International journal of medical sciences*, 15(6): 603-609. doi: 10.7150/ijms.2449215.
- Lefkowitz, R. J. (2007). Seven Transmembrane Receptors: A Brief Personal Retrospective. *Biochimica et Biophysica Acta*, 1768(4): 748-755.
- Li, W., Zhao, W., Wu, Q., Lu, Y., Shi, J. and Chen, X. (2016). Puerarin Improves Diabetic Aorta Injury by Inhibiting NADPH Oxidase-Derived Oxidative Stress in STZ-Induced Diabetic Rats. *Journal of Diabetes Research*, <http://dx.doi.org/10.1155/2016/8541520>
- Li, B., Yang, N., Li, C., Li, C., Gao, K., Xie, X., Dong, X., Yang, J., Yang, Q., Tong, Z. and Lu, G. (2018). INT-777, A Bile Acid Receptor Agonist, Extenuates Pancreatic Acinar Cells Necrosis in a Mouse Model of Acute Pancreatitis. *Biochemical and Biophysical Research Communications*, 503(1), 38-44.
- Libby, P., Ridker, P. M. and Hansson, G. K. (2011). Progress and Challenges in Translating the Biology of Atherosclerosis. *Nature*, 473(7347): 317-325.
- Lin, Y. and Sun, Z. (2010). Current Views on Type 2 Diabetes. *The Journal of Endocrinology*, 204(1), 1.
- Ling, S. K., Mazura, M. P. and Salbiah, M. (2007). Platelet-Activating Factor (PAF) Receptor- Binding Antagonist Activity of the Methanol Extracts and Isolated Flavonoids from *Chromolaena odorata* (L.) King and Robinson. *Biological and Pharmaceutical Bulletin*, 30: 1150-1152.
- Lipinski, B., (2001). Pathophysiology of Oxidative Stress in Diabetes Mellitus. *Journal of Diabetes and Its Complications* 15(4): 203-210.
- Liu, D., Zhen, W., Yang, Z., Carter, J. D., Si, H. and Reynolds, K. A. (2006). Genistein Acutely Stimulates Insulin Secretion in Pancreatic B-Cells Through A cAMP-Dependent Protein Kinase Pathway. *Diabetes*, 55, 1043-1050.
- Lo, S. H., Cheng, K. C., Li, Y. X., Chang, C. H., Cheng, J. T. and Lee, K. S. (2016). Development of Betulinic Acid as an Agonist of TGR5 Receptor Using A New *in vitro* Assay. *Drug Design, Development and Therapy*, 10: 2669. <http://dx.doi.org/10.2147/DDDT.S113197>
- Lokman, F. E., Gu, H. F., Wan Mohamad, W. N., Yusoff, M. M., Chia, K. L. and Östenson, C. G. (2013). Antidiabetic Effect of Oral Borapetol B Compound, Isolated from the plant *Tinospora crispera*, by Stimulating Insulin Release. *Evidence-Based Complementary and Alternative Medicine*. <http://dx.doi.org/10.1155/2013/727602>
- Lovell, S. C., Davis, I. W., Arendall III, W. B., De Bakker, P. I., Word, J. M., Prisant, M. G. and Richardson, D. C. (2003). Structure Validation by C $\alpha$  Geometry:  $\phi$ ,  $\psi$  and C $\beta$  Deviation. *Proteins: Structure, Function, and Bioinformatics*, 50(3), 437-450.
- Lovshin, J. A. and Drucker, D. J. (2009). Incretin-Based Therapies for Type 2 Diabetes Mellitus. *Nature Reviews Endocrinology*, 5: 262-269.
- Lunde, I. G., Aronsen, J. M., Kvaløy, H., Qvigstad, E., Sjaastad, I., Tønnessen, T. and Carlsson, C. R. (2012). Cardiac O-GlcNAc Signaling is Increased in Hypertrophy and Heart Failure. *Physiological Genomics*, 44(2), 162-172.
- Ma, J. and Hart, G. W. (2013). Protein O-GlcNAcylation in Diabetes and Diabetic Complications. *Expert Review of Proteomics*, 10(4): 365-380.
- MacDonald, P. E., El-kholy, W., Riedel, M. J., Salapatek, A. M. F., Light, P. E. and Wheeler, M. B. (2002). The Multiple Actions of GLP-1 on the Process of Glucose-Stimulated Insulin Secretion. *Diabetes*, 51(suppl 3): S434-S442.
- MacKenzie, T., Leary, L. and Brooks, W. B. (2007). The Effect of an Extract of Green and Black Tea on Glucose Control in Adults with Type 2 Diabetes Mellitus: Double-Blind Randomized Study. *Metabolism*, 56: 1340-1344.

- Maczewsky, J., Kaiser, J., Gresch, A., Gerst, F., Düfer, M., Krippeit-Drews, P. and Drews, G. (2019). TGR5 Activation Promotes Stimulus-Secretion Coupling of Pancreatic  $\beta$ -Cells via a PKA-Dependent Pathway. *Diabetes*, 68(2): 324-336.
- Mahomoodally, M. F. (2013). Traditional medicines in Africa: An Appraisal of Ten Potent African Medicinal Plants. *Evidence-based complementary and alternative medicine*. Article ID 617459. <https://doi.org/10.1155/2013/617459>
- Malik, J. and Roohi, N. (2018). GLP-1, A Powerful Physiological Incretin: An Update. *Journal of Biological Regulators and Homeostatic Agents*, 32(5), 1171-1176.
- Mao, C. P. and Gu, Z. L. (2005). Puerarin Reduces Increased c-fos, c-jun, and Type IV Collagen Expression Caused by High Glucose in Glomerular Mesangial Cells. *Acta Pharmacologica Sinica*, 26: 982.
- Martens, S., Preuß, A. and Matern, U. (2010). Multifunctional Flavonoid Dioxygenases: Flavonol and Anthocyanin Biosynthesis in *Arabidopsis thaliana* L. *Phytochemistry*, 71(10), 1040-1049.
- Maritim, A. C., Sanders, R. A. and Watkins, J. B. (2003). Diabetes Mellitus is a Metabolic Disorder Characterized by Hyperglycemia and Insufficiency of Secretion or Action of Endogenous Insulin. *Journal of Biochemical and Molecular Toxicology*, 17, 24-38.
- Maruyama, T., Miyamoto, Y., Nakamura, T., Tamai, Y., Okada, H., Sugiyama, E., Nakamura, T., Itadani, H. and Tanaka, K. (2002). Identification of Membrane-Type Receptor for Bile Acids (M-BAR). *Biochemical and Biophysical Research Communications*, 298(5): 714-719.
- Maury, E., Ehala-Aleksejev, K. Guiot, Y., Detry, R., Vandenhooff, A. and Brichard, S. M. (2007). Adipokines Oversecreted by Oriental Adipose Tissue in Human Obesity. *American Journal of Physiology-Endocrinology and Metabolism*, 293: E656-E665.
- May, O. (2008). Diabetes and insulin signaling: A New Strategy to Promote Pancreatic  $\beta$  Cell Survival. Article Library. Cayman Chemical, Supplier. [online] Caymanchem.com. (accessed 2019 Oct 30). Available from: URL: <https://www.caymanchem.com/app/template/Article.vm/article/2108>.
- McCullough, M. L., Peterson, J. J., Patel, R., Jacques, P. F., Shah, R. and Dwyer, J. T. (2012). Flavonoid Intake and Cardiovascular Disease Mortality in a Prospective Cohort of US Adults. *The American Journal of Clinical Nutrition*, 95(2), 454-464.
- Mendenhall, E., Norris, S. A., Shidhaye, R. and Prabhakaran, D. (2014). Depression and Type 2 Diabetes in Low- and Middle-Income Countries: A Systematic Review. *Diabetes Research and Clinical Practice*, 103(2): 276-285.
- Middleton, E., Kandaswami, C. and Theoharides, T. C. 2000. The Effects of Plant Flavonoids on Mammalian Cells: Implications for Inflammation, Heart Disease, and Cancer. *Pharmacological Reviews*, 52(4): 673-751.
- Mishra, D., Sarkar, D. K., Nayak, B. S., Rout, P. K., Ellaiah, P. and Ramakrishna, S. (2010). Phytochemical Investigation and Evaluation of anthelmintic Activity of Extract from Leaves of *Eupatorium odoratum* Linn. *Indian Journal of Pharmaceutical Education and Research*, 44(4): 369-374.
- Miyata, Y., Tanaka, H., Shimada, A., Sato, T., Ito, A. and Yamanouchi, T. (2011). Regulation of Adipocytokine Secretion and Adipocyte Hypertrophy by Polymethoxyflavonoids, Nobiletin and Tangeretin. *Life Sciences*, 88(13-14): 613-618.
- Moghaddam, H. S., Samarghandian, S. and Farkhondeh, T. (2015). Effect of bisphenol A on Blood Glucose, Lipid Profile and Oxidative Stress Indices in Adult Male Mice. *Toxicology Mechanisms and Methods*, 25: 507-513.

- Mohamed, B., Abderrahim, Z., Hassane, M., Abdelhafid, T. and Abdelkhalq, L. (2006). Medicinal Plants with Potential Antidiabetic Activity – A review of Ten Years of Herbal Medicine Research. *International Journal of Diabetes Metabolism*, 14: 1-25.
- Murphy, K. G., Dhillon, W. S. and Bloom, S. R. (2006). Gut Peptides in the Regulation of Food Intake and Energy Homeostasis. *Endocrine Reviews*, 27(7), 719-727.
- Naito, M., Fujikura, J., Ebihara, K., Miyana, F., Yokoi, H., Kusakabe, T., Yamamoto, Y., Son, C., Mukoyama, M., Hosoda, K. and Nakao, K. (2011). Therapeutic Impact of Leptin on Diabetes, Diabetic Complications, and Longevity in Insulin-Deficient Diabetic Mice. *Diabetes*, 60(9): 2265-2273.
- Najafian, M., Ebrahim-Habibi, A., Yaghmaei, P., Parivar, K., Larijani, B. (2010). Core Structure of Flavonoids Precursor as an Antihyperglycemic and Antihyperlipidemic Agent: An *in vivo* study in Rats. *Acta Biochimica Polonica*, 57(4):553-560.
- Narayana, K. R., Reddy, M. S., Chaluvadi, M. R., Krishna, D. R., (2001). Bioflavonoids Classification, Pharmacological, Biochemical Effects and Therapeutic Potential. *Indian Journal of Physiology and Pharmacology*, 33: 2-16.
- Nasri, S., Roghani, M., Baluchnejadmojarad, T., Rabani, T. and Balvardi, M. (2011). Vascular Mechanisms of Cyanidin-3-Glucoside Response in Streptozotocin-Diabetic Rats. *Pathophysiology*, 18: 273-278.
- Nathan, D. M., Buse, J. B., Davidson, M. B., Ferrannini, E., Holman, R. R., Sherwin, R., and Zinman, B. (2009). American Diabetes Association; European Association for Study of Diabetes. Medical Management of Hyperglycemia in Type 2 Diabetes: A Consensus Algorithm for the Initiation and Adjustment of Therapy: A Consensus Statement of the American Diabetes Association and the European Association for the Study of Diabetes. *Diabetes Care*, 32(1), 193-203.
- Nauck, M. A. (2009). Unraveling the Science of Incretin Biology. *European Journal of Internal Medicine*, 20, S303-S308.
- Nauck, M. A., Homberger, E., Siegel, E. G., Allen, R. C., Eaton, R. P., Ebert, R. and Creutzfeldt, W. (1986). Incretin Effects of Increasing Glucose Loads in Man Calculated from Venous Insulin and C-peptide Responses. *The Journal of Clinical Endocrinology and Metabolism*, 63(2), 492-498.
- Newman, D. J. (2008). Natural Products as Leads to Potential Drugs: An Old Process or the New Hope for Drug Discovery? *Journal of Medicinal Chemistry*, 51: 2589-2599.
- Nicolle, E., Souard, F., Faure, P. and Boumendjel, A. (2011). Flavonoids as Promising Lead Compounds in Type 2 Diabetes Mellitus: Molecules of Interest and Structure-Activity Relationship. *Current Medicinal Chemistry*, 18(17): 2661-2672.
- Nurdiana, S., Goh, Y. M., Ahmad, H., Dom, S. M., Azmi, N. S. A., Zin, N. S. N. M., and Ebrahimi, M. (2017). Changes in Pancreatic Histology, Insulin Secretion and Oxidative Status in Diabetic Rats Following Treatment with *Ficus deltoidea* and Vitexin. *BMC Complementary and Alternative Medicine*, 17(1): 290. <https://doi.org/10.1186/s12906-017-1762-8>.
- Odugbemi, T., 2006. *Outlines and Pictures of Medicinal Plants from Nigeria*. 1st Edn., University of Lagos Press, Nigeria. ISBN: 978-38235-9-0, Pages: 283.
- Odugbemi, T. and Akinsulire, O. (2006). *Medicinal Plants by Species Names. Outlines and Pictures of Medicinal plants from Nigeria*, 112.
- Oh, Y. S. (2015). Plant-Derived Compounds Targeting Pancreatic Beta Cells for the Treatment of Diabetes. *Evidence-Based Complementary and Alternative Medicine*. <http://dx.doi.org/10.1155/2015/629863>.
- Okwu, D. E. (2001). Evaluation of the Chemical Composition of Indigenous Spices and Flavouring Agents. *Global Journal of Pure and Applied Science*, 7(3): 455-459.
- Olokoba, A. B., Obateru, O. A. and Olokoba B. L. (2012). Type 2 Diabetes Mellitus: A Review of Current Trends. *Oman Medical Journal*, 27(40): 269-273.

- Mohamed, B., Abderrahim, Z., Hassane, M., Abdelhafid, T. and Abdelkhalq, L. (2006). Medicinal Plants with Potential Antidiabetic Activity – A review of Ten Years of Herbal Medicine Research. *International Journal of Diabetes Metabolism*, 14: 1-25.
- Murphy, K. G., Dhillon, W. S. and Bloom, S. R. (2006). Gut Peptides in the Regulation of Food Intake and Energy Homeostasis. *Endocrine Reviews*, 27(7), 719-727.
- Naito, M., Fujikura, J., Ebihara, K., Miyayama, F., Yokoi, H., Kusakabe, T., Yamamoto, Y., Son, C., Mukoyama, M., Hosoda, K. and Nakao, K. (2011). Therapeutic Impact of Leptin on Diabetes, Diabetic Complications, and Longevity in Insulin-Deficient Diabetic Mice. *Diabetes*, 60(9): 2265-2273.
- Najafian, M., Ebrahim-Habibi, A., Yaghmaei, P., Parivar, K., Larijani, B. (2010). Core Structure of Flavonoids Precursor as an Antihyperglycemic and Antihyperlipidemic Agent: An *in vivo* study in Rats. *Acta Biochimica Polonica*, 57(4):553-560.
- Narayana, K. R., Reddy, M. S., Chaluvadi, M. R., Krishna, D. R., (2001). Bioflavonoids Classification, Pharmacological, Biochemical Effects and Therapeutic Potential. *Indian Journal of Physiology and Pharmacology*, 33: 2-16.
- Nasri, S., Roghani, M., Baluchnejadmojarad, T., Rabani, T. and Balvardi, M. (2011). Vascular Mechanisms of Cyanidin-3-Glucoside Response in Streptozotocin-Diabetic Rats. *Pathophysiology*, 18: 273-278.
- Nathan, D. M., Buse, J. B., Davidson, M. B., Ferrannini, E., Holman, R. R., Sherwin, R., and Zinman, B. (2009). American Diabetes Association; European Association for Study of Diabetes. Medical Management of Hyperglycemia in Type 2 Diabetes: A Consensus Algorithm for the Initiation and Adjustment of Therapy: A Consensus Statement of the American Diabetes Association and the European Association for the Study of Diabetes. *Diabetes Care*, 32(1), 193-203.
- Nauck, M. A. (2009). Unraveling the Science of Incretin Biology. *European Journal of Internal Medicine*, 20, S303-S308.
- Nauck, M. A., Homberger, E., Siegel, E. G., Allen, R. C., Eaton, R. P., Ebert, R. and Creutzfeldt, W. (1986). Incretin Effects of Increasing Glucose Loads in Man Calculated from Venous Insulin and C-peptide Responses. *The Journal of Clinical Endocrinology and Metabolism*, 63(2), 492-498.
- Newman, D. J. (2008). Natural Products as Leads to Potential Drugs: An Old Process or the New Hope for Drug Discovery? *Journal of Medicinal Chemistry*, 51: 2589-2599.
- Nicolle, E., Souard, F., Faure, P. and Boumendjel, A. (2011). Flavonoids as Promising Lead Compounds in Type 2 Diabetes Mellitus: Molecules of Interest and Structure-Activity Relationship. *Current Medicinal Chemistry*, 18(17): 2661-2672.
- Nurdiana, S., Goh, Y. M., Ahmad, H., Dom, S. M., Azmi, N. S. A., Zin, N. S. N. M., and Ebrahimi, M. (2017). Changes in Pancreatic Histology, Insulin Secretion and Oxidative Status in Diabetic Rats Following Treatment with *Ficus deltoidea* and Vitexin. *BMC Complementary and Alternative Medicine*, 17(1): 290. <https://doi.org/10.1186/s12906-017-1762-8>.
- Odugbemi, T., 2006. *Outlines and Pictures of Medicinal Plants from Nigeria*. 1st Edn., University of Lagos Press, Nigeria, ISBN: 978-38235-9-0, Pages: 283.
- Odugbemi, T. and Akinsulire, O. (2006). Medicinal Plants by Species Names. *Outlines and Pictures of Medicinal plants from Nigeria*, 112.
- Oh, Y. S. (2015). Plant-Derived Compounds Targeting Pancreatic Beta Cells for the Treatment of Diabetes. *Evidence-Based Complementary and Alternative Medicine*. <http://dx.doi.org/10.1155/2015/629863>.
- Okwu, D. E. (2001). Evaluation of the Chemical Composition of Indigenous Spices and Flavouring Agents. *Global Journal of Pure and Applied Science*, 7(3): 455-459.
- Olokoba, A. B., Obateru, O. A. and Olokoba B. L. (2012). Type 2 Diabetes Mellitus: A Review of Current Trends. *Oman Medical Journal*, 27(40): 269-273.

- Omotuyi, I. O., Elekofehinti, O. O., Ejelonu, O. C. and Obi, F. O. (2013). Mass Spectra Analysis of *H. sabdarifia* L Anthocyanidins and their *in silico* Corticosteroid-Binding Globulin Interactions. *Pharmacol OnLine*, 1, 206-217.
- Omotuyi, O. I., Nash, O., Inyang, O.K., Ogidigo, J., Enejoh, O., Okpalefe, O. and Hamada, T. (2018). Flavonoid-rich extract of *Chromolaena odorata* Modulate Circulating GLP-1 in Wistar Rats: Computational Evaluation of TGR5 Involvement. *3 Biotech*, 8(2): 124
- Onkaramurthy, M., Veerapur, V. P., Thippeswamy, B. S., Reddy, T. N., Rayappa, H. and Badami S. (2013). Anti-diabetic and Anti-cataract Effects of *Chromolaena Odorata* Linn, in Streptozotocin-Induced Diabetic Rats. *Journal of Ethnopharmacology*, 145(1): 363-72.
- Orchard, T. J., Costacou, T., Kretowski, A. and Nesto, R. W. (2006). Type 1 Diabetes and Coronary Artery Disease. *Diabetes Care*, 29(11): 2528-2538.
- Oskouei, B. G., Abbaspour-Ravaşjani, S., Jamal, S. M., Ahmad, S. S., Abdolhosseinzadeh A., Hamishhekar, H., Ghahremanzadeh, K., Shokouhi, B. (2019). *in vivo* Evaluation of Anti-hyperglycemic, Anti-hyperlipidemic and Anti-oxidant Status of Liver and Kidney of Thymol in STZ-induced Diabetic Rats. *Drug Research*, (Stuttg) 69(1):46-52. doi: 10.1055/a-0646-3803.
- Owoyele, V. B., Adediji, J. O. and Soladoye, A. O. (2005). Anti-inflammatory Activity of Aqueous Leaf Extract of *Chromolaena odorata*. *Inflammopharmacology*, 13(5-6): 479-484.
- Pandith, H., Zhang, X., Thongpraditchote, S., Wongkrajang, Y., Gritsanapan, W. and Baek, S. J. (2013). Effect of Siam Weed Extract and its Bioactive Component Scutellarein Tetramethyl Ether on Anti-Inflammatory Activity Through NF- $\kappa$ B Pathway. *Journal of Ethnopharmacology*, 147: 434-441.
- Paneni, F., Beckman, J. A., Creager, M. A. and Cosentino, F. (2013). Diabetes and Vascular Disease: Pathophysiology, Clinical Consequences, and Medical Therapy: Part 1. *European Heart Journal*, 34(31): 2436-2443.
- Papaccio G, Pisanti FA, Latronico MV, Ammendola E, Galdieri M. (2000). Multiple Low Dose and Single High Dose Treatments with Streptozotocin do not Generate Nitric Oxide. *Journal of Cellular Biochemistry*, 77(1): 82-91.
- Park, S. A., Choi, M. S., Cho, S. Y., Seo, J. S., Jung, U. J., Kim, M. J. and Lee, M. K. (2006). Genistein and Daidzein Modulate Hepatic Glucose and Lipid Regulating Enzyme Activities in C57BL/KsJ-db/db Mice. *Life Sciences*, 79: 1207-1213.
- Patel, J., Kumar, G. S., Qureshi, M. S. and Jena, P. K. (2010). Anthelmintic Activity of Ethanolic Extract of Whole Plant of *Eupatorium Odoratum*. *L. International Journal of Phytomedicine*, 2(2).
- Pennemans, V., Rigo, J. M., Penders, J. and Swennen, Q. (2012). Collection and Storage Requirements for Urinary Kidney Injury Molecule-1 (KIM-1) Measurements in Humans. *Clinical Chemistry and Laboratory Medicine*, 50(3), 539-543.
- Pellicciari, R., Gioiello, A., Macchiariulo, A., Thomas, C., Rosatelli, E., Natalini, B., Sardella, R., Pruzanski, M., Roda, A., Pastorini, E. and Schoonjans, K. (2009). Discovery of 6 $\alpha$ -ethyl-23 (S)-methylcholic acid (S-EMCA, INT-777) as a Potent and Selective Agonist for the TGR5 Receptor, A Novel Target for Diabesity. *Journal of Medicinal Chemistry*, 52(24): 7958-7961. <http://dx.doi.org/10.1021/jm901390p>.
- Pelfetti, R., Zhou, J., Doyle, M.E. and Egan, J. M. (2000). Glucagon-Like Peptide-1 Induces Cell Proliferation and Pancreatic-Duodenum Homeobox-1 Expression and Increases Endocrine Cell Mass in the Pancreas of Old, Glucose-Intolerant Rats. *Endocrinology*, 141: 4600-4605.

- Petersen, M. C., Vatner, D. F. and Shulman, G. I. (2017). Regulation of Hepatic Glucose Metabolism in Health and Disease. *Nature Reviews Endocrinology*, 13(10): 572.
- Petrache, H. I., Dodd, S. W. and Brown, M. F. (2000). Area Per Lipid and Acyl Length Distributions in Fluid Phosphatidylcholines Determined by <sup>2</sup>H NMR Spectroscopy. *Biophysical Journal*, 79(6), 3172-3192.
- Petersen, E. F., Goddard, T. D., Huang, C. C., Couch, G. S., Greenblatt, D. M., Meng, E. C. and Ferrin, T. E. (2004). UCSF Chimera—A Visualization System for Exploratory Research and Analysis. *Journal of Computational Chemistry*, 25(13), 1605-1612.
- Phan, T. T., Wang, L., See, P., Grayer, R. J., Chan, S. Y., Lee, S. T., (2001). Phenolic Compounds of *Chromolaena odorata* Protect Cultured Skin Cells from Oxidative Damage: Implication for Cutaneous Wound Healing. *Biological Pharmaceutical Bulletin*, 24: 1373-1379.
- Piero, M. N., Njagi, J. M., Kibiti, C. M., Ngeranwa, J. J. N., Njagi, A. N. M., Njue, W. M. and Gathumbi, P. K. (2012). Herbal Management of Diabetes Mellitus: A Rapidly Expanding Research Avenue. *International Journal of Current Pharmaceutical Research*, 4(2): 1-4.
- Pinet, M., Blay, M., Blade, M. C., Salvado, M. J., Arola, L., Ardevol, A. (2004). Grape Seed-Derived Procyanidins have an Antihyperglycemic Effect in Streptozotocin-Induced Diabetic Rats and Insulinomimetic Activity in Insulin-Sensitive Cell Lines. *Endocrinology*, 145: 4985-4990
- Poitout, V., J. Amyot, M. Semache, B. Zarrouki, D. Hagman, and G. Fontés, (2010). "Glucolipotoxicity of the Pancreatic Beta Cell". *Biochimica et Biophysica Acta*, 1801(3): 289-298.
- Portha, B., Tourrel-Cuzin, C. and Movassat, J. (2011). Activation of the GLP-1 Receptor Signalling Pathway: A Relevant Strategy to Repair a Deficient Beta-Cell Mass. *Experimental Diabetes Research*, doi:10.1155/2011/376509.
- Prasad, S., Phromnoi, K., Yadav, V. R., Chaturvedi, M. M. and Aggarwal, B. B. (2010). Targeting Inflammatory Pathways by Flavonoids for Prevention and Treatment of Cancer. *Planta Medica*, 76: 1044-1063.
- Prasath, G. S., Pillai, S. and Subramanian, S. P. (2014). Fisetin Improves Glucose Homeostasis Through the Inhibition of Gluconeogenic Enzymes in Hepatic Tissues of Streptozotocin-Induced Diabetic Rats. *European Journal of Pharmacology*, 740: 248-54.
- Prigeon, R.L., Quddusi, S., Paty, B. and D'Alessio, D.A. (2003). Suppression of Glucose Production by GLP-1 Independent of Islet Hormones: A Novel Extrapancreatic Effect. *American Journal of Physiology-Endocrinology and Metabolism*, 285: E701-E707.
- Procházková, D., Boušová, I. and Wilhelmová, N. (2011). Antioxidant and Prooxidant Properties of Flavonoids. *Fitoterapia*, 82(4), 513-523.
- Puddu, A., Storace, D., Durante, A., Odetti, P. and Viviani, G. L., (2010). "Glucagon-Like peptide-1 Counteracts the Detrimental Effects of Advanced Glycation End-Products in the Pancreatic Beta Cell Line HIT-T 15," *Biochemical and Biophysical Research Communications*, 398(3): 462-466.
- Pulok, K. M., Kuntal, M., Kakali, M. and Peter, J. H. (2006). Leads from Indian Medicinal Plants with Hypoglycemic Potentials. *Journal of Ethnopharmacology*, 106: 1-28.
- Qin, Y., Niu, K., Zeng, Y., Liu, P., Yi, L., Zhang, T., Zhang, Q.Y., Zhu, J. D. and Mi, M. T. (2013). Isoflavones for Hypercholesterolaemia in Adults. *Cochrane Database of Systematic Reviews*, (6): 9518.
- Quianzon, C. C. and Cheikh, I. (2012). History of Insulin. *Journal of community hospital internal medicine perspectives*, 2(2), 18701.

- Ramachandran, A., Snehalatha, C., Shetty, A. S. and Nanditha, A. (2012). Trends in Prevalence of Diabetes in Asian Countries. *World Journal of Diabetes*, 3: 110-117.
- Raman, G., Jayaprakasha, G. K., Brodbelt, J., Cho, M. and Patil, B. S. (2004). Isolation of Structurally Similar Citrus Flavonoids by Flash Chromatography. *Analytical Letters*, 37(14), 3005-3016.
- Ramasamy, R., Vannucci, S. J., Du Yan, S. S., Herold, K., Yan, S. F. and Schmidt, A. M. (2005). Advanced Glycation End Products and RAGE: A Common Thread in Aging, Diabetes, Neurodegeneration, and Inflammation. *Glycobiology*, 15(7): 16R-28R.
- Rambuda, T. D. and Johnson, S. D. (2004). Breeding Systems of Invasive Alien Plants in South Africa: Does Baker's Rule Apply? *Diversity and Distributions*, 10(5-6): 409-416.
- Rejitha, G., Sunilson, J. A. J., Suraj, R., Amitava, D. and Kiran, N. (2009). Diuretic Activity of *Eupatorium odoratum* Linn. *Journal of Pharmacy Research*, 2(5): 844-846.
- Remuzzi, G., Macia, M. and Ruggenenti, P. (2006). Prevention and Treatment of Diabetic Renal Disease in Type 2 Diabetes: The BENEDICT Study. *Journal of the American Society of Nephrology*, 17: S90-97.
- Rendell, M. (2004). The role of Sulphonylureas in the Management of Type 2 Diabetes Mellitus. *Drugs*, 64(12), 1339-1358.
- Reuter, S., Gupta, S. C., Chaturvedi, M. M. and Aggarwal, B. B. (2010). Oxidative Stress, Inflammation, and Cancer: How are they Linked? *Free Radical Biology and Medicine*, 49(11): 1603-1616.
- Rice-Evans, C. A., Miller, N. J. and Paganga, G. (1996). Structure-Antioxidant Activity Relationships of Flavonoids and Phenolic Acids. *Free Radical Biology and Medicine*, 20(7): 933-956.
- Rifaai, R. A., El-Tahawy, N. F., Saber, E. A. and Ahmed, R. (2012). Effect of Quercetin on the Endocrine Pancreas of the Experimentally Induced Diabetes in Male Albino Rats: A Histological and Immunohistochemical Study. *Journal of Diabetes and Metabolism*, 3(182): 2 doi:10.4172/scientificreports.330.
- Robertson, R., Zhou, H., Zhang, T. and Harmon, J. S. (2007). "Chronic Oxidative Stress as a Mechanism for Glucose Toxicity of the Beta Cell in Type 2 Diabetes." *Cell Biochemistry and Biophysics*, 48(2-3): 139-146.
- Robertson R. P. (2009). "β-Cell Deterioration During Diabetes: What's in the Gun?" *Trends in Endocrinology and Metabolism*, 20(8): 388-393.
- Rorsman, P. (1997). The Pancreatic Beta-Cell as a Fuel Sensor: An Electrophysiologist's Viewpoint. *Diabetologia*, 40(5): 487-495.
- Rorsman, P., Eliasson, L., Renström, E., Gromada, J., Barg, S. and Göpel, S. (2000). "The Cell Physiology of Biphasic Insulin Secretion," *News in Physiological Sciences*, 15(2): 72-77.
- Rösen, P., Nawroth, P., King, G., Möller, W., Tritschler, H. and Packer, L. (2001). The Role of Oxidative Stress in the Onset and Progression of Diabetes and its Complications: A Summary of a Congress Series Sponsored by UNESCO-MCBN, the American Diabetes Association and the German Diabetes Society. *Diabetes Metabolism Research and Review*, 17(3): 189-212.
- Sabu, M. C., Smitha, K., Kuttan, R. (2002). Antidiabetic Activity Of Green Tea Polyphenols and their Role in Reducing Oxidative Stress in Experimental Diabetes. *Journal of Ethnopharmacology*, 83: 109-116.
- Saini, V. (2010). Molecular Mechanisms of Insulin Resistance in Type 2 Diabetes Mellitus. *World Journal of Diabetes*, 1(3): 68.
- Samarghandian, S., Azimi-Nezhad, M., Afshari, R., Farkhondeh, T. and Karimnezhad, F. (2015). Effects of Buprenorphine on Balance of Oxidant/ Antioxidant System in the

- Different Ages of Male Rat Liver. *Journal of Biochemical and Molecular Toxicology*, 29: 249-25.
- Scheen, A. J. (2003). Pathophysiology of Type 2 Diabetes. *International Journal of Clinical and Laboratory Medicine*, 58(6), 335-341.
- Scheen, A. J. and Paquot, N. (2015). 2015 Updated Position Statement of the Management of Hyperglycaemia in Type 2 Diabetes. *Revue medicale suisse*, 11(483), 1518-1520.
- Schiekofer, S., Andrassy, M., Chen, J., Rudofsky, G., Schneider, J., Wendt, T., Stefan, N., Humpert, P., Fritsche, A. and Stumvoll, M. (2003). Acute Hyperglycemia Causes Intra-Cellular Formation of CML and Activation of Ras, p42/44 MAPK, and Nuclear Factor  $\kappa$ B in PBMCs. *Diabetes*, 52(3): 621-633.
- Schwartz, C.J., Valente, A.J., Sprague, E.A., Kelley, J.L., Cayatte, A.J. and Rozek, M.M. 1992. Pathogenesis of the Atherosclerotic Lesion: Implications for Diabetes Mellitus. *Diabetes Care*, 15(9): 1156-1167.
- Selway, J. T. (1986). Antiviral Activity of Flavones and Flavans. *Progress in Clinical and Biological Research*, 213: 521-536.
- Sena, C. M., Pereira, A. M. and Seica, R. (2013). Endothelial Dysfunction—A Major Mediator of Diabetic Vascular Disease. *Biochimica et Biophysica Acta (BBA)-Molecular Basis of Disease*, 1832(12), 2216-2231.
- Shaw, J. E., Sicree, R. A. and Zimmet, P. Z. (2010). Global Estimates of the Prevalence of Diabetes for 2010 and 2030. *Diabetes Research and Clinical Practice*, 87(1), 4-14.
- Sheehan, M. T. (2003). Current Therapeutic Options in Type 2 Diabetes Mellitus: A Practical Approach. *Clinical Medicine and Research*, 1: 189-200.
- Shen, H., Shao, M., Cho, K. W., Wang, S., Chen, Z., Sheng, L. and Rui, L. (2012). Herbal Constituent Sequoyitol Improves Hyperglycemia and Glucose Intolerance by Targeting Hepatocytes, Adipocytes, and  $\beta$ -cells. *American Journal of Physiology-Endocrinology and Metabolism*, 302(8), E932-E940.
- Slaoui, M. and Fiette, L. (2011). Histopathology Procedures: from Tissue Sampling to Histopathological Evaluation. In *Drug Safety Evaluation* (pp. 69-82). Humana Press.
- Soares, J. M. D., Leal, A. E. B. P., Silva, J. C., Almeida, J. R., and de Oliveira, H. P. (2017). Influence of Flavonoids on Mechanism of Modulation of Insulin Secretion. *Pharmacognosy Magazine*, 13(52), 639.
- Sonne, D. P., Hansen, M. and Knop, F. K. (2014). Bile Acid Sequestrants in Type 2 Diabetes: Potential Effects on GLP1 Secretion. *European Journal of Endocrinology*, 171: R47-R65. doi: 10.1530/EJE-14-0154
- Spiegelman, B. M. (1998). "PPAR- $\gamma$ : Adipogenic Regulator and Thiazolidinedione Receptor," *Diabetes*, 47, (4): 507-514.
- Srinivasan, S. and Pari, L. (2012). Ameliorative Effect of Diosmin, a Citrus Flavonoid Against Streptozotocin-Nicotinamide Generated Oxidative Stress Induced Diabetic Rats. *Chemical Biology Interactions*, 195: 43-51.
- Stanley, N., Pardo, L. and De Fabritiis, G. (2016). The Pathway of Ligand Entry from the Membrane Bilayer to a Lipid G Protein-Coupled Receptor. *Scientific Reports*, 6(1), 1-9.
- Stote, K. S., Clevidence, B. A., Novotny, J. A., Henderson, T., Radecki, S. V. and Baer, D. J. (2012). Effect of Cocoa and Green Tea on Biomarkers of Glucose Regulation, Oxidative Stress, Inflammation and Hemostasis in Obese Adults at Risk for Insulin Resistance. *European Journal of Clinical Nutrition*, 66(10), 1153-1159.
- Stumvoll, M., Goldstein, B. J. and van Haefen, T. W. (2005). "Type 2 Diabetes: Principles of Pathogenesis and Therapy," *The Lancet*, 365(9467): 1333-1346.

- Sundaram, R., Shanthi, P., and Sachdanandam, P. (2014). Effect of Tangeretin, a Polymethoxylated Flavones on Glucose Metabolism in Streptozotocin-Induced Diabetic Rats. *Phytomedicine*, 21: 793–799.
- Tadera, K., Minami, Y., Takamatsu, K. and Matsuoka, T. (2006). Inhibition of  $\alpha$ -glucosidase and  $\alpha$ -amylase by Flavonoids. *Journal of Nutritional Science and Vitaminology*, 52(2), 149-153.
- Taiwo, O. B., Olajide, O. A., Soyannwo, O. O. and Makinde, J. M. (2000). Anti-Inflammatory, Antipyretic and Antispasmodic Properties of *Chromolaena odorata*. *Pharmaceutical Biology*, 38(5): 367-370.
- Takaori, K. and Yanagita, M. (2016). Insights into the Mechanisms of the Acute Kidney Injury-to-Chronic Kidney Disease Continuum. *Nephron*, 134(3): 172-6.
- Tang, Y., Choi, E. J., Han, W. C., Oh, M., Kim, J., Hwang, J. Y., Park, P. J., Moon, S. H., Kim, Y. S. and Kim, E. K. (2017). *Moringa oleifera* from Cambodia Ameliorates Oxidative Stress, Hyperglycemia, and Kidney Dysfunction in Type 2 Diabetic Mice. *Journal of Medicinal Food* 20(5): 502-10.
- Tang-Christensen, M., Vrang, N. and Larsen, P. J. (1998). Glucagon-Like Peptide 1(7–36) Amide's Central Inhibition of Feeding and Peripheral Inhibition of Drinking are Abolished by Neonatal Monosodium Glutamate Treatment. *Diabetes*, 47: 530-537.
- Thang, P. T., Teik, L. S. and Yung, C. S. (2001). Anti-Oxidant Effects of the Extracts from the Leaves of *Chromolaena odorata* on Human Dermal Fibroblasts and Epidermal Keratinocytes Against Hydrogen Peroxide and Hypoxanthine-Xanthine Oxidase Induced Damage. *Burns*, 27(4):319-327.
- Thent, Z. C., Seong Lin, T., Das, S. and Zakaria, Z. (2012). Effect of *Piper sarmentosum* Extract on the Cardiovascular System of Diabetic Sprague-Dawley Rats: Electron Microscopic Study. *Evidence-Based Complementary and Alternative Medicine*, Article ID 628750 <https://doi.org/10.1155/2012/628750>
- Thomas, C., Pellicciari, R., Pruzanski, M., Auwerx, J. and Schoonjans, K. (2008). Targeting Bile-Acid Signalling for Metabolic Diseases. *Nature Reviews Drug Discovery*, 7: 678–693.
- Thomas, C., Giociello, A., Noriega, L., Strehle, A., Oury, J., Rizzo, G. and Pellicciari, R. (2009). TGR5- Mediated Bile Acid Sensing Controls Glucose Homeostasis. *Cell Metabolism*, 10(3): 167-177.
- Thomas, M. E., Blaine, C., Dawnay, A., Devonald, M. A., Ftouh, S., Laing, C., Latchem, S., Lewington, A., Milford, D. V. and Ostermann, M. (2015). The Definition of Acute Kidney Injury and its Use in Practice. *Kidney International*, 87(1): 62-73.
- Torrenegra, R. D. and Rodríguez, O. E. (2011). Chemical and Biological Activity of Leaf Extracts of *Chromolaena leivensis*. *Natural Product Communications*, 6: 947-950.
- Unnikrishnan, M. K., Veerapur, V., Nayak, Y., Mudgal, P. P. and Mathew, G. (2014). Antidiabetic, Antihyperlipidemic and Antioxidant Effects of the Flavonoids. In *Polyphenols in human health and disease* (pp. 143-161). Academic Press.
- Uyi, O. O., Ekhatfor F., Ikuenobe C. E., Borokini T. I., Aigbokhan E. I. and Egbon I. N. (2014) *Chromolaena odorata* Invasion in Nigeria: A Case for Coordinated Biological Control. *Management of Biological Invasions*, 5: 377–393.
- Van Belle, T. L., Coppieters, K. T. and Von Herrath, M. G. (2011). Type 1 Diabetes: Etiology, Immunology, and Therapeutic Strategies. *Physiological Reviews*, 91(1): 79-118.
- Van Der Spoel, D., Lindahl, E., Hess, B., Groenhof, G., Mark, A. E. and Berendsen, H. J. (2005). GROMACS: Fast, Flexible, and Free. *Journal of Computational Chemistry*, 26(16): 1701-18.
- Vaquero, M. R., Alberto, M. R. and De Nadra, M. M. (2007). Antibacterial Effect of Phenolic Compounds from Different Wines. *Food Control*, 18(2), 93-101.

- Vijayaraghavan K., Rajkumar J., Bukhari, S. N. A., Al-sayed, B. and seyed, M. A. (2017). Pharmacological Enhancement of Wound Healing Potential by *C. odorata*. *Molecular Medicine Reports*, 15: 1007-1016. DOI: 10.3892/mmr.2017.6133
- Vosseller, K., Sakabe, K., Wells, L. and Hart, G. W. (2002). Diverse Regulation of Protein Function by O-GlcNAc: A Nuclear and Cytoplasmic Carbohydrate Post-Translational Modification. *Current Opinion in Chemical Biology*, 6(6): 851-857.
- Wald, D. S., Law, M. and Morris, J. K. (2002). Homocysteine and Cardiovascular Disease: Evidence on Causality from a Meta Analysis. *British Medical Journal*, 325(7374):1202.
- Wan, X., Huo, Y., Johns, M., Piper, E., Mason, J. C., Carling, D., Haskard, D.O. and Boyle, J. J. (2013). 5'-AMP-Activated Protein Kinase-Activating Transcription Factor 1 Cascade Modulates Human Monocyte-Derived Macrophages to Atheroprotective Functions in Response to Heme or Metformin. *Arteriosclerosis, Thrombosis, and Vascular Biology*, 33(11), 2470-2480.
- Wang, X., Zhou, J., Doyle, M. E. and Egan, J. M. (2001). "Glucagon-Like Peptide-1 Causes Pancreatic Duodenal Homeobox-1 Protein Translocation from the Cytoplasm to the Nucleus of Pancreatic  $\beta$ -cells by a Cyclic Adenosine Monophosphate/Protein Kinase A-Dependent Mechanism," *Endocrinology*, 142(5): 1820-1827.
- Wang, Y. D., Chen, W. D., Yu, D., Forman, B. M. and Huang, W. (2011). The G-Protein-Coupled Bile Acid Receptor, Gpbar1 (TGR5), Negatively Regulates Hepatic Inflammatory Response through Antagonizing Nuclear Factor Kappa Light-Chain Enhancer of Activated B Cells (NF-Kappab) in Mice. *Hepatology*, 54: 1421-1432.
- Wang, D., Zhuang, Y., Tian, Y., Thomas, G. N., Ying, M. and Tomlinson, B. (2012). Study of the Effects of Total Flavonoids of *Astragalus* on Atherosclerosis Formation and Potential Mechanisms. *Oxidative Medicine and Cellular Longevity*. <https://doi.org/10.1155/2012/282383>.
- Wang, Y. H., Liu, Y. H., He, G. R., Lv, Y., Du, G. H. (2015). Esculin Improves Dyslipidemia, Inflammation and Renal Damage in Streptozotocin-Induced Diabetic Rats. *BMC Complementary and Alternative Medicine*, 15(1): 402.
- Wang, L., Cheng, K. C., Li, Y., Niu, C., Cheng, J., Niu, H. (2017). Glycyrrhizic Acid Increases Glucagon Like Peptide-1 Secretion via TGR5 Activation in Type 1-Like Diabetic Rats. *Biomedicine and Pharmacotherapy*, 95: 599-604.
- Wang, T., Li, Q., Bi, K. (2018). Bioactive Flavonoids in Medicinal Plants: Structure, Activity and Biological Fate. *Asian Journal of Pharmaceutical Sciences*, 13: 12-23.
- Weisberg, S. P., McCann, D., Desai, M., Rosenbaum, M., Leibel, R. L. and Ferrante, A. W. (2003). Obesity is Associated with Macrophage Accumulation in Adipose Tissue. *Journal of Clinical Investigation*, 112: 1796-1808.
- Weiss, R. B. (1982). Streptozocin: A Review of Its Pharmacology, Efficacy, and Toxicity. *Cancer Treatment Reports*, 66(3): 427-438.
- Whiting, D. R., Guariguata, L., Weil, C. and Shaw, J. (2011). IDF Diabetes Atlas: Global Estimates of the Prevalence of Diabetes for 2011 and 2030. *Diabetes Research and Clinical Practice*, 94(3), 311-321.
- Wilkinson, A., Bian, L., Khalil, D., Gibbons, K., Wong, P. F., Hart, D. N., Harris, M., Cotterill, A. and Vuckovic, S. (2011). Type 1 Diabetic Children and Siblings Share a Decrease in Dendritic Cell and Monocyte Numbers but are Differentiated by Expansion of CD4+ T Cells Expressing IL-17. *Journal of Clinical and Cellular Immunology*, 2(001): 1-9.
- Williams, R. (2009). Diabetes in the UK—How Big is the Problem? *Journal of Dentistry*, 8(37): S573-S574.

- Winer, N. and Sowers, J. R. (2004). Epidemiology of Diabetes. *Journal of Clinical Pharmacology*, 44(4): 397-405.
- Wu, C. and Yen, G. (2005). Inhibitory Effect of Naturally Occurring Flavonoids on the Formation of Advanced Glycation End Products. *Journal of Agriculture and Food Chemistry*, 53(8): 3167-3173.
- Wu, T., Rayner, C. K. and Horowitz, M. (2015). Incretins. *Metabolic Control*, 137-171.
- Xie, Z., Zhong, L., Wu, Y., Wan, X., Yang, H., Xu, X. and Li, P. (2018). Carnosic Acid Improves Diabetic Nephropathy by Activating Nrf2/ARE and Inhibition of NF- $\kappa$ B Pathway. *Phytomedicine*, 47: 161-173.
- Xu, H. Y.; Barnes, G.T.; Yang, Q.; Tan, Q.; Yang, D.S.; Chou, C.J.; Sole, J.; Nichols, A.; Ross, J.S.; Tartaglia, L.A and Chen, H. (2003). Chronic Inflammation in Fat Plays a Crucial Role in the Development of Obesity-Related Insulin Resistance. *Journal of Clinical Investigation*, 112(12): 1821-1830.
- Xu, H. X. and Lee, S. F. (2001). Activity of Plant Flavonoids Against Antibiotic - Resistant Bacteria. *Phytotherapy Research: An International Journal Devoted to Pharmacological and Toxicological Evaluation of Natural Product Derivatives*, 15(1), 39-43.
- Yan, S. D., Schmidt, A. M., Anderson, G. M., Zhang, J., Brett, J., Zou, Y. S., Pinsky, D. and Stern, D. (1994). Enhanced Cellular Oxidant Stress by the Interaction of Advanced Glycation End Products with their Receptors/Binding Proteins. *Journal of Biological Chemistry*, 269(13): 9889-9897.
- Yang, W. J., Li, Y. R., Gao, H., Wu, X. Y., Wang, X. L., Wang, X. N., Xiang, L., Ren, D. M., Lou, H. X. and Shen, T. (2018). Protective Effect of the Ethanol Extract from *Ligusticum chuanxiong* Rhizome against Streptozotocin-Induced Diabetic Nephropathy in Mice. *Journal of Ethnopharmacology*, 227: 166- 175.
- Yang, X. and Qian, K. (2017). Protein O-GlcNAcylation: Emerging Mechanisms and Functions. *Nature Reviews Molecular Cell Biology*, 18(7): 452.
- Ye, J. H., Liu, M. H., Zhang, X. L. and He, J. Y. (2015). Chemical Profiles and Protective Effect of *Hedyotis diffusa* wild in Lipopolysaccharide-Induced Renal Inflammation Mice. *International Journal of Molecular Sciences*, 16: 27252-27269.
- Yu, R., Kim, C. S., Kwon, B. S. and Kawada, T. (2006). Mesenteric Adipose Tissue-Derived Monocyte Chemoattractant Protein-1 Plays a Crucial Role in Adipose Tissue Macrophage Migration and Activation in Obese Mice. *Obesity*, 14: 1353-1362.
- Yuan, S., Filipek, S., Palczewski, K. and Vogel, H. (2014). Activation of G-protein-Coupled Receptors Correlates with the Formation of a Continuous Internal Water Pathway. *Nature Communications*, 5: 4733.
- Zachariades, C., Day, M., Muniappan, R. and Reddy, G. V. B. (2009). *Chromolaena odorata* (L.) King and Robinson (Asteraceae). In: Muniappan, R. (Ed.). *Biological Control of Tropical Weeds using Arthropods*. Cambridge University Press, Cambridge, UK. Pp 130-162.
- Zander, M., Madsbad, S., Madsen, J. L. and Holst, J. J. (2002). Effect of 6-week course of Glucagon-Like Peptide 1 on Glycaemic Control, Insulin Sensitivity, and Beta-Cell Function in Type 2 Diabetes: A Parallel-Group Study. *Lancet*, 359: 824-830.
- Zarrinpar, A. and Loomba, R. (2012). The Emerging Interplay Among the Gastrointestinal Tract, Bile Acids and Incretins in the Pathogenesis of Diabetes And Non - Alcoholic Fatty Liver Disease. *Alimentary Pharmacology and Therapeutics*, 36(10), 909-921.
- Zeidan, Q. and Hart, G. W. (2010). The Intersections Between O-GlcNAcylation and Phosphorylation: Implications for Multiple Signaling Pathways. *Journal of Cell Science*, 123(1): 13-22.

- Zeka, K., Ruparella, K., Arroo, R. R. J., Budriesi R. and Micucci, M. (2017). Flavonoids and Their Metabolites: Prevention in Cardiovascular Diseases and Diabetes. *Diseases*, 5: 19; doi:10.3390/diseases5030019.
- Zhang, M. L., Irwin, D., Li, X. N., Sauriol, F., Shi, X. W., Wang, Y. F., Huo, C. H., Li, L. G., Gu, Y. C. and Shi, Q. W. (2012). PPAR $\gamma$  Agonist from *Chromolaena odorata*. *Journal of Natural Products*, 75: 2076-2081.
- Zheng, C., Zhou, W., Wang, T., You, P., Zhao, Y., Yang, Y., Wang, X., Luo, J., Chen, Y., Liu, M. and Chen, H. (2015). A Novel TGR5 Activator WB403 Promotes GLP-1 Secretion and Preserves Pancreatic  $\beta$ -Cells in Type 2 Diabetic Mice. *PLoS ONE*, 10(7): e0134051.
- Zheng, Y. C., He, H., Wei, X., Ge, S., Lu, Y. H. (2016). Comparison of Regulation Mechanisms of Five Mulberry Ingredients on Insulin Secretion under Oxidative Stress. *Journal of Agricultural and Food Chemistry*, 64: 8763-8772.
- Zimmet, P. Z., Magliano, D. J., Herman, W. H. and Shaw, J. E. (2014). Diabetes: A 21st Century Challenge. *The Lancet Diabetes and Endocrinology*, 2(1), 56-64.
- Zou, W., Yang, Y., Gu, Y., Zhu, P., Zhang, M., Cheng, Z., Liu X, Yu Y, and Peng, X. (2017). Repeated Blood Collection from Tail Vein of Non-Anesthetized Rats with a Vacuum Blood Collection System. *Journal of Visualized Experiments*, 130: e55852.